A QUATERNION FRAMEWORK FOR ANALYSIS OF THREE-PHASE LINEAR LOADS

ANDRÉ SEIKI FIGUEIREDO KOMENO

MASTERS DISSERTATION
DEPARTAMENTO DE ENGENHARIA ELÉTRICA

FACULDADE DE TECNOLOGIA

UNIVERSIDADE DE BRASÍLIA

UNIVERSIDADE DE BRASÍLIA

FACULDADE DE TECNOLOGIA

DEPARTAMENTO DE ENGENHARIA ELÉTRICA

A QUATERNION FRAMEWORK FOR ANALYSIS OF THREE-PHASE LINEAR LOADS

ANDRÉ SEIKI FIGUEIREDO KOMENO

ORIENTADOR: JOÃO YOSHIYUKI ISHIHARA

COORIENTADOR: ANÉSIO DE LELES FERREIRA FILHO

DISSERTAÇÃO DE MESTRADO EM ENGENHARIA ELÉTRICA

PUBLICAÇÃO: PPGENE.DM - 776/21

BRASÍLIA/DF: DEZEMBRO – 2021.

FICHA CATALOGRÁFICA

KOMENO, ANDRÉ SEIKI FIGUEIREDO

A QUATERNION FRAMEWORK FOR ANALYSIS

OF THREE-PHASE LINEAR LOADS. [Distrito Federal] 2021.

xv, 80p., 210 x 297 mm (ENE/FT/UnB, Mestre, Dissertação de Mestrado – Universidade de Brasília, Faculdade de Tecnologia).

Departamento de Engenharia Elétrica

1. Power Quality
2. Quaternions
3. Circuit Theory
4. Linear Loads

I. ENE/FT/UnB
II. Título

REFERÊNCIA BIBLIOGRÁFICA

KOMENO, A. S. F. (2021). A QUATERNION FRAMEWORK FOR ANALYSIS OF THREE-PHASE LINEAR LOADS, Dissertação de Mestrado, Publicação PPGENE.DM-776/21, Departamento de Engenharia Elétrica, Universidade de Brasília, Brasília, DF, 80 p.

André Seiki Figueiredo Komeno

Departamento de Eng. Elétrica (ENE) - FT

Universidade de Brasília (UnB)

Campus Darcy Ribeiro

CEP 70919-970 - Brasília - DF - Brasil

Universidade de Brasília
Faculdade de Tecnologia
Departamento de Engenharia Elétrica

A QUATERNION FRAMEWORK FOR ANALYSIS OF THREE-PHASE LINEAR LOADS

André Seiki Figueiredo Komeno

Dissertação de mestrado submetida ao Departamento de Engenharia Elétrica da Faculdade de Tecnologia da Universidade de Brasília, como parte dos requisitos necessários para a obtenção do grau de mestre.

APROVADA POR:

João Yoshiyuki Ishihara, Dr., ENE/UnB

(Orientador)

Francisco Damasceno Freitas, Dr., ENE/UnB

(Examinador interno)

Rodrigo Andrade Ramos, Dr., EESC/USP

(Examinador externo)

Brasília/DF, 03 de Dezembro de 2021.

To my baachan Michiko Komeno,
rest in peace.

André Seiki Figueiredo Komeno

Acknowledgments

I would like to express my gratitude to my supervisors João and Anésio, who were really helpful in the development of this work. Our long meetings were always insightful and improved a lot the quality of my work. I also want to say thank you a lot to Victor, who actively participated in many of our reunions, always bringing useful comments and sharing his great experience with the research topic.

I also am very thankful to my parents and my brother, who are always supportive and helped me a lot when I broke my leg this year. It was essential for my recovery and to make it possible to finish this dissertation.

I can't do an acknowledgment section without mentioning my girlfriend Letícia, who for almost 7 years now has been on my side sharing all the good and bad moments of my life. Our love is a source of strength, hope, and a lot of happiness for me. No matter how much I try I can never express how grateful I am for having you in my life.

I also want to mention my best friends for life Fernanda and Eloah. Regardless of how crazy life gets and how little time we have, whenever I meet you it is like time hasn't passed.

My thanks to Fischer and Pedro, my closest friends from school who followed me in the tortuous path of Electrical Engineering. Talking to you guys is always inspiring.

Thanks to the friends Enetec gave me whom I am looking forward to keeping all my life: Carol, Cadu, Leão, Guto, Igor, Rebeca, Malu, Zanatta, Helena, Augusto and Nat. Especially to Rebeca, for the friendship we have grown in these last two years. I already consider you one of my very best friends.

The difficulties of writing a monograph are already considerable, but having a global pandemic in effect during essentially all my master didn't help. Additionally, breaking my leg in the last semester, when I needed to concentrate on writing was a major challenge. All the people mentioned here were essential for enduring these challenges and finishing my dissertation.

I want to extend my thanks to:

My friends from Supervaust: Allan, Arthur, Borba, Celote, Hiandra, Mucilon, Sid, and Thiago.

My friends from school: Leandro, Egler, Gabriel, Gilberto, Greimel, Jhonny, Naty, Rogério and Vicky.

Thanks a lot to all of you!

This study was financed in part by the Coordenação de Aperfeiçoamento de Pessoal de Nível Superior - Brasil (CAPES) - Finance Code 001.

André Seiki Figueiredo Komeno

RESUMO

Nome: André Seiki Figueiredo Komeno

Título: Modelagem Quaterniônica para a Análise de Cargas Lineares Trifásicas

Nome do Programa: Programa de Pós-Graduação em Engenharia Elétrica

Data da defesa: Brasília, 3 de dezembro de 2021

Orientador: João Yoshiyuki Ishihara

Co-orientador: Anésio de Leles Ferreira Filho

Palavras-Chave: Qualidade da Energia, Quatérnios, Teoria de Circuitos, Cargas Lineares.

A teoria de potência instantânea tem um importante papel para a análise de sistemas de potência. Entre as ferramentas matemáticas utilizadas no desenvolvimento dessa teoria, quatérnions têm sido empregados para descrever grandezas elétricas em trabalhos recentes. Neste contexto, este estudo tem por objetivo modelar cargas trifásicas por meio de quatérnions. Considerando esse objetivo, os conceitos de impedância e potência quaterniônicas são generalizados, considerando o regime permanente e o regime transitório. Usando esses conceitos e considerando fontes de tensão equilibradas, cargas trifásicas lineares são analisadas. No caso de cargas balanceadas, realiza-se a análise de diversos tipos de impedâncias conectadas na configuração estrela. Mais especificamente, em cada caso são considerados resitores, indutores, capacitores, além das suas combinações. O caso desbalanceado é modelado considerando o estado permanente de cargas genéricas em sistemas de três e quatro fios. As configurações delta e estrela são analisadas em sistemas de três fios. Nos sistemas de quatro fios, considera-se a estrela aterrada e a estrela aterrada por impedância. Mostra-se que é simples se obter as correntes ou a potência quaterniônicas utilizando as expressões obtidas para a admitância quaterniônica, desde que as tensões trifásicas sejam conhecidas. A expressão obtida para a admitância quaterniônica também torna natural a introdução em sistemas a três fios da decomposição da carga trifásicas desbalanceada em termos de um componente balanceado e um componente desbalanceado com potência média nula. Obtém-se também uma decomposição para a estrela aterrada por impedância, mostrando que ela é equivalente à combinação em paralelo de uma carga em delta e de uma estrela aterrada. Os resultados obtidos estendem a teoria de sistemas de potência no domínio dos quatérnions e enfatizam as vantagens dessa representação. Particularmente, o modelo desenvolvido permite a representação das grandezas trifásicas numa notação compacta e prática.

ABSTRACT

Name: André Seiki Figueiredo Komeno

Title: A Quaternion Framework For Analysis of Three-phase Linear Loads

Name of Program: Programa de Pós-Graduação em Engenharia Elétrica

Date of Defense: Brasília, December 3rd, 2021

Supervisor: João Yoshiyuki Ishihara

Co-supervisor: Anésio de Leles Ferreira Filho

Keywords: Power Quality, Quaternions, Circuit Theory, Linear Loads.

Instantaneous power theory has an important role in power systems analysis. Among mathematical settings used for the development of this theory, quaternion algebra has been used for describing electrical variables in recent works. In this context, this study aims to model three-phase loads in a quaternion framework. Having in view this goal, the concepts of quaternionic power and impedance are generalized, considering steady and transient states. Using these concepts and considering balanced three-phase voltage sources, three-phase loads are analyzed. In the balanced case, several types of impedance are considered in the wye configuration. More specifically resistive, inductive, and capacitive impedances as well as their combinations are considered in each case. The unbalanced case is modeled considering the steady-state of generic loads in three and four-wire systems. In three-wire systems, both delta and wye configurations are analyzed. In four-wire systems, the solidly grounded and the grounded wye loads are examined. The expressions obtained for the admittance quaternion make it easy to obtain the three-phase current or the power quaternion if the three-phase voltages are known. The admittance quaternion expression obtained also makes it natural to introduce a decomposition of the three-wire unbalanced load in terms of a balanced load and an unbalanced load with null average power. It is also observed from the admittance quaternion of the grounded wye load that this configuration can be decomposed in a delta load in parallel with a solidly grounded wye load. The results obtained extend the power systems theory in the quaternion domain and emphasize the advantages of using this framework. Particularly, it is noteworthy that the model developed allows for a compact and practical representation of three-phase quantities.

CONTENTS

LIST OF FIGURES

LIST OF TABLES

LIST OF SYMBOLS

$\mathbb{H}$	Hamiltonian space	
$\mathbb{R}$	Real space	
t	time variable	[s]
ω	Angular electrical frequency	[rad/s]
$p(t)$	Instantaneous active power	[W]
$v_x(t)$	Instantaneous voltage of phase "x"	[V]
$i_x(t)$	Instantaneous current of phase "x"	[V]
R	Resistance	[Ω]
L	Inductance	[H]
C	Capacitance	[F]
ζ	Damping factor of a second order circuit	
ω_0	Resonance frequency of a second order circuit	[rad/s]
$\mathbf{V}(t)$	Voltage quaternion	[V]
$\mathbf{I}(t)$	Current quaternion	[A]
$\mathbf{S}(t)$	Power quaternion	[VA]
$\mathbf{Z}$	Impedance quaternion	[Ω]
$\mathbf{Y}$	Admittance quaternion	[S]
$\boldsymbol{\iota}$	Transient current quaternion	[A]
$\boldsymbol{\varsigma}$	Transient power quaternion	[VA]
$\boldsymbol{\upsilon}$	Transient admittance quaternion	[S]
$\mathrm{Re}(\mathbf{X})$	Real part of quaternion "$\mathbf{X}$"	
$\lvert\mathbf{X}\rvert$	Norm of quaternion "$\mathbf{X}$"	
$X \cdot Y$	Inner product between X and Y vectors	
$X \times Y$	Cross product between X and Y vectors	

Subscripts

T	Including transient state
pp	Phase to phase

Superscript

$\hat{}$	Phasor
$*$	Conjugate
-1	Inverse
$\vec{}$	Vectorial part of a quaternion

Abbreviations

Q-voltage	Voltage quaternion
Q-current	Current quaternion
Q-power	Power quaternion
Q-impedance	Impedance quaternion
Q-admittance	Admittance quaternion
RL	Resistor and inductor
RC	Resistor and capacitor
RLC	Resistor, inductor and capacitor

1 INTRODUCTION

The use of power electronics devices has risen in recent years, as the technologies are improved and renewable sources become more prominent in the market [1]. In this context, the importance of the compensation of harmonics and load unbalance is highlighted with several dedicated studies [2–5]. To mitigate these effects, accurate mathematical models need to be employed in order to correctly design compensators. However, phasors, the main tool used for evaluating power systems, have limitations when such non-ideal conditions are considered [6].

Originally, phasors were introduced to electrical circuit theory to simplify differential equations involving sinusoidal functions into algebraic equations. Since alternating current systems voltages and currents in ideal conditions consist of sinusoidal functions with a single frequency, phasors were a natural choice for modeling them. Other definitions such as electrical power and impedance could also be introduced in this framework, in which products and sums of sines became basic operations between complex numbers.

In practical applications, it was observed that power definitions via phasors occurred in some inconsistencies [7]. The presence of harmonics caused issues in the measurements of apparent, active, and reactive powers [6]. It was also observed that pure resistive loads present reactive power, which is not accounted for by phasors complex power [8]. Moreover, it is desirable to interpret three-phase systems as one entity, instead of a group of three individual systems [6, 9].

The analysis of power systems under unbalanced conditions is mainly classified into two different domains: the time-domain and the frequency domain. Particularly, the time-domain characterization has been utilized to develop powerful analysis tools [10–12]. In [10], the instantaneous p-q power theory was proposed employing the Clark transformation of instantaneous voltages and currents of a three-phase system. This theory allows the compensation of reactive power without energy storage components. The theory was extended by [11]. The author presented another interpretation that allows instantaneous reactive power characterization without the need of performing a Clark transformation. It makes possible analysis of polyphase networks. In [12], a generalized theory of instantaneous reactive power was proposed and analyzed for its physical meaning.

All the above-mentioned authors considered instantaneous space vectors to represent voltages and cur-

rents. More recently, some researchers have investigated instantaneous power quantities using a more general mathematical setting such as geometric algebra [13, 14], tensor analysis [15, 16], and quaternion algebra [17–20].

A framework based on quaternions seems to be promising for analysis of several problems in power systems and has already produced some interesting results [17–20]. The representation of three or four-dimensional quantities is an ideal scenario for employing them, making them an excellent tool for representing power systems [17–20]. Although they were applied in several problems, the foundations of three-phase circuit theory in this framework were not completely investigated in the literature.

1.1 QUATERNIONS IN ELECTRICAL ENGINEERING PROBLEMS

In this section, the literature on the application of quaternions in electrical engineering problems will be discussed.

Quaternions are a four-dimensional generalization of complex numbers [21]. They were discovered by Sir William Rowan Hamilton, who was searching for an algebra that represented three-dimensional rotations in the same way that complex numbers are employed to represent two-dimensional rotations. The solution found was to define three imaginary units, forming numbers with a real part and three mutually orthogonal imaginary parts. The established algebra was denoted $\mathbb{H}$ in honor of its creator.

Quaternions have been traditionally used for the problem of modeling three-dimensional rotations in a computationally efficient manner [22–24]. The invertibility property of nonzero quaternions allows concise and mathematically tractable solutions with fewer restrictions than those obtainable in the real domain and also avoids problems associated with gimbal lock [22, 23]. Additionally, higher-quality computer graphics is obtained by the smooth interpolations of rotations that quaternions produce [25].

For power systems, the usage of quaternion seems promising due to the possibility of i) operating the three phases as one entity and ii) representing electrical quantities in the time-domain, following the tendency of developing tools in this domain. Quaternion-based algorithms have been shown to be computationally efficient and accurate [26–29]. Consequently, a diverse niche of applications has been found for quaternions in power systems.

An algebraic approach was employed by the authors of [30] for defining three-phase quantities. Ac-

cording to the authors, this approach is more convenient for the quantitative analysis of the electric system behavior than the geometrical approach discussed in [31]. In this quaternionic framework, instantaneous line voltage and currents were defined. Instantaneous hypercomplex power was also defined and using this concept, the three-phase current is separated into "real" and "imaginary" components. It was shown that this decomposition generates the same currents as those discussed by Willems' power theory [11]. The author also generalizes the notion of impedance and admittance, defining instantaneous impedance and admittance. However, the authors only suggested the definitions for these quantities, not using them for further analysis.

The authors of [17] analyzed the electromagnetic transients in a three-phase squirrel-cage induction motor employing quaternions. The author used Pauli spin matrices representation of quaternions for calculating the linear transformations. This approach showed the advantage of using only 4 kinematic Caylen-Klein parameters instead of 9 direction cosines necessary in the traditional way. The method also allows performing the separate compensation of "active" and "reactive" losses in the induction motor, according to the author.

The authors of [32,33] designed an active power filter for compensating harmonics and reactive power. Quaternions were employed for obtaining the compensating currents. The filter was used for compensating the power of unbalanced non-linear three-phase loads in computational simulations, decreasing the total harmonic distortion from 37.45% to 8.24%. It was concluded that the generation of compensating reference on a quaternion basis is about ten times faster than the control operation based on the original Akagi-Nabae p-q theory [10]. This method for designing active power filters was revisited in [34], in which a shunt active power filter was projected and simulated for compensating currents of an unbalanced non-linear three-phase load. This paper also explored the properties of the instantaneous power definition in the hypercomplex space. The control laws of the active power filter presented in [32–34] were summarized in [35].

The authors of [36] developed a frequency estimation algorithm for three-phase systems based on quaternions. According to the authors, the algorithm developed is robust to noise and distortions. The $\mathbb{H}$ calculus was employed to derive a state-space estimator based on the quaternion extended Kalman filter proposed in [28]. The quaternion-valued state-space model was compared to the complex-valued state-space model in simulations. The simulations consisted of a balanced system that suffered a voltage

sag, an unbalanced system experiencing a frequency rise, and real-world data recorded at a 110/20/10 kV transformer station. The performance of this algorithm outperformed conventional complex linear estimators.

In [37], the author summarized the results achieved in [19] and [38]. In this paper, a single-phase RLC circuit was analyzed using quaternions. The differential equation of this circuit was written in terms of two orthogonal axes. Then, the power vector was represented in the remaining two quaternion axis, enlightening that these quantities are in quadrature with each other. The author also applied quaternions to analyze a direct current motor circuit. The Lorenz's force was computed for several cases with varying relative positions of flux and current.

The authors of [39] proposed harmonic distortion detection in three-phase power systems employing of quaternions. The frequency sweeping vector was rewritten considering a hypercomplex axis. Using this vector, the well-known processing algorithms MVDR and MUSIC were applied. Simulations showed that the model can detect all-order harmonics effectively and has similar estimation accuracy with the complex-valued model. Additionally, it can detect the zero-sequence voltages that are ignored by traditional Clarke's transformation.

A dynamic model of an induction motor with a squirrel-cage rotor in a quaternion framework was presented in [40]. Clark and Park's transformations were described in the hypercomplex space by quaternion rotations. These transformations were employed to obtain voltage differential equations and flux equations in dq coordinates. Afterward, instantaneous power and electric torque quaternions were found. The authors concluded that their model allows to split up the vector control design in sub-tasks and ensures the high-performance of speed response as well as reduction of active losses.

A quaternion quantitative analysis on harmonics of three-phase systems was carried out in [41]. Different compensation objectives were formulated based on this analysis, showing which terms of instantaneous power should be addressed by the active power filter for full compensation. These objectives permit to provide balanced or/and sinusoidal source currents with the desired phase shift relative to the corresponding voltage.

In 2018, [18] modeled three-phase circuits using quaternions. The voltage locus was analyzed for both balanced and unbalanced situations. It was shown that in the unbalanced case, it describes an ellipse while in the balanced case, it describes a circle. A three-phase series RLC balanced wye load was also

studied. Expressions for impedance and power of this load were obtained and it was shown that they are analogous to the representation of a single-phase RLC load using phasors. Additionally, it was pointed out that quaternion characterization of three-phase quantities serves as a link between the usual time and frequency domains. More specifically, with quaternions, it is possible to define three-phase electrical quantities analogously to single-phase definitions with phasors.

A hyper-impedance model was defined using quaternions in [42]. This hyper-impedance differed from the impedance model proposed in [18] by the inclusion of voltage and temperature in the formulation. A hypercomplex impedance model was also presented, using the octonion algebra. It added time, length, mass, amount of matter, and intensity of light in the hyper-impedance model, besides considering a dynamic parameter of the object. The use of these models made it possible to expand the capabilities of the Sawyer-Tower method for indirect measurements of the electrophysical parameters of ferroelectrics. According to the authors, their model opens up the possibility of taking into account the influence of heterogeneous factors on the object of study.

A control strategy for a four-leg full-bridge inverter using quaternions was proposed in [20]. It was based on the decomposition of three-phase voltages into balanced sinusoidal and unbalanced multi-harmonic components in the $\mathbb{H}$-domain. The quaternion representation of Clark and Park transformations was employed for modeling the feedback controller. Computational simulations showed that the quaternion control strategy provided the expected steady-state accuracy and fast-response transient behavior in the three-phase four-wire system. The control strategy presented in this work makes possible full characterization of voltage source inverter operations under unbalanced and/or non-sinusoidal load conditions.

A unified framework for filtering and controlling quaternion-valued state vector processes through multi-agent networked systems is presented in [43]. A distributed quaternion Kalman filter algorithm is introduced, as well as a decentralized quaternion-valued widely-linear quadrature regulator algorithm. The derived framework's performance is evaluated by computational simulations, comparing traditional centralized approaches to the distributed approaches proposed by the authors. It was observed that the developed framework reaches comparable performance levels to that of its centralized counterpart. According to the authors, the advantages of modeling three-dimensional signals with quaternions were demonstrated by simulations.

In synthesis, quaternions have been used for

1. representing three-phase electrical quantities (voltage, current, impedance, admittance) [18, 30, 44];

2. representing linear transformations in induction motors models [17, 38, 40];

3. analyzing single phase systems [18, 19, 37];

4. designing compensators [20, 32–35];

5. estimating electrical frequency [36];

6. treating harmonics [39, 41];

7. algorithms for distributed filter and control [43].

Although linear loads have been studied before in a quaternion framework, the transients were not analyzed. Also, the expression for the admittance of three-phase unbalanced loads was not presented in the literature. Considering the aforementioned facts, a comprehensive analysis of linear loads would be a useful study for quaternion's flourishing literature.

1.2 OBJECTIVES

This study aims to present the evaluation of voltage, current, instantaneous power, and admittance in the time domain, using quaternions. In other words, the objective of this dissertation is to extend the three-phase circuit theory based on quaternions, making feasible the application of this theory in the various problems studied in power systems. The analysis of the various load configurations is the approach chosen to accomplish this goal.

1.3 CONTRIBUTIONS

The contributions of this dissertation are

1. Modelling and analysis of current, admittance and power of three-phase balanced loads composed of resistors, inductors, capacitors and their combinations in a quaternion framework, considering transient and steady-states in the time domain;

2. Modelling and analysis of current, admittance and power of unbalanced three-phase delta and wye loads in a quaternion framework, considering the steady-state;

3. Modelling and analysis of current, admittance and power of unbalanced solidly grounded and grounded wye loads in a quaternion framework, considering the steady-state;

4. Decomposition of the unbalanced delta load into a balanced load in parallel with an unbalanced load with null average power;

5. Decomposition of the unbalanced grounded wye load into a delta load in parallel with a solidly grounded wye load.

The parts of these results related to the analysis of current and power of delta loads in the steady-state and the decomposition of delta loads were also published in [44].

1.4 DISSERTATION ORGANIZATION

In chapter 2, some basic theoretical background on the quaternion non-commutative algebra is presented. Several operations and properties necessary for working with quaternion three-phase circuit theory are shown. Afterward, in the chapter 3, the modeling of three-phase linear loads in the quaternion domain is presented. The modeling considers three and four-wire systems, balanced and unbalanced loads, and transient and steady-states. Finally, conclusions and guidelines for future works are addressed in chapter 4.

2 THEORETICAL BACKGROUND

In this chapter, the theoretical background of this dissertation is presented. First, quaternions are defined. Then, quaternion algebra is detailed, providing the mathematical foundation necessary for the construction of the hypercomplex three-phasic concepts of this monograph.

2.1 QUATERNION ALGEBRA

Quaternions were discovered by the Irish mathematician Sir William Rowan Hamilton (1805-1865). His initial motivation was inventing a set of numbers that related to the three-dimensional space in the same way as the complex numbers relate to the plane. This set would make it possible to represent three-dimensional rotations in the same way that complex numbers can represent two-dimensional rotations. His first conjecture proposed to add a second imaginary component to complex numbers for defining these numbers. However, after about 10 years of researching this subject, he still had not accomplished any success defining hypercomplex numbers. His struggle was even known by his children, who would ask if he already could multiply his “triplets”, to which he would deny, due to the inconsistency of his initial idealized algebra. But on 16th of October, in 1843, as he was walking along the Royal Canal in Dublin with his wife, came the inspiration: using three imaginary components instead of two, he could define an algebra that had the properties he was looking after. Thus, the quaternions were born (from Latin, quaternio, meaning "set of four"). He was so excited with his discovery that he drew his pocketknife and carved into the stone of Broome Bridge the famous formulas

$$\mathbf{i}^2 = \mathbf{j}^2 = \mathbf{k}^2 = \mathbf{ijk} = -1. \tag{2.1}$$

Unfortunately, the carvings faded with time. Nevertheless, even nowadays the Mathematics Department of the National University of Ireland, Maynooth, organizes a Hamilton Walk to Broome Bridge every year on October 16, in honor of his discovery [21].

Putting aside history, quaternions are an excellent tool for problems involving three dimensions, especially when rotations are involved. In this dissertation, instead of using **i**, **j** and **k**, **a**, **b** and **c** are used for representing the imaginary units of the quaternion domain, in allusion to the phases in three-phase systems.

In the subsections that follow, quaternions definitions and properties will be presented. The theory

discussed here is based in [21].

2.1.1 The standard Quadrinomial Form

Quaternions are a set of numbers denoted by $\mathbb{H}$, in honor of its discoverer. Since this set is one of the possible generalizations of complex numbers, its elements are considered hypercomplex numbers. An element of $\mathbb{H}$ can be defined in the quadrinomial form as

$$\mathbf{Q} = q_0 + q_1\mathbf{a} + q_2\mathbf{b} + q_3\mathbf{c}, \tag{2.2}$$

where q_0, q_1, q_2 and q_3 are real numbers and **a**, **b** and **c** form, along with 1, the orthonormal basis of their hypercomplex space. The quaternion **Q** can be unequivocally associated to an ordered quadruple of real numbers (q_0, q_1, q_2, q_3), so every point in $\mathbb{R}^4$ has a corresponding quaternion.

2.1.2 Scalar and vectorial parts

Analogously to complex numbers real and imaginary parts, quaternions can be separated into real (or scalar) and imaginary (or vectorial) parts. Considering the quaternion presented in (2.2), its real part $\mathrm{Re}(\mathbf{Q})$ and vectorial part $\vec{\mathbf{Q}}$ are, respectively, given by

$$\mathrm{Re}(\mathbf{Q}) = q_0, \tag{2.3}$$

$$\vec{\mathbf{Q}} = q_1\mathbf{a} + q_2\mathbf{b} + q_3\mathbf{c}. \tag{2.4}$$

If a quaternion has its real part equal to 0, it is said to be a purely vectorial quaternion. Notice that the vectorial part of a quaternion is always a purely vectorial quaternion. In the same way that quaternions are related to vectors in $\mathbb{R}^4$, purely vectorial quaternions can be unequivocally associated to vectors in $\mathbb{R}^3$ which are represented by the ordered triplet (q_1, q_2, q_3). From this point on, the terms purely vectorial quaternion and vector will be used as synonyms.

2.1.3 Sum and Subtraction

Considering two quaternions **Q** and **P** where $\mathbf{Q} = q_0 + q_1\mathbf{a} + q_2\mathbf{b} + q_3\mathbf{c}$ and $\mathbf{P} = p_0 + p_1\mathbf{a} + p_2\mathbf{b} + p_3\mathbf{c}$, their sum and subtraction can be calculated respectively as

$$\mathbf{Q} + \mathbf{P} = (q_0 + p_0) + (q_1 + p_1)\mathbf{a} + (q_2 + p_2)\mathbf{b} + (q_3 + p_3)\mathbf{c}, \tag{2.5}$$

$$\mathbf{Q} - \mathbf{P} = (q_0 - p_0) + (q_1 - p_1)\mathbf{a} + (q_2 - p_2)\mathbf{b} + (q_3 - p_3)\mathbf{c}. \tag{2.6}$$

It is noteworthy that these operations are equivalent to the sum and subtraction of vectors in $\mathbb{R}^4$. Furthermore, the addition of quaternions is associative and commutative, *i.e.*

$$(\mathbf{Q} + \mathbf{P}) + \mathbf{R} = \mathbf{Q} + (\mathbf{P} + \mathbf{R}), \tag{2.7}$$

$$\mathbf{Q} + \mathbf{P} = \mathbf{P} + \mathbf{Q}. \tag{2.8}$$

2.1.4 Basic Units

The imaginary units of $\mathbb{H}$ are related according to the famous expression

$$\mathbf{a}^2 = \mathbf{b}^2 = \mathbf{c}^2 = \mathbf{abc} = -1. \tag{2.9}$$

Using these relations it can be shown that

$$\mathbf{ab} = \mathbf{c} = -\mathbf{ba}, \tag{2.10}$$

$$\mathbf{bc} = \mathbf{a} = -\mathbf{cb}, \tag{2.11}$$

$$\mathbf{ca} = \mathbf{b} = -\mathbf{ac}. \tag{2.12}$$

It is observed from eqs. (2.10) to (2.12) that **a**, **b** and **c** pairwise anti-commute. As a consequence, quaternion product is non-commutative, as will be presented next.

2.1.5 Product

In quaternion algebra, the product of two quaternions **Q** and **P** is defined by

$$\begin{aligned}\mathbf{QP} = (q_0p_0 - q_1p_1 - q_2p_2 - q_3p_3) + (q_0p_1 + q_1p_0 + q_2p_3 - q_3p_2)\mathbf{a} \\ + (q_0p_2 - q_1p_3 + q_2p_0 + q_3p_1)\mathbf{b} + (q_0p_3 + q_1p_2 - q_2p_1 + q_3p_0)\mathbf{c}.\end{aligned} \tag{2.13}$$

The quaternion product can be rewritten in terms of the inner product and the cross product of the vectorial parts of the operands. The inner product between $\vec{\mathbf{Q}}$ and $\vec{\mathbf{P}}$ is defined as

$$\vec{\mathbf{Q}} \cdot \vec{\mathbf{P}} = q_1p_1 + q_2p_2 + q_3p_3 \tag{2.14}$$

and the cross product is given by the following determinant

$$\vec{\mathbf{Q}} \times \vec{\mathbf{P}} = \begin{vmatrix} \mathbf{a} & \mathbf{b} & \mathbf{c} \\ q_1 & q_2 & q_3 \\ p_1 & p_2 & p_3 \end{vmatrix}.$$

Notice that the definition of these operations is the same regardless if the vectorial part of quaternions or vectors in $\mathbb{R}^3$ are considered. Using these definitions, the product between $\mathbf{Q}$ and $\mathbf{P}$ can be rewritten as

$$\mathbf{QP} = (\mathrm{Re}(\mathbf{Q})\,\mathrm{Re}(\mathbf{P}) - \vec{\mathbf{Q}} \cdot \vec{\mathbf{P}}) + (\mathrm{Re}(\mathbf{Q})\vec{\mathbf{P}} + \mathrm{Re}(\mathbf{P})\vec{\mathbf{Q}} + \vec{\mathbf{Q}} \times \vec{\mathbf{P}}). \tag{2.15}$$

In particular, if $\mathbf{Q}$ and $\mathbf{P}$ are purely vectorial quaternions, then their product can be simplified to

$$\mathbf{QP} = -\vec{\mathbf{Q}} \cdot \vec{\mathbf{P}} + \vec{\mathbf{Q}} \times \vec{\mathbf{P}}. \tag{2.16}$$

The product of quaternions is associative, but not commutative. This comes from the cross product found on eq. (2.15) being non-commutative. More specifically, the cross-product is anti-commutative, $i.e.$

$$\vec{\mathbf{Q}} \times \vec{\mathbf{P}} = -\vec{\mathbf{P}} \times \vec{\mathbf{Q}}. \tag{2.17}$$

There is an exception to the non-commutativity of the product between quaternions. If the vectorial part of two quaternions is co-linear, their cross product is 0 and their product is commutative. In this case, it is said that these quaternions commute. Naturally, real numbers also commute with every quaternion.

2.1.6 Conjugate

Analogously to complex numbers, quaternions also have a conjugate. The conjugate of the quaternion $\mathbf{Q}$ is the quaternion

$$\mathbf{Q}^* = \mathrm{Re}(\mathbf{Q}) - \vec{\mathbf{Q}}. \tag{2.18}$$

Its noteworthy that, if the quaternion is purely vectorial, the conjugate is equivalent to multiplying it to -1, $i.e.$

$$\mathbf{Q}^* = -\mathbf{Q}. \tag{2.19}$$

Another important property of the conjugate of a product between quaternions is that

$$(\mathbf{QP})^* = \mathbf{P}^*\mathbf{Q}^*. \tag{2.20}$$

2.1.7 Norm

The norm of a quaternion $\mathbf{Q}$ is equivalent to the Euclidean distance of their correspondent point on $\mathbb{R}^4$ to the origin. It is defined as

$$|\mathbf{Q}| = \sqrt{q_0^2 + q_1^2 + q_2^2 + q_3^2}. \tag{2.21}$$

Particularly, the norm of a purely vectorial quaternion is

$$|\vec{\mathbf{Q}}| = \sqrt{q_1^2 + q_2^2 + q_3^2}. \tag{2.22}$$

Naturally, eq. (2.21) can also be expressed in terms of the norm of the vectorial part of the quaternion

$$|\mathbf{Q}| = \sqrt{q_0^2 + |\vec{\mathbf{Q}}|^2}. \tag{2.23}$$

The norm can also be defined in terms of quaternion conjugate

$$\mathbf{Q}\mathbf{Q}^* = \mathbf{Q}^*\mathbf{Q} = |\mathbf{Q}|^2. \tag{2.24}$$

2.1.8 Inverse

The inverse of a non zero quaternion $\mathbf{Q}$ is defined in terms of its conjugate and norm according to

$$\mathbf{Q}^{-1} = \frac{\mathbf{Q}^*}{|\mathbf{Q}|^2}. \tag{2.25}$$

Using this definition, the division between quaternions can also be defined. The right division of $\mathbf{Q}$ by $\mathbf{P}$ is defined as $\mathbf{Q}\mathbf{P}^{-1}$ and the left division of $\mathbf{Q}$ by $\mathbf{P}$ is defined as $\mathbf{P}^{-1}\mathbf{Q}$. In general, $\mathbf{Q}\mathbf{P}^{-1} \neq \mathbf{P}^{-1}\mathbf{Q}$, unless $\mathbf{Q}$ and $\mathbf{P}$ commute. The inverse applied to a product of quaternions follows the property

$$(\mathbf{Q}\mathbf{P})^{-1} = \mathbf{P}^{-1}\mathbf{Q}^{-1}. \tag{2.26}$$

2.1.9 Polar Form

The polar form (or trigonometric representation) of a quaternion $\mathbf{Q}$ similarly to complex numbers is defined in terms of its norm and an angle θ. The polar form is defined as

$$\mathbf{Q} = |\mathbf{Q}|e^{\mathbf{d}\theta} = |\mathbf{Q}|(\cos(\theta) + \mathbf{d}\sin(\theta)), \tag{2.27}$$

where $\mathbf{d}$ is given by

$$\mathbf{d} = \frac{\vec{\mathbf{Q}}}{|\vec{\mathbf{Q}}|} \tag{2.28}$$

and θ is the angle between $\mathbf{Q}$ and the real axis. The quaternion $|\mathbf{Q}|\mathbf{d}\sin(\theta)$ is equivalent to the projection of $\mathbf{Q}$ to $\mathbb{R}^3$.

2.1.10 Rotation Quaternion

Considering a purely vectorial quaternion $\mathbf{q}$, the clockwise rotation in the $\mathbb{H}$ domain of this vector around an axis $\mathbf{p}$ by an angle θ is calculated as

$$\mathbf{q}_{rot} = \mathbf{R}\mathbf{q}\mathbf{R}^*, \tag{2.29}$$

where $\mathbf{R}$ is a unity quaternion defined as

$$\mathbf{R} = \cos\left(\frac{\theta}{2}\right) + \mathbf{p}\sin\left(\frac{\theta}{2}\right) = e^{\mathbf{p}\frac{\theta}{2}}. \tag{2.30}$$

The axis $\mathbf{p}$ is a unity purely vectorial quaternion.

It is noteworthy that if $\mathbf{q}$ is rotated along an perpendicular axis, the rotation can be rewritten as

$$\mathbf{q}_{rot} = e^{\mathbf{p}\theta}\mathbf{q} = \mathbf{q}e^{-\mathbf{p}\theta}. \tag{2.31}$$

This is a consequence of the inner product between two perpendicular vectors being null and the cross product being anticommutative.

2.1.11 $\mathbb{H}$ calculus

In this dissertation, $\mathbb{H}$ calculus is applied in relation to a scalar. This implies that quaternion derivatives and integrals will be discussed only with respect to a real number. In the quaternion domain, these operands are also linear. Considering $\mathbf{Q}(t) = q_0(t) + q_1(t)\mathbf{a} + q_2(t)\mathbf{b} + q_3(t)\mathbf{c}$, then

$$\frac{d\mathbf{Q}(t)}{dt} = \frac{dq_0(t)}{dt} + \frac{dq_1(t)}{dt}\mathbf{a} + \frac{dq_2(t)}{dt}\mathbf{b} + \frac{dq_3(t)}{dt}\mathbf{c}, \tag{2.32}$$

$$\int \mathbf{Q}(t)\,dt = \int q_0(t)\,dt + \left(\int q_1(t)\,dt\right)\mathbf{a} + \left(\int q_2(t)\,dt\right)\mathbf{b} + \left(\int q_3(t)\,dt\right)\mathbf{c}. \tag{2.33}$$

Derivatives of quaternions rotating in circular motions are mapped into products between them, their rotation axis and their angular momentum. Assuming a quaternion is represented in its polar form as $\mathbf{Q}(t) = |\mathbf{Q}(t)|e^{\mathbf{n}\theta(t)}$, then

$$\frac{d\mathbf{Q}(t)}{dt} = \frac{d\theta(t)}{dt}\mathbf{n}\mathbf{Q}(t). \tag{2.34}$$

In particular, if the angle is a proportional to time, $i.e.$, $\theta(t) = \omega t$, then its derivative is

$$\frac{d\mathbf{Q}(t)}{dt} = \omega \mathbf{n}\mathbf{Q}(t) \tag{2.35}$$

and its integral is

$$\int \mathbf{Q}(t)\, dt = -\frac{1}{\omega}\mathbf{n}\mathbf{Q}(t). \tag{2.36}$$

If the quaternion describes a uniform circular motion around an perpendicular axis, it can be written according to eq. (2.31) as

$$\mathbf{Q}(t) = e^{\mathbf{n}\omega t}\mathbf{Q}_0, \tag{2.37}$$

where $\mathbf{Q}_0 = \mathbf{Q}(0)$. In this case, it can be shown that

$$\frac{d\mathbf{Q}(t)}{dt} = \omega \mathbf{n}\mathbf{Q}(t), \tag{2.38}$$

$$\int \mathbf{Q}(t)\, dt = -\frac{1}{\omega}\mathbf{n}\mathbf{Q}(t). \tag{2.39}$$

In other words, the derivatives and integrals map quaternions to products, analogously as phasors.

2.1.12 Exponential

Considering the quaternion $\mathbf{Q}$ as defined by eq. (2.2), the quaternion natural exponential function is defined as

$$e^{\mathbf{Q}} = e^{q_0}\left(\cos|\vec{\mathbf{Q}}| + \mathbf{n}\sin|\vec{\mathbf{Q}}|\right), \tag{2.40}$$

where $\mathbf{n}$ is given by

$$\mathbf{n} = \frac{\vec{\mathbf{Q}}}{|\vec{\mathbf{Q}}|}. \tag{2.41}$$

The product of two exponential of commuting quaternions follows the property

$$e^{\mathbf{Q}}e^{\mathbf{P}} = e^{\mathbf{Q}+\mathbf{P}}. \tag{2.42}$$

2.1.13 Isomorphic subsets of $\mathbb{H}$

Through the development of the quaternionic three-phase power theory in this study, quaternions written in a particular form are found. More specifically, a subset of quaternions isomorphic to $\mathbb{C}$ is especially useful.

For defining this subset, consider the equation $\mathbf{Q}^2 + 1 = 0$. In the $\mathbb{H}$ domain, it has infinite solutions. To solve this equation, the square is expanded, obtaining four equations

$$q_0^2 - q_1^2 - q_2^2 - q_3^2 = -1, \tag{2.43}$$

$$2q_0q_1 = 0, \tag{2.44}$$

$$2q_0q_2 = 0, \tag{2.45}$$

$$2q_0q_3 = 0. \tag{2.46}$$

From eqs. (2.44) to (2.46), $q_1 = q_2 = q_3 = 0$ or $q_0 = 0$. If we substitute the first case in eq. (2.43), we obtain $q_0^2 = -1$, which has no solution since q_0 is a real number. Then, we conclude that $q_0 = 0$. Using this in eq. (2.43)

$$q_1^2 + q_2^2 + q_3^2 = 1. \tag{2.47}$$

Since there is no other restriction, this implies that every unity purely vectorial quaternion is a solution to the equation.

The complex numbers $\mathbb{C}$ are isomorphic to the subsets of $\mathbb{H}$ in the form $S = \{\mathbf{q} \in \mathbb{H} | \ \mathbf{q} = w + \mathbf{n}x,\ w \text{ and } x \in \mathbb{R},\ \mathbf{n} \in \mathbb{H},\ \mathbf{n}^2 = -1\}$. Additionally, the quaternion in these subsets commute. In fact, considering the quaternions $\mathbf{p} = w + \mathbf{n}x$ and $\mathbf{q} = y + \mathbf{n}z$ with the same unity purely vectorial quaternion $\mathbf{n}$. Notice that

$$\mathbf{pq} = \mathbf{qp} = (wy - xz) + \mathbf{n}(wz + xy). \tag{2.48}$$

2.2 FINAL CONSIDERATIONS

In this chapter, the quaternion algebra $\mathbb{H}$, its properties, and its calculus operators were presented. The theoretical background presented in this chapter, particularly the quaternion description of rotation, will help analyze balanced and unbalanced three-phase loads in the next chapter.

3 QUATERNION CHARACTERIZATION OF THREE-PHASE LOADS

In this chapter voltage and current quaternions are presented. Initially, considering a balanced source, these definitions are used to obtain an expression for power, impedance, and admittance quaternions. The balanced case is investigated for resistive, inductive, and capacitor three-phase loads, as well as their combinations. After that, expressions are obtained for the admittance quaternion of delta and wye loads for the unbalanced case. The admittance quaternions of unbalanced solidly grounded and grounded wye loads are obtained. Lastly, the power quaternions of balanced loads, unbalanced delta load, and solidly grounded load are analyzed

3.1 QUATERNION QUANTITIES IN THREE-PHASE SYSTEMS

In three-phase systems, balanced phase voltages can be written in the time-domain as

$$v_a(t) = \sqrt{2}V_o \cos(\omega t), \tag{3.1}$$

$$v_b(t) = \sqrt{2}V_o \cos(\omega t - 120^\circ), \tag{3.2}$$

$$v_c(t) = \sqrt{2}V_o \cos(\omega t + 120^\circ), \tag{3.3}$$

where $v_a(t)$, $v_b(t)$ and $v_c(t)$ are phase to ground voltages, V_o is the RMS voltage in V, t is the time in s, and ω is the electrical frequency in deg/s.

Using eqs. (3.1) to (3.3), the voltage quaternion (Q-voltage) can be defined according to [30] by

$$\mathbf{V}(t) = v_a(t)\mathbf{a} + v_b(t)\mathbf{b} + v_c(t)\mathbf{c}. \tag{3.4}$$

Analogously, the three-phase current quaternion (Q-current) is defined by

$$\mathbf{I}(t) = i_a(t)\mathbf{a} + i_b(t)\mathbf{b} + i_c(t)\mathbf{c}, \tag{3.5}$$

in which $i_a(t)$, $i_b(t)$ and $i_c(t)$ are line currents flowing through phases A, B and C, respectively.

In [18], it is shown that, in steady-state, the Q-voltage and Q-current describe elliptical movements. Particularly, a circular motion is traced in the balanced case. The balanced Q-voltage defined by eq. (3.4), for example, can be written in terms of quaternion rotations using eq. (2.31) as

$$\mathbf{V}(t) = \sqrt{3}V_o e^{\mathbf{n}\omega t}\mathbf{q}_p, \tag{3.6}$$

where $\mathbf{q}_p$ is an unity quaternion in the same direction of $\mathbf{V}(0)$ and is given by

$$\mathbf{q}_p = \frac{\mathbf{V}(0)}{|\mathbf{V}(0)|} = \frac{2\mathbf{a} - \mathbf{b} - \mathbf{c}}{\sqrt{6}}, \tag{3.7}$$

and $\mathbf{n}$ is an unity quaternion perpendicular to Q-voltage's plane and given by

$$\mathbf{n} = \frac{\mathbf{a} + \mathbf{b} + \mathbf{c}}{\sqrt{3}}. \tag{3.8}$$

Figs. 3.1 and 3.2 show, respectively, the components and the locus of the Q-voltage for $V_o = 220$ V and $\omega = 2\pi 60$ rad/s.

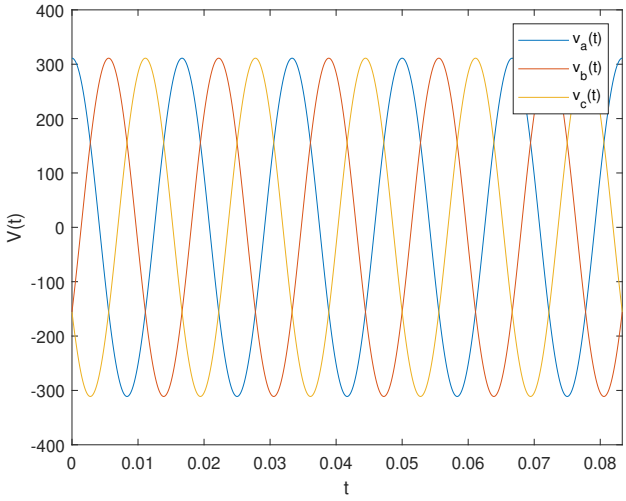

Figure 3.1: Balanced three-phase voltages.

There are some different definitions of the power quaternion (Q-power) in the literature. In [33] and subsequent works [34, 35, 40, 41], the Q-power was defined by the product of Q-voltage and Q-current. However, [18] showed that it is more appropriated to define the Q-power as

$$\mathbf{S}(t) = \mathbf{V}(t)\mathbf{I}^*(t). \tag{3.9}$$

The definition in eq. (3.9) will also be used in this work since the direction of the Q-power has a physical meaning using this definition. With this expression, the scalar part's sign and vectorial part direction of

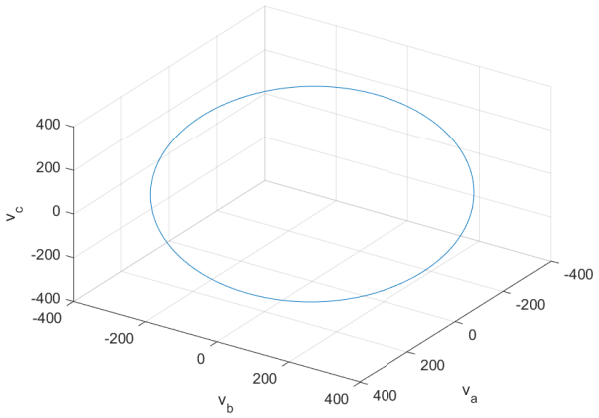

Figure 3.2: Balanced three-phase Q-voltage.

Q-power indicates active and reactive power consumption, respectively [18]. Other possible definitions, e.g. $\mathbf{I}(t)\mathbf{V}(t)$ fails to preserve this property.

In [18] it is also shown that the Q-power can be written as

$$\mathbf{S}(t) = p_{abc}(t) - \vec{\mathbf{Q}}(t), \tag{3.10}$$

where $p_{abc}(t)$ is the instantaneous three-phase active power and $\vec{\mathbf{Q}}(t)$ is

$$\vec{\mathbf{Q}}(t) = q_a(t)\mathbf{a} + q_b(t)\mathbf{b} + q_c(t)\mathbf{c}, \tag{3.11}$$

$$q_a(t) = v_b(t)i_c(t) - v_c(t)i_b(t), \tag{3.12}$$

$$q_b(t) = v_c(t)i_a(t) - v_a(t)i_c(t), \tag{3.13}$$

$$q_c(t) = v_a(t)i_b(t) - v_b(t)i_a(t). \tag{3.14}$$

The instantaneous reactive Q-power $\vec{\mathbf{Q}}(t)$ is equivalent to instantaneous reactive power representation via vectors [12, 18].

The three-phase impedance quaternion (Q-impedance) [30] is defined as

$$\mathbf{Z} = \mathbf{V}\mathbf{I}^{-1}. \tag{3.15}$$

It is defined as Q-voltage right divided by Q-current instead of other combinations for consistency with the geometrical interpretation of Q-power. Using eq. (3.15), Q-power eq. (3.9) can be rewritten in terms of Q-impedance as shown in [18].

$$\mathbf{S} = \mathbf{Z}|\mathbf{I}|^2, \tag{3.16}$$

$$\mathbf{S} = (\mathbf{Z}^{-1})^* |\mathbf{V}|^2. \tag{3.17}$$

Another concept that comes naturally considering the definition of the Q-impedance is the three-phase admittance quaternion (Q-admittance). It was defined by [30] as

$$\mathbf{Y} = \mathbf{Z}^{-1} = \mathbf{I}\mathbf{V}^{-1}. \tag{3.18}$$

Naturally, Q-power can also be written in terms of Q-admittance using eq. (3.18) in eq. (3.9).

$$\mathbf{S} = \mathbf{Y}^{-1} |\mathbf{I}|^2, \tag{3.19}$$

$$\mathbf{S} = \mathbf{Y}^* |\mathbf{V}|^2. \tag{3.20}$$

A parallel association rule can be obtained from the definition of Q-admittance eq. (3.18). If two three-phase loads are connected to the line, they share the same Q-voltage $\mathbf{V}$ and the Q-current supplied to them $\mathbf{I}$ is the sum of the current of each load, so

$$\mathbf{Y}_1 + \mathbf{Y}_2 = \mathbf{I}_1\mathbf{V}^{-1} + \mathbf{I}_2\mathbf{V}^{-1} = \mathbf{I}\mathbf{V}^{-1} = \mathbf{Y}_{eq}, \tag{3.21}$$

where $\mathbf{Y}_1$ and $\mathbf{Y}_2$ are the Q-admittances of both loads, $\mathbf{I}_1$ and $\mathbf{I}_2$ are their Q-currents, $\mathbf{Y}_{eq}$ is the Q-admittance of their parallel association.

In the rest of this chapter, different combinations of loads and their response to Q-voltage will be analyzed in detail.

3.2 THREE-PHASE BALANCED LOADS

Having defined the quaternionic electrical quantities in three-phase systems, the next natural step is to study simple loads in this framework. Nevertheless, the formulation of Q-admittance of basic loads is missing from the literature. In [18], the Q-impedance of a three-phase RLC balanced load in the wye configuration was presented. However, the authors presented the formulation exclusively for the steady-state, despite doing a time-domain analysis. In this sense, a novel formulation of balanced loads is presented in this section, considering the transient and steady states. The expression of Q-admittance is obtained instead of Q-impedance since its relation to Q-power is more straightforward. The choice of Q-admittance is also justified by the transient and steady-state components being independent, as will be discussed later in this chapter.

For analyzing three-phase balanced loads, first, the formulation of a generic load in the steady-state will be presented. Next, a systematic analysis of different configurations is made, considering the transient state of each kind of load. The Q-voltage is considered the input of each circuit and is given by eq. (3.4). The Q-current is then obtained using circuit analysis and utilizing it, the Q-admittance is calculated.

Starting this analysis, consider a balanced three-phase load with admittances connected in each phase equal to $Ye^{-j\theta}$. This load is shown in Fig. 3.3.

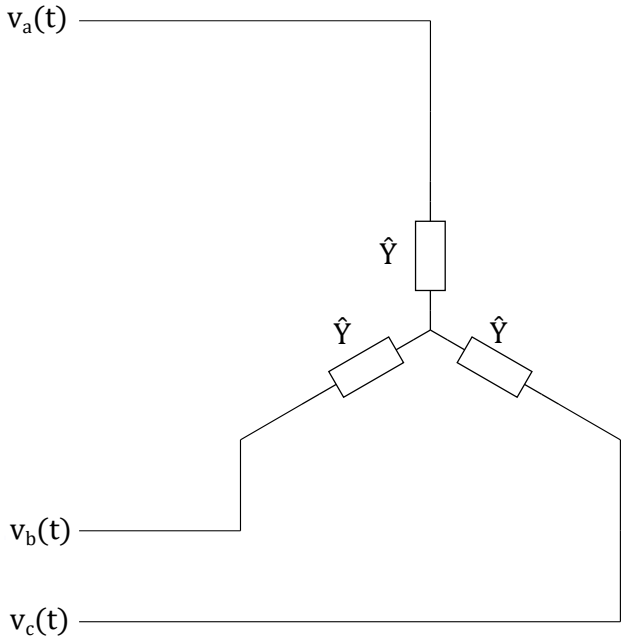

Figure 3.3: Balanced three-phase load.

Assuming a balanced source with Q-voltage described by eq. (3.4), steady-state Q-current is given by

$$\mathbf{I}(t) = \sqrt{2}V_o Y(\cos(\omega t - \theta)\mathbf{a} + \cos(\omega t - 120^\circ - \theta)\mathbf{b} + \cos(\omega t + 120^\circ - \theta)\mathbf{c}) \tag{3.22}$$

It is noteworthy that, if the Q-voltage is dislocated by an angle α, eq. (3.6) can be written as

$$\mathbf{V}\left(t + \frac{\alpha}{\omega}\right) = \sqrt{3}V_o e^{\mathbf{n}(\omega t + \alpha)}\mathbf{q}_p. \tag{3.23}$$

As a consequence, the Q-current can also be written in terms of quaternion rotations using eq. (3.23)

$$\boxed{\mathbf{I}(t) = \sqrt{3}V_o Y e^{\mathbf{n}(\omega t - \theta)}\mathbf{q}_p.} \tag{3.24}$$

Since Q-voltage is given by $\sqrt{3}V_o e^{\mathbf{n}\omega t}\mathbf{q}_p$, it is observed that, in the steady-state, the Q-current rotates in circular motion with a θ rad delay in relation to voltage. Also, the radius of the circumference is multiplied

by Y. The Q-current considering a RLC balanced load with $R = 100\,\Omega$, $C = 100\,\mu$F and $L = 1$ H is presented in Fig. 3.4.

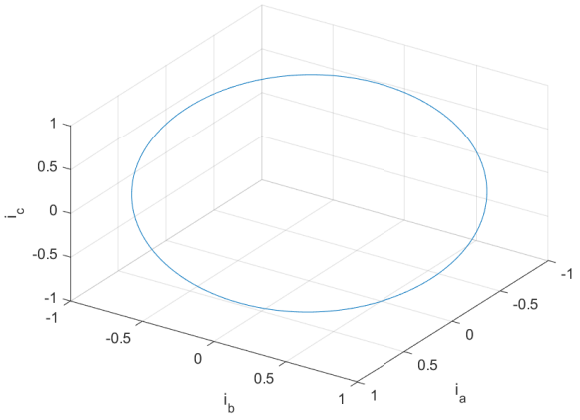

Figure 3.4: Steady-state Q-current in the balanced load.

The steady-state Q-admittance can be calculated as well. First, computing $\mathbf{V}^{-1}(t)$

$$\mathbf{V}^{-1}(t) = \frac{1}{\sqrt{3}V_o}\mathbf{q}_p^{-1}e^{-\mathbf{n}\omega t}. \tag{3.25}$$

Then, using eqs. (3.24) and (3.25) in eq. (3.18)

$$\boxed{\mathbf{Y} = \mathbf{I}\mathbf{V}^{-1} = Ye^{-\mathbf{n}\theta}.} \tag{3.26}$$

It is noteworthy that the expression obtained is equivalent to the expression of the single-phase admittance, substituting the j for $\mathbf{n}$. For the balanced case in the steady-state, the quaternion representation is similar to the single-phase equivalent circuit using phasors. Since quaternions are more computationally expensive, it would make an argument for sticking with the phasor representation. Nevertheless, as a time-domain representation, quaternions allow the inclusion of transients in a unique formulation. This fact is explored in the next subsections, where different combinations of loads are analyzed.

3.2.1 R load

For the first case, a pure resistive three-phase load is considered. This load is shown in Fig. 3.5.

The voltage in each phase is simply

$$v_a(t) = Ri_a(t), \tag{3.27}$$

$$v_b(t) = Ri_b(t), \tag{3.28}$$

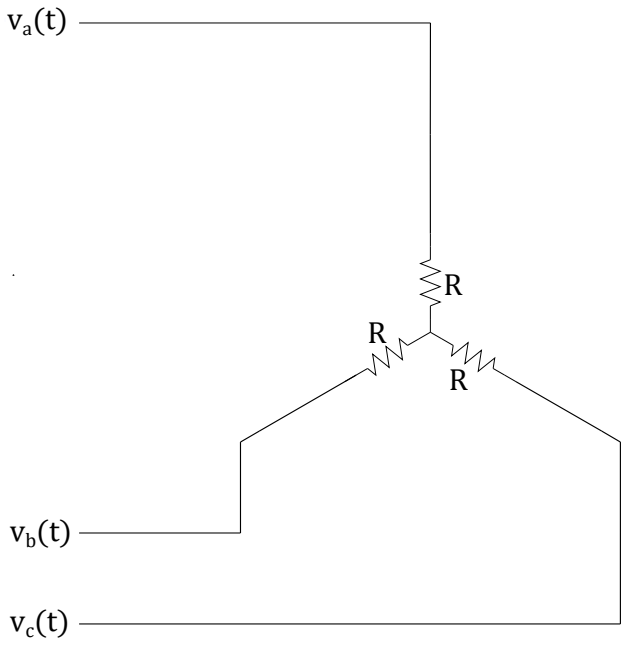

Figure 3.5: Resistive three-phase load.

$$v_c(t) = Ri_c(t), \tag{3.29}$$

which can be written as the Q-voltage

$$\boxed{\mathbf{V}(t) = R\mathbf{I}_T(t).} \tag{3.30}$$

From eq. (3.30) it is observed that the resistive balanced load can be described by the steady-state model of eqs. (3.24) and (3.26), with $Y = 1/R$ and $\theta = 0$.

3.2.2 L load

Next, a pure inductive three-phase load is considered. This load is shown in Fig. 3.6.

The voltage in each phase is given by

$$v_a(t) = L\frac{di_a(t)}{dt}, \tag{3.31}$$

$$v_b(t) = L\frac{di_b(t)}{dt}, \tag{3.32}$$

$$v_c(t) = L\frac{di_c(t)}{dt}, \tag{3.33}$$

which can be written as the Q-voltage

$$\mathbf{V}(t) = L\frac{d\mathbf{I}_T(t)}{dt}. \tag{3.34}$$

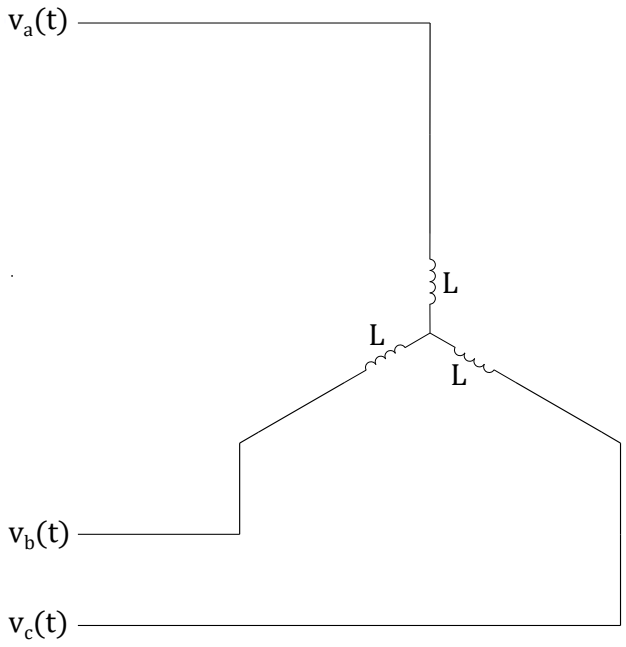

Figure 3.6: Inductive three-phase load.

Solving for $\mathbf{I}_T(t)$

$$\mathbf{I}_T(t) = \frac{1}{L}\int_0^t \mathbf{V}(\tau)d\tau + \mathbf{I}_T(0). \tag{3.35}$$

Since **V**(t) is given by eq. (3.6)

$$\mathbf{I}_T(t) = -\mathbf{n}\frac{\sqrt{3}V_o}{\omega L}e^{\mathbf{n}\omega t}\mathbf{q}_p + \mathbf{n}\frac{\sqrt{3}V_o}{\omega L}\mathbf{q}_p + \mathbf{I}_T(0), \tag{3.36}$$

The Q-current can be simplified to

$$\mathbf{I}_T(t) = \frac{\sqrt{3}V_o}{\omega L}e^{\mathbf{n}(\omega t-\frac{\pi}{2})}\mathbf{q}_p - \frac{\sqrt{3}V_o}{\omega L}e^{-\mathbf{n}(\frac{\pi}{2})}\mathbf{q}_p + \mathbf{I}_T(0). \tag{3.37}$$

Defining

$$\mathbf{k} = \mathbf{I}_T(0) - \frac{\sqrt{3}V_o}{\omega L}e^{-\mathbf{n}(\frac{\pi}{2})}\mathbf{q}_p, \tag{3.38}$$

the Q-current eq. (3.37) can be written as

$$\boxed{\mathbf{I}_T(t) = \frac{\sqrt{3}V_o}{\omega L}e^{\mathbf{n}(\omega t-\frac{\pi}{2})}\mathbf{q}_p + \mathbf{k}.} \tag{3.39}$$

The Q-admittance of this load can be calculated as well using eqs. (3.25) and (3.39) in eq. (3.18)

$$\boxed{\mathbf{Y}_T = \frac{1}{\omega L}e^{-\mathbf{n}\frac{\pi}{2}} + \frac{1}{\sqrt{3}V_o}\mathbf{k}\mathbf{q}_p^{-1}e^{-\mathbf{n}\omega t}.} \tag{3.40}$$

It is observed that the initial value of the Q-current is relevant in the behavior of a purely inductive load, adding a constant term in the steady model of eqs. (3.24) and (3.26). Nevertheless, if $\mathbf{k} = 0$, eqs. (3.39) and (3.40) are equivalent to eqs. (3.24) and (3.26). In this case, from eqs. (3.39) and (3.40) it is observed that the inductive balanced load can be described by the steady-state model of eqs. (3.24) and (3.26), with $Y = 1/\omega L$ and $\theta = \pi/2$.

3.2.3 C load

In this case, a pure capacitive three-phase balanced load is considered. This load is shown in Fig. 3.7.

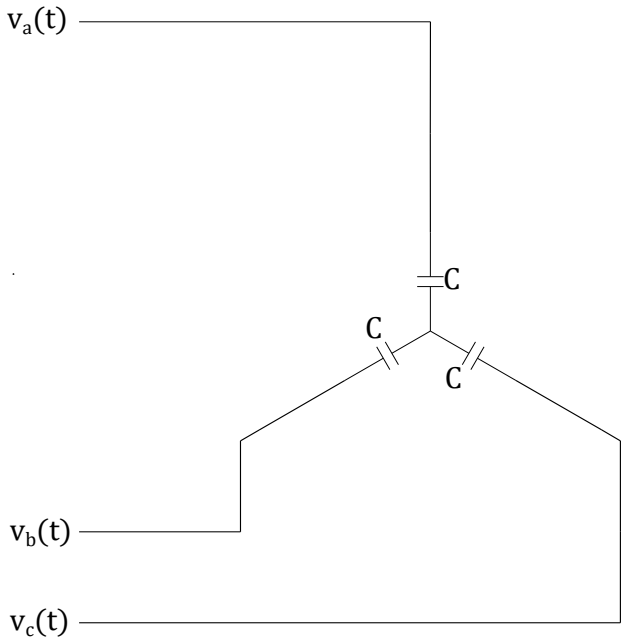

Figure 3.7: Capacitive three-phase load.

The voltages in each phase are given by

$$v_a(t) = \frac{1}{C}\int_{-\infty}^{t} i_a(\tau)\, d\tau, \tag{3.41}$$

$$v_b(t) = \frac{1}{C}\int_{-\infty}^{t} i_b(\tau)\, d\tau, \tag{3.42}$$

$$v_c(t) = \frac{1}{C}\int_{-\infty}^{t} i_c(\tau)\, d\tau, \tag{3.43}$$

which can be written with quaternions as

$$\mathbf{V}(t) = \frac{1}{C}\int_{-\infty}^{t} \mathbf{I}_T(\tau)\, d\tau. \tag{3.44}$$

Solving for $\mathbf{I}_T(t)$

$$C\frac{d\mathbf{V}(t)}{dt} = \mathbf{I}_T(t). \tag{3.45}$$

Since **V**(t) is given by eq. (3.6)

$$\mathbf{I}_T(t) = \mathbf{n}\omega C\sqrt{3}V_o e^{\mathbf{n}\omega t}\mathbf{q}_p, \tag{3.46}$$

which can be written as

$$\boxed{\mathbf{I}_T(t) = \sqrt{3}V_o\omega C e^{\mathbf{n}(\omega t+\frac{\pi}{2})}\mathbf{q}_p,} \tag{3.47}$$

From eq. (3.47) it is observed that the capacitive balanced load can be described by the steady-state model of eqs. (3.24) and (3.26), with $Y = \omega C$ and $\theta = -\pi/2$.

3.2.4 RL load

In this case, an RL wye load, as presented in Fig. 3.8 is analyzed. The phase loads are series connected resistors and inductors.

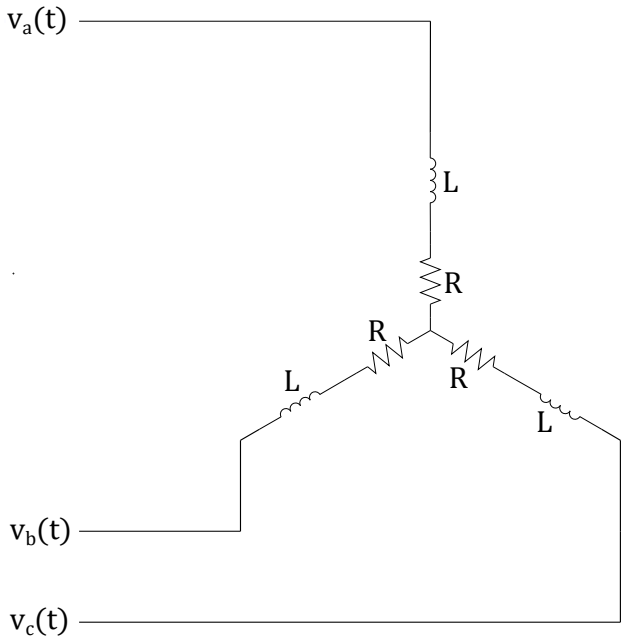

Figure 3.8: RL three-phase load.

The voltage in each phase could be described by a set of differential equations

$$v_a(t) = Ri_a(t) + L\frac{di_a(t)}{dt}, \tag{3.48}$$

$$v_b(t) = Ri_b(t) + L\frac{di_b(t)}{dt}, \tag{3.49}$$

$$v_c(t) = Ri_c(t) + L\frac{di_c(t)}{dt}. \tag{3.50}$$

Rewriting eqs. (3.48) to (3.50) in the quaternion form

$$\mathbf{V}(t) = R\mathbf{I}_T(t) + L\frac{d\mathbf{I}_T(t)}{dt}. \tag{3.51}$$

Solving the differential equation eq. (3.51) is equivalent to solving eqs. (3.48) to (3.50) separately. The solution is given by the combination of homogeneous and particular solutions, which means

$$\mathbf{I}_T(t) = \mathbf{I}_h(t) + \mathbf{I}_p(t). \tag{3.52}$$

The particular solution represents the steady-state of the Q-current. It is given by eq. (3.24) where

$$Y = \frac{1}{\sqrt{R^2 + (\omega L)^2}}, \tag{3.53}$$

$$\theta = \tan^{-1}\left(\frac{\omega L}{R}\right). \tag{3.54}$$

The homogeneous solution represents the transient state and is given by

$$\mathbf{I}_h(t) = k_a e^{-\frac{R}{L}t}\mathbf{a} + k_b e^{-\frac{R}{L}t}\mathbf{b} + k_c e^{-\frac{R}{L}t}\mathbf{c} = e^{-\frac{R}{L}t}\mathbf{k}, \tag{3.55}$$

where

$$\mathbf{k} = k_a\mathbf{a} + k_b\mathbf{b} + k_c\mathbf{c}. \tag{3.56}$$

The constants k_a, k_b and k_c are determined by the initial value of $\mathbf{I}_T(t)$. The solution for the differential equation eq. (3.51) is then given by

$$\boxed{\mathbf{I}_T(t) = \sqrt{3}V_o Y e^{\mathbf{n}(\omega t - \theta)}\mathbf{q}_p + e^{-\frac{R}{L}t}\mathbf{k}.} \tag{3.57}$$

It is noteworthy that the second term in eq. (3.57) is a quaternion with constant direction and decreasing modulus. The Q-current in this situation is given by the composition of an escalated, delayed Q-voltage with this modulus decreasing transient Q-current.

Fig. 3.9 presents the components of the Q-current in the time domain, considering $R = 100\,\Omega$, $L = 1$ H and $\mathbf{I}_T(0) = 0$. It is observed that the currents have different amplitudes in the transient state and in the steady state, they are balanced. In Fig. 3.10 the transient state of the components of the Q-current are presented separately.

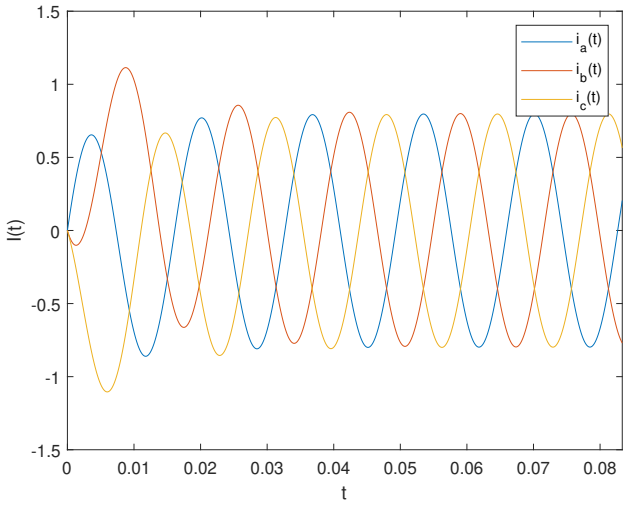

Figure 3.9: Currents of the RL three-phase load.

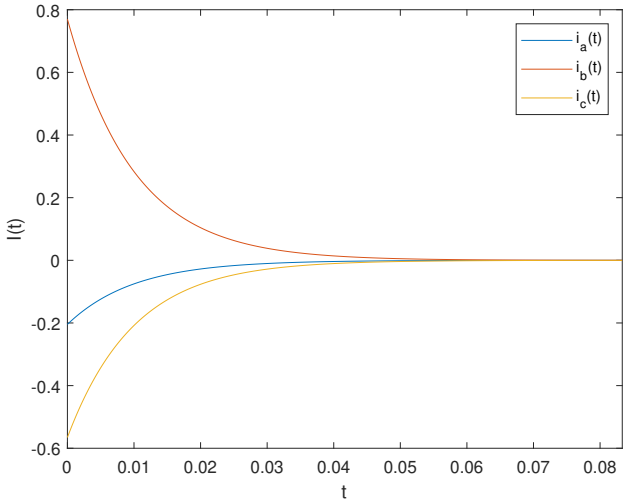

Figure 3.10: Transient state currents of the RL three-phase load.

The transient part of Q-current represents the center of its locus circumference. As observed in Fig. 3.10, the center dislocates until it stabilizes in the origin. The resultant motion is a spiral-like movement that approaches a perfect circular motion as time increases. Fig. 3.11 presents the Q-current locus. The Q-current starts at the initial value and then circles around in a spiral shape until it reaches the steady-state.

It is noteworthy that, in this case, the Q-current is in a single plan in the $\mathbb{H}$ domain. As such, it can be represented as presented in Fig. 3.12. In Fig. 3.12, $\mathbf{q}_r$ is a unity quaternion perpendicular to $\mathbf{q}_p$ and $\mathbf{n}$ and given by

$$\mathbf{q}_r = e^{-\mathbf{n}(\frac{\pi}{2})}\mathbf{q}_p. \tag{3.58}$$

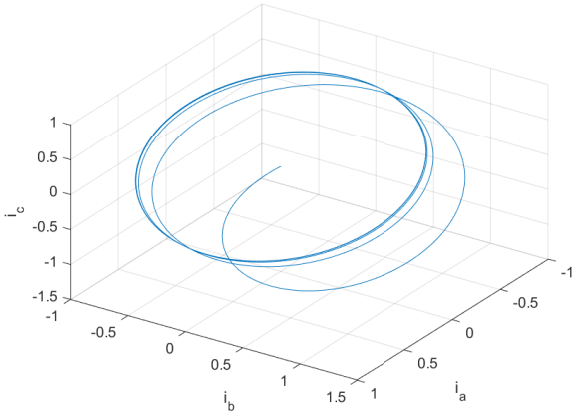

Figure 3.11: Currents of the RL three-phase load in **abc** space.

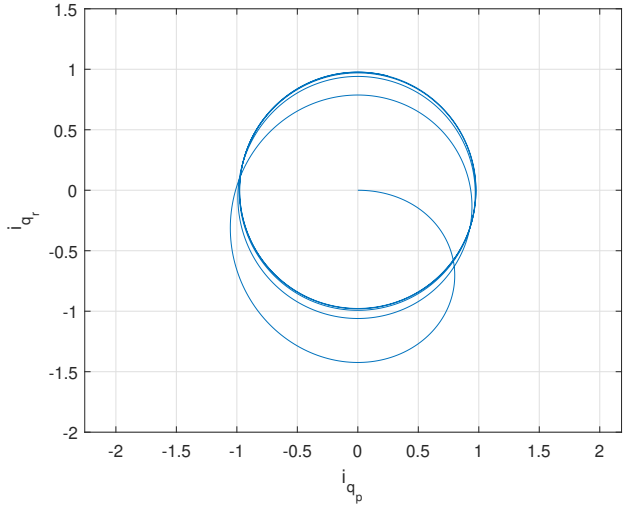

Figure 3.12: Currents of the RL three-phase load.

The instantaneous Q-admittance can be defined as

$$\mathbf{Y}_T = \mathbf{I}_T\mathbf{V}^{-1} = \mathbf{I}_h(t)\mathbf{V}^{-1} + \mathbf{I}_p(t)\mathbf{V}^{-1}. \tag{3.59}$$

Using eq. (3.25), eq. (3.59) can be computed as

$$\boxed{\mathbf{Y}_T(t) = Ye^{-\mathbf{n}\theta} + \frac{e^{-\frac{R}{L}t}}{\sqrt{3}V_o}\mathbf{k}\mathbf{q}_p^{-1}e^{-\mathbf{n}\omega t},} \tag{3.60}$$

where $Ye^{-\mathbf{n}\theta}$ is the steady-state part and $(e^{-\frac{R}{L}t}/\sqrt{3}V_o)\mathbf{k}\mathbf{q}_p^{-1}e^{-\mathbf{n}\omega t}$ is the transient part of the Q-admittance.

3.2.5 RC load

In this case, it is considered that the three-phase wye load is formed by resistors and capacitors connected in series, as shown in Fig. 3.13.

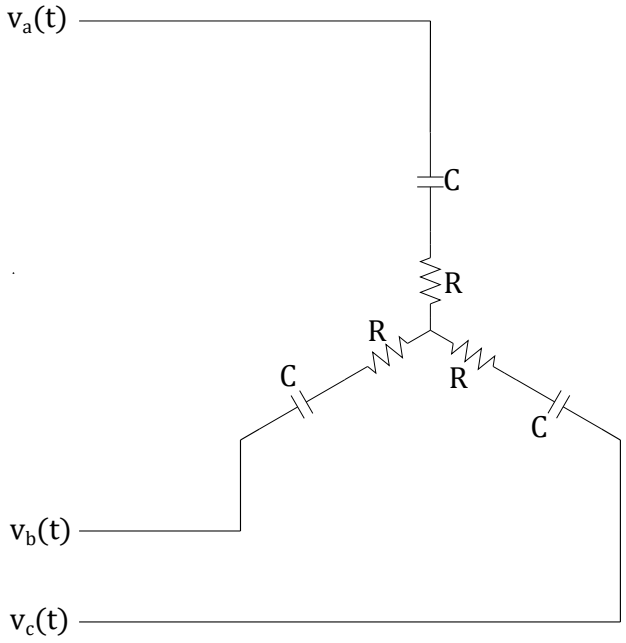

Figure 3.13: RC three-phase load.

The voltage in each phase is described by the differential equations

$$v_a(t) = Ri_a(t) + \frac{1}{C}\int_{-\infty}^{t} i_a(\tau)\, d\tau, \tag{3.61}$$

$$v_b(t) = Ri_b(t) + \frac{1}{C}\int_{-\infty}^{t} i_b(\tau)\, d\tau, \tag{3.62}$$

$$v_c(t) = Ri_c(t) + \frac{1}{C}\int_{-\infty}^{t} i_c(\tau)\, d\tau, \tag{3.63}$$

which can be written with quaternions as

$$\mathbf{V}(t) = R\mathbf{I}_T(t) + \frac{1}{C}\int_{-\infty}^{t} \mathbf{I}_T(\tau)\, d\tau. \tag{3.64}$$

Applying the derivative in both sides

$$\frac{d\mathbf{V}(t)}{dt} = R\frac{d\mathbf{I}_T(t)}{dt} + \frac{\mathbf{I}_T(t)}{C}. \tag{3.65}$$

The solution to eq. (3.65) is the sum of homogeneous and particular solutions eq. (3.52) where the particular solution is given by eq. (3.24) where

$$Y = \frac{1}{\sqrt{R^2 + \frac{1}{(\omega C)^2}}}, \tag{3.66}$$

$$\theta = -\tan^{-1}\left(\frac{1}{\omega CR}\right). \tag{3.67}$$

On the other hand, the natural response is given by

$$\mathbf{I}_h(t) = k_a e^{-\frac{t}{RC}}\mathbf{a} + k_b e^{-\frac{t}{RC}}\mathbf{b} + k_c e^{-\frac{t}{RC}}\mathbf{c} = e^{-\frac{t}{RC}}\mathbf{k}. \tag{3.68}$$

The constants k_a, k_b and k_c are determined by the initial value of $\mathbf{I}_T(t)$. The solution for the differential equation eq. (3.65) is then given by

$$\boxed{\mathbf{I}_T(t) = \sqrt{3}V_o Y e^{\mathbf{n}(\omega t-\theta)}\mathbf{q}_p + e^{-\frac{t}{RC}}\mathbf{k}.} \tag{3.69}$$

It is noteworthy that the second term in eq. (3.69) is a quaternion with constant direction and decreasing modulus.

Fig. 3.14 presents the Q-current transients considering $R = 100\,\Omega$, $C = 100\,\mu$F and $\mathbf{I}_T(0) = 0$.

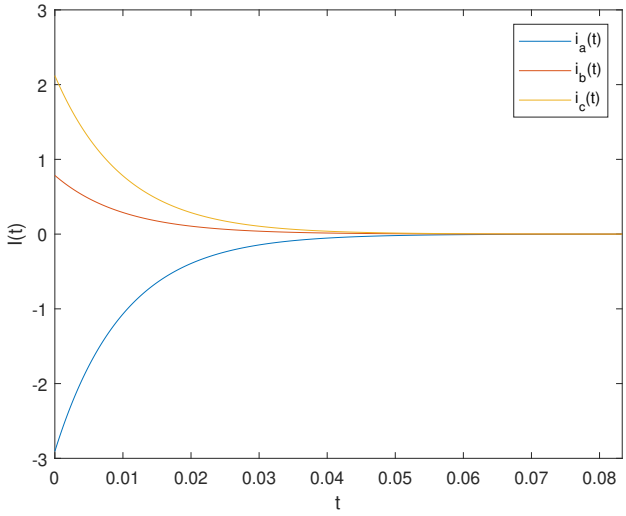

Figure 3.14: Transient state currents of the RC three-phase load.

Fig. 3.15 presents the Q-current locus. As the RL case, the Q-current resultant motion is a spiral-like movement that approaches an circular motion as time increases. The center of the circumference, represented by the transient term of Q-current, has the same behaviour observed in the RL case, the difference being that it starts at a different point in the $\mathbb{H}$ domain.

Using the definition eq. (3.59), the instantaneous admittance is calculated as

$$\boxed{\mathbf{Y}_T(t) = Y e^{-\mathbf{n}\theta} + \frac{e^{-\frac{t}{RC}}}{\sqrt{3}V_o}\mathbf{k}\mathbf{q}_p^{-1}e^{-\mathbf{n}\omega t},} \tag{3.70}$$

where $Y e^{-\mathbf{n}\theta}$ is the steady-state part and $(e^{-\frac{t}{RC}}/\sqrt{3}V_o)\mathbf{k}\mathbf{q}_p^{-1}e^{-\mathbf{n}\omega t}$ is the transient part of the Q-admittance.

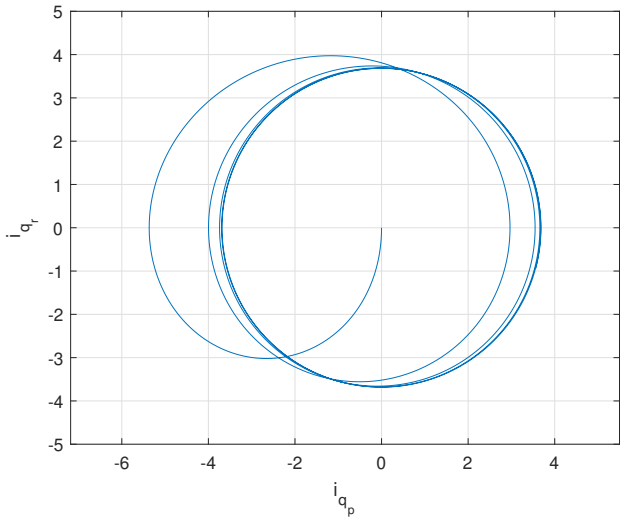

Figure 3.15: Currents of the RC three-phase load.

3.2.6 RLC load

Considering a RLC wye load, as presented in Fig. 3.16.

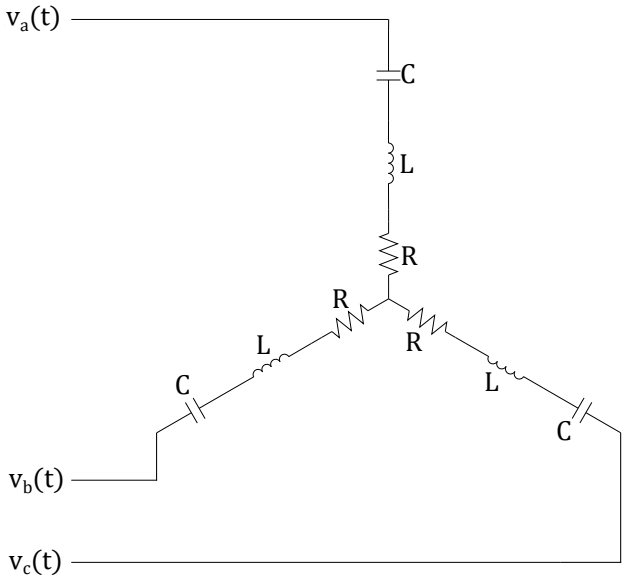

Figure 3.16: RLC three-phase load.

This load is described by the equations

$$v_a(t) = L\frac{di_a(t)}{dt} + Ri_a(t) + \frac{1}{C}\int_{-\infty}^{t} i_a(\tau)\,d\tau, \tag{3.71}$$

$$v_b(t) = L\frac{di_b(t)}{dt} + Ri_b(t) + \frac{1}{C}\int_{-\infty}^{t} i_b(\tau)\,d\tau, \tag{3.72}$$

$$v_c(t) = L\frac{di_c(t)}{dt} + Ri_c(t) + \frac{1}{C}\int_{-\infty}^{t} i_c(\tau)\,d\tau, \tag{3.73}$$

which can be written using quaternion as

$$\mathbf{V}(t) = L\frac{d\mathbf{I}_T(t)}{dt} + R\mathbf{I}_T(t) + \frac{1}{C}\int_{-\infty}^{t} \mathbf{I}_T(\tau)\, d\tau. \tag{3.74}$$

Applying the derivative on both sides and dividing by L

$$\frac{1}{L}\frac{d\mathbf{V}(t)}{dt} = \frac{d^2\mathbf{I}_T(t)}{dt^2} + \frac{R}{L}\frac{d\mathbf{I}_T(t)}{dt} + \frac{\mathbf{I}_T(t)}{LC}. \tag{3.75}$$

The solution of eq. (3.75) is in the form eq. (3.52). The particular solution in given by eq. (3.24) where

$$Y = \frac{1}{\sqrt{R^2 + (\omega L - \frac{1}{\omega C})^2}}, \tag{3.76}$$

$$\theta = \tan^{-1}\left(\frac{1}{R}\left(\omega L - \frac{1}{\omega C}\right)\right). \tag{3.77}$$

Next, the natural response of this load is obtained. Considering that $\frac{R}{L} = 2\zeta\omega_0$ and $\frac{1}{LC} = \omega_0^2$, then eq. (3.75) can be written as

$$\frac{1}{L}\frac{d\mathbf{V}(t)}{dt} = \frac{d^2\mathbf{I}_T(t)}{dt^2} + 2\zeta\omega_0\frac{d\mathbf{I}_T(t)}{dt} + \omega_0^2\mathbf{I}_T(t). \tag{3.78}$$

The natural response depends on the value of ζ. In the next subsections, it will be discussed.

3.2.6.1 $\zeta > 1$

This case is known as overdamped. The natural response is given by

$$\mathbf{I}_h(t) = (k_{a1}e^{-s_1 t} + k_{a2}e^{-s_2 t})\mathbf{a} + (k_{b1}e^{-s_1 t} + k_{b2}e^{-s_2 t})\mathbf{b} + (k_{c1}e^{-s_1 t} + k_{c2}e^{-s_2 t})\mathbf{c}, \tag{3.79}$$

$$\mathbf{I}_h(t) = e^{-s_1 t}\mathbf{k}_1 + e^{-s_2 t}\mathbf{k}_2. \tag{3.80}$$

where $s_1 = \zeta\omega_0 - \omega_0\sqrt{\zeta^2 - 1}$ and $s_2 = \zeta\omega_0 + \omega_0\sqrt{\zeta^2 - 1}$. The constants k_{a1}, k_{a2}, k_{b1}, k_{b2}, k_{c1} and k_{c2} are determined by initial values. The solution to eq. (3.78) is then given as

$$\boxed{\mathbf{I}_T(t) = \sqrt{3}V_o Y e^{\mathbf{n}(\omega t - \theta)}\mathbf{q}_p + e^{-\zeta\omega_0 t}(e^{\omega_0\sqrt{\zeta^2-1}t}\mathbf{k}_1 + e^{-\omega_0\sqrt{\zeta^2-1}t}\mathbf{k}_2).} \tag{3.81}$$

In this case, unlike the first-order systems, the transient part does not have a constant direction. Given that, the spiral motion is irregular. Nevertheless, as the steady-state is reached, it becomes a circular motion, like the first-order circuits. Fig. 3.17 presents the transient part of the Q-current considering $R = 100\,\Omega$, $L = 50$ mH, $C = 100\,\mu$F and $\mathbf{I}_T(0) = 0$.

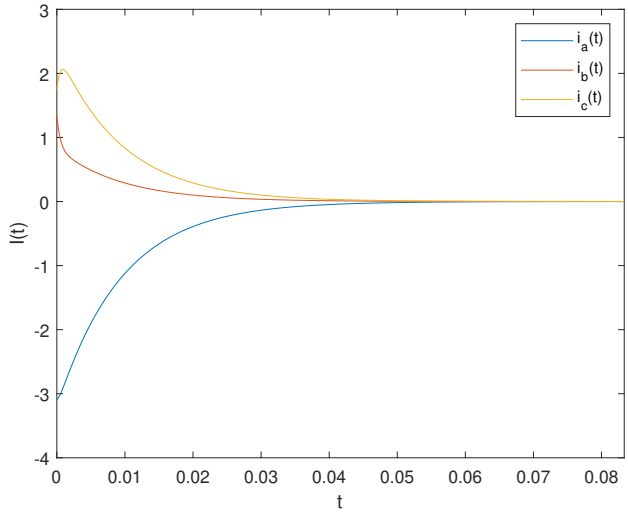

Figure 3.17: Transient state currents of the RLC three-phase load (overdamped).

In Fig. 3.18 the locus of Q-current is presented. The behaviour of Q-current has a subtle difference when compared to first order circuits, due to the transient part increasing in the beginning, as observed in Fig. 3.17.

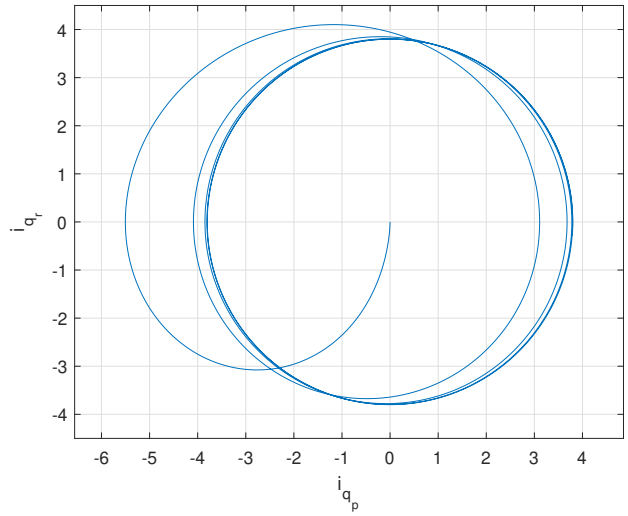

Figure 3.18: Currents of the RLC three-phase load (overdamped).

The instantaneous Q-admittance can be calculated using eq. (3.59) and is computed as

$$\boxed{\mathbf{Y}_T(t) = Ye^{-\mathbf{n}\theta} + \frac{e^{-\zeta\omega_0 t}}{\sqrt{3}V_o}(e^{\omega_0\sqrt{\zeta^2-1}t}\mathbf{k}_1 + e^{-\omega_0\sqrt{\zeta^2-1}t}\mathbf{k}_2)\mathbf{q}_p^{-1}e^{-\mathbf{n}\omega t},} \tag{3.82}$$

where $Ye^{-\mathbf{n}\theta}$ is the steady-state part and $(e^{-\zeta\omega_0 t}/\sqrt{3}V_o)(e^{\omega_0\sqrt{\zeta^2-1}t}\mathbf{k}_1 + e^{-\omega_0\sqrt{\zeta^2-1}t}\mathbf{k}_2)\mathbf{q}_p^{-1}e^{-\mathbf{n}\omega t}$ is the transient part of the Q-admittance.

3.2.6.2 $\zeta = 1$

This case is known as critically damped. The natural response is given by

$$\mathbf{I}_h(t) = (k_{a1}e^{-\zeta\omega_0 t} + k_{a2}te^{-\zeta\omega_0 t})\mathbf{a} + (k_{b1}e^{-\zeta\omega_0 t} + k_{b2}te^{-\zeta\omega_0 t})\mathbf{b} + (k_{c1}e^{-\zeta\omega_0 t} + k_{c2}te^{-\zeta\omega_0 t})\mathbf{c}, \quad (3.83)$$

$$\mathbf{I}_h(t) = e^{-\zeta\omega_0 t}(\mathbf{k}_1 + t\mathbf{k}_2). \quad (3.84)$$

The constants k_{a1}, k_{a2}, k_{b1}, k_{b2}, k_{c1} and k_{c2} are determined by initial values. The solution to eq. (3.78) is then given as

$$\boxed{\mathbf{I}_T(t) = \sqrt{3}V_o Y e^{\mathbf{n}(\omega t-\theta)}\mathbf{q}_p + e^{-\zeta\omega_0 t}(\mathbf{k}_1 + t\mathbf{k}_2).} \quad (3.85)$$

Fig. 3.19 presents the transient components of the Q-current considering $R = 200\Omega$, $L = 1$ H, $C = 100\,\mu$F and $\mathbf{I}_T(0) = 0$.

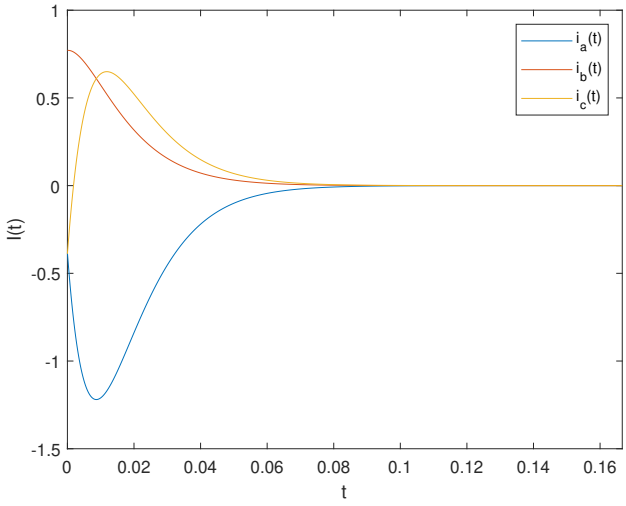

Figure 3.19: Transient state currents of the RLC three-phase load (critically damped).

In Fig. 3.20 the locus of Q-current is presented. It is observed that Q-current oscillates more than in overdamped case. This is a consequence of a more prominent increase of the Q-current transient component, as observed in Fig. 3.19. As the steady-state approaches, it also stabilizes in a circular motion.

The instantaneous Q-admittance can be calculated using eq. (3.59) and is computed as

$$\boxed{\mathbf{Y}_T(t) = Ye^{-\mathbf{n}\theta} + \frac{e^{-\zeta\omega_0 t}}{\sqrt{3}V_o}(\mathbf{k}_1 + t\mathbf{k}_2)\mathbf{q}_p^{-1}e^{-\mathbf{n}\omega t},} \quad (3.86)$$

where $Ye^{-\mathbf{n}\theta}$ is the steady-state part and $(e^{-\zeta\omega_0 t}/\sqrt{3}V_o)(\mathbf{k}_1 + t\mathbf{k}_2)\mathbf{q}_p^{-1}e^{-\mathbf{n}\omega t}$ is the transient part of the Q-admittance.

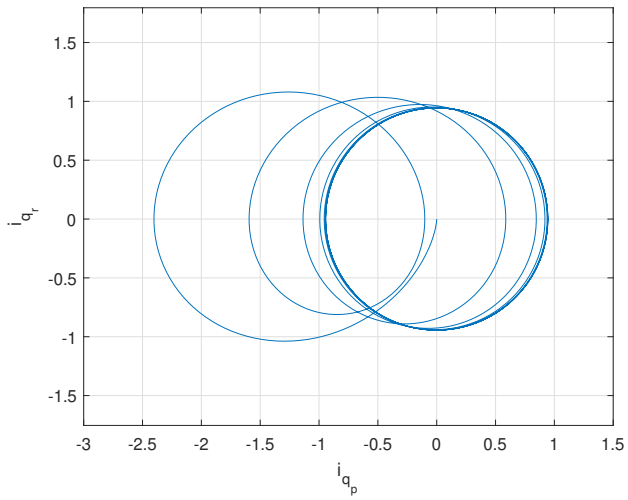

Figure 3.20: Currents of the RLC three-phase load (critically damped).

3.2.6.3 $0 < \zeta < 1$

This case is known as underdamped. The natural response is given by

$$\mathbf{I}_h(t) = e^{-\zeta\omega_0 t}[(k_{a1}\cos(\omega_0\sqrt{1-\zeta^2}t) + k_{a2}\sin(\omega_0\sqrt{1-\zeta^2}t))\mathbf{a} + (k_{b1}\cos(\omega_0\sqrt{1-\zeta^2}t)+ k_{b2}\sin(\omega_0\sqrt{1-\zeta^2}t))\mathbf{b} + (k_{c1}\cos(\omega_0\sqrt{1-\zeta^2}t) + k_{c2}\sin(\omega_0\sqrt{1-\zeta^2}t))\mathbf{c}], \quad (3.87)$$

$$\mathbf{I}_h(t) = e^{-\zeta\omega_0 t}[\cos(\omega_0\sqrt{1-\zeta^2}t)\mathbf{k}_1 + \sin(\omega_0\sqrt{1-\zeta^2}t)\mathbf{k}_2]. \quad (3.88)$$

The constants k_{a1}, k_{a2}, k_{b1}, k_{b2}, k_{c1} and k_{c2} are determined by initial values. The solution to eq. (3.78) is then given as

$$\boxed{\mathbf{I}_T(t) = \sqrt{3}V_o Y e^{\mathbf{n}(\omega t-\theta)}\mathbf{q}_p + e^{-\zeta\omega_0 t}[\cos(\omega_0\sqrt{1-\zeta^2}t)\mathbf{k}_1 + \sin(\omega_0\sqrt{1-\zeta^2}t)\mathbf{k}_2].} \quad (3.89)$$

Fig. 3.21 presents the transient components of the Q-current considering $R = 100\,\Omega$, $L = 1$ H, $C = 100\,\mu$F and $\mathbf{I}_T(0) = 0$.

In Fig. 3.22 the locus of the Q-current is presented. The shape described is similar to other RLC cases, but with more oscillations. The center of the circles also oscillate back and forth through the origin as the Q-current approaches the steady state. This is observed in the Q-current locus of Fig. 3.22 by the rightmost part of the curve, which comes from a center with component in the $\mathbf{q}_p$ direction greater than zero.

The instantaneous Q-admittance can be calculated using eq. (3.59) and is computed as

$$\boxed{\mathbf{Y}_T(t) = Ye^{-\mathbf{n}\theta} + \frac{e^{-\zeta\omega_0 t}}{\sqrt{3}V_o}[\cos(\omega_0\sqrt{1-\zeta^2}t)\mathbf{k}_1 + \sin(\omega_0\sqrt{1-\zeta^2}t)\mathbf{k}_2]\mathbf{q}_p^{-1}e^{-\mathbf{n}\omega t},} \quad (3.90)$$

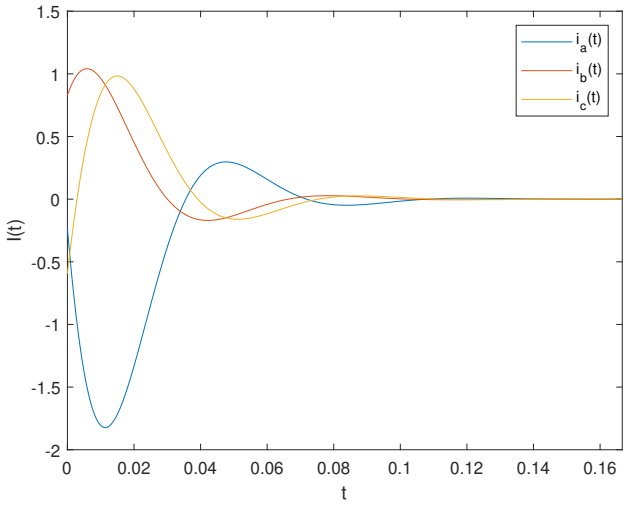

Figure 3.21: Transient state currents of the RLC three-phase load (underdamped).

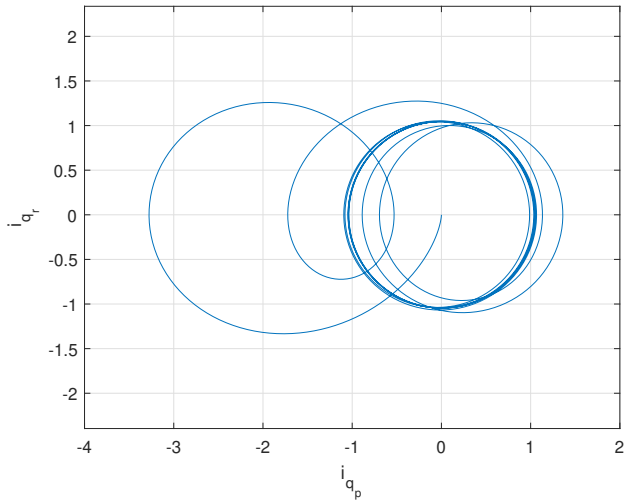

Figure 3.22: Currents of the RLC three-phase load (underdamped).

where $Ye^{-\mathbf{n}\theta}$ is the steady-state part and $(e^{-\zeta\omega_0 t}/\sqrt{3}V_o)[\cos(\omega_0\sqrt{1-\zeta^2}t)\mathbf{k}_1+\sin(\omega_0\sqrt{1-\zeta^2}t)\mathbf{k}_2]\mathbf{q}_p^{-1}e^{-\mathbf{n}\omega t}$ is the transient part of the Q-admittance.

3.2.7 LC load

For the last case, a three-phase wye load consisting of capacitors and inductors connected in series will be considered, as presented in Fig. 3.23.

The voltage in each phase is described by the differential equations

$$v_a(t) = L\frac{di_a(t)}{dt} + \frac{1}{C}\int_{-\infty}^{t} i_a(\tau)\,d\tau, \tag{3.91}$$

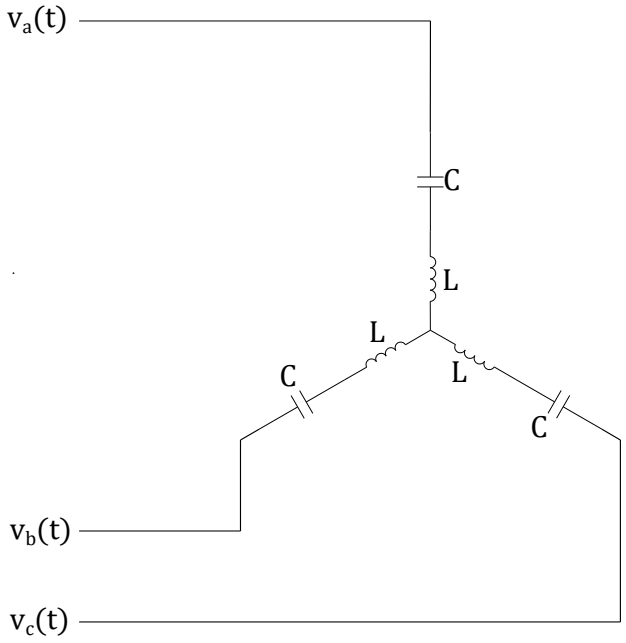

Figure 3.23: LC three-phase load.

$$v_b(t) = L\frac{di_b(t)}{dt} + \frac{1}{C}\int_{-\infty}^{t} i_b(\tau)\,d\tau, \tag{3.92}$$

$$v_c(t) = L\frac{di_c(t)}{dt} + \frac{1}{C}\int_{-\infty}^{t} i_c(\tau)\,d\tau. \tag{3.93}$$

which can be simplified in the quaternion format to

$$\mathbf{V}(t) = L\frac{d\mathbf{I}_T(t)}{dt} + \frac{1}{C}\int_{-\infty}^{t} \mathbf{I}_T(\tau)\,d\tau. \tag{3.94}$$

Applying the derivative on both sides and dividing by L

$$\frac{1}{L}\frac{d\mathbf{V}(t)}{dt} = \frac{d^2\mathbf{I}_T(t)}{dt^2} + \frac{\mathbf{I}_T(t)}{LC}. \tag{3.95}$$

The solution to eq. (3.95) is also in the form eq. (3.52) where the particular solution is eq. (3.24) where

$$Y = \frac{1}{|\omega L - \frac{1}{\omega C}|}, \tag{3.96}$$

$$\theta = \operatorname{sgn}\left(\omega L - \frac{1}{\omega C}\right) 90^\circ. \tag{3.97}$$

On the other hand, the natural response is given by

$$\mathbf{I}_h(t) = k_a \cos(\omega_0 t + \phi_a)\mathbf{a} + k_b \cos(\omega_0 t + \phi_b)\mathbf{b} + k_c \cos(\omega_0 t + \phi_c)\mathbf{c}. \tag{3.98}$$

Using $\cos(\alpha+\beta)=\cos(\alpha)\cos(\beta)-\sin(\alpha)\sin(\beta)$, eq. (3.98) can be written as

$$\mathbf{I}_h(t)=\cos(\omega_0 t)(k_a\cos(\phi_a)\mathbf{a}+k_b\cos(\phi_b)\mathbf{b}+k_c\cos(\phi_c)\mathbf{c}) \\ -\sin(\omega_0 t)(k_a\sin(\phi_a)\mathbf{a}+k_b\sin(\phi_b)\mathbf{b}+k_c\sin(\phi_c)\mathbf{c}), \quad (3.99)$$

$$\mathbf{I}_h(t)=\cos(\omega_0 t)\mathbf{k}_1-\sin(\omega_0 t)\mathbf{k}_2. \quad (3.100)$$

The constants k_a, ϕ_a, k_b, ϕ_b, k_c and ϕ_c are determined by the initial values. The solution for the differential equation eq. (3.95) is then given by

$$\boxed{\mathbf{I}_T(t)=\sqrt{3}V_o Y e^{\mathbf{n}(\omega t-\theta)}\mathbf{q}_p+\cos(\omega_0 t)\mathbf{k}_1-\sin(\omega_0 t)\mathbf{k}_2.} \quad (3.101)$$

It is observed that, as expected from an LC circuit, the transient term is not damped, resulting in a composition of oscillating motions. Fig. 3.24 presents the transient components of the Q-current considering $L=1$ H, $C=1\ \mu$F and $\mathbf{I}_T(0)=0$.

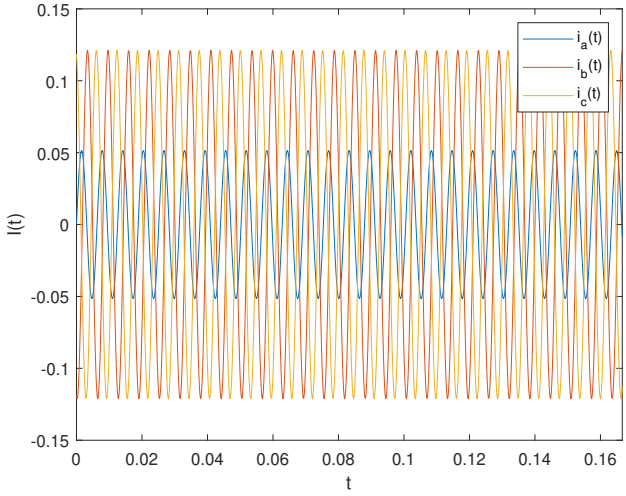

Figure 3.24: Transient state currents of the LC three-phase load.

In Fig. 3.24 the locus of the Q-current is presented. Naturally, the motion does not stabilize in a circular shape, since the steady-state is never reached.

The instantaneous Q-admittance can be calculated using eq. (3.59) and is computed as

$$\boxed{\mathbf{Y}_T(t)=Ye^{-\mathbf{n}\theta}+\frac{1}{\sqrt{3}V_o}(\cos(\omega_0 t)\mathbf{k}_1-\sin(\omega_0 t)\mathbf{k}_2)\mathbf{q}_p^{-1}e^{-\mathbf{n}\omega t},} \quad (3.102)$$

where $Ye^{-\mathbf{n}\theta}$ is the steady-state part and $(1/\sqrt{3}V_o)(\cos(\omega_0 t)\mathbf{k}_1-\sin(\omega_0 t)\mathbf{k}_2)\mathbf{q}_p^{-1}e^{-\mathbf{n}\omega t}$ is the transient part of the Q-admittance.

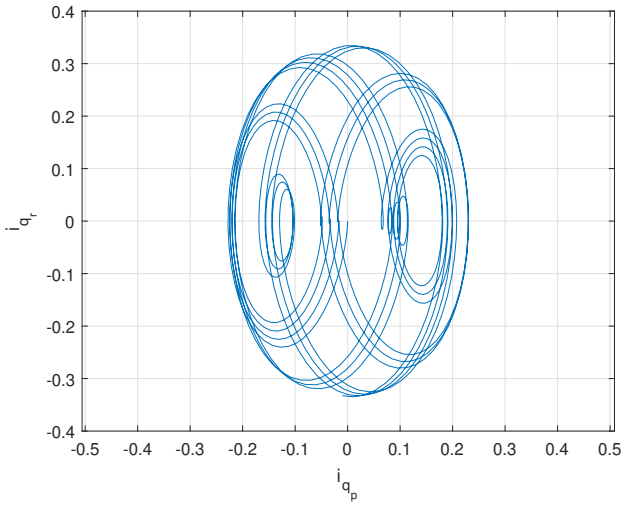

Figure 3.25: Currents of the LC three-phase load.

3.3 INSTANTANEOUS POWER, ADMITTANCE, AND IMPEDANCE

The expressions obtained for current, admittance, and power in the section 3.2 considered the complete response in time for these quantities, representing both steady and transient states for some load types. Here, these definitions are generalized, defining instantaneous quantities.

In three-phase systems, usually, it is assumed that the voltage of loads connected to the line is known. Then, currents are a consequence of voltage and load characteristics. In this context, assuming that a source with Q-voltage $\mathbf{V}(t)$ is connected to an arbitrary three-phase load. Instantaneous Q-current can be defined as the sum of the transient and steady-state quantities.

$$\mathbf{I}_T = \mathbf{I} + \boldsymbol{\iota}, \tag{3.103}$$

where $\mathbf{I}$ is the steady-state Q-current, $\boldsymbol{\iota}$ is the transient Q-current and $\mathbf{I}_T$ is the instantaneous Q-current. Applying the instantaneous Q-current in eqs. (3.9) and (3.18)

$$\mathbf{S}_T = \mathbf{V}\mathbf{I}^* + \mathbf{V}\boldsymbol{\iota}^* = \mathbf{S} + \boldsymbol{\varsigma}, \tag{3.104}$$

$$\mathbf{Y}_T = \mathbf{I}\mathbf{V}^{-1} + \boldsymbol{\iota}\mathbf{V}^{-1} = \mathbf{Y} + \boldsymbol{\upsilon}. \tag{3.105}$$

where $\mathbf{S}$, $\mathbf{Y}$, $\boldsymbol{\varsigma}$, $\boldsymbol{\upsilon}$, $\mathbf{S}_T$ and $\mathbf{Y}_T$ are, respectively, Q-power and Q-admittance in steady-state, transient state and time-domain (instantaneous). These expressions are in agreement with those found in section 3.2, where it was observed that Q-current, Q-admittance, and Q-power can be separated in steady and transient states.

An analogous expression would not be found for the impedance. If eq. (3.15) is used, the expression obtained is

$$\mathbf{Z}_T = \frac{\mathbf{V}\mathbf{I}^*}{|\mathbf{I}_T|^2} + \frac{\mathbf{V}\boldsymbol{\iota}^*}{|\mathbf{I}_T|^2}, \tag{3.106}$$

and it is observed that $\mathbf{I}^*/|\mathbf{I}_T|^2 \neq \mathbf{I}^{-1}$. As a consequence, the instantaneous Q-impedance is not the sum of our previous definition for steady-state Q-impedance with a transient Q-impedance. For this reason, the admittance notation is focused on in this work. It is important to notice that eqs. (3.59) and (3.106) are consequences of choosing voltage as the input and would appear reverted if the input was current. Nevertheless, in power systems, voltage is usually used as the input, as stated previously. Additionally, the definitions of instantaneous Q-impedance and Q-admittance using eqs. (3.15) and (3.18) do not depend on whether voltage or current are chosen as input.

3.4 THREE-PHASE UNBALANCED LOADS

In this section, the quaternion representation of three-phase unbalanced loads is discussed. Voltages and currents are assumed to be in the steady-state. In the unbalanced case, there are numerous possible combinations of impedances connected in each phase, e.g. an RLC impedance in the first phase, an RC impedance in the second, and an RL impedance in the last. Additionally, there are several load configurations to consider, such as delta, ungrounded wye, solidly grounded wye, and grounded wye. Given these facts, an exhaustive analysis of the expressions of Q-current, Q-admittance, and Q-power is beyond the scope of this work. For obtaining these quantities for a specific case, three differential equations need to be solved separately, since each phase is decoupled. Here the steady-state formulation is focused on, in view of the fact that it can be easily generalized and is the main focus of most of the studies.

3.4.1 Three-wire systems

3.4.1.1 Delta load

An unbalanced Delta load, as presented in Fig. 3.26, is analyzed in this subsection. The admittances of this load can be written as $Y_{ab}e^{-j\theta_{ab}}$, $Y_{bc}e^{-j\theta_{bc}}$ and $Y_{ca}e^{-j\theta_{ca}}$, where $Y_{mn}e^{-j\theta_{mn}}$ is the complex representation of the admittance between phases m and n.

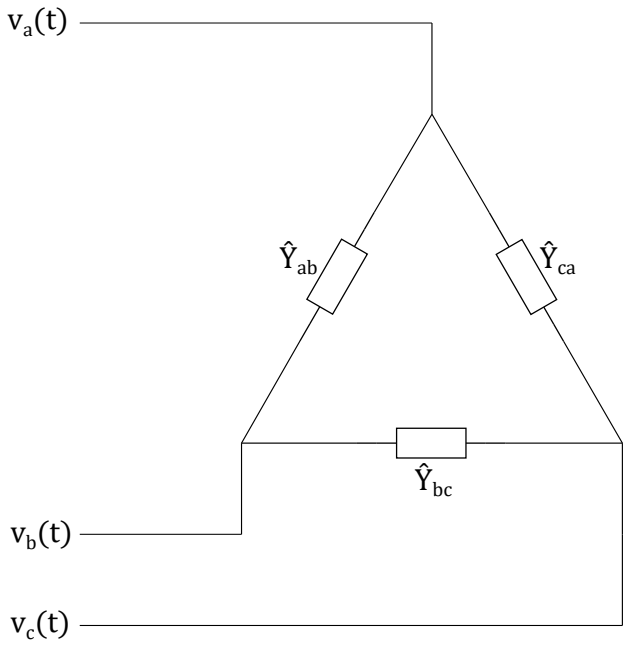

Figure 3.26: Unbalanced Delta three-phase load.

The phase to phase Q-voltage is given by

$$\mathbf{V}_{pp}(t) = \sqrt{6}V_o(\cos(\omega t + 30^\circ)\mathbf{a} + \cos(\omega t - 90^\circ)\mathbf{b} + \cos(\omega t + 150^\circ)\mathbf{c}). \tag{3.107}$$

The phase to phase Q-current can be written as

$$\mathbf{I}_{pp}(t) = \sqrt{6}V_o(Y_{ab}\cos(\omega t + 30^\circ - \theta_{ab})\mathbf{a} + Y_{bc}\cos(\omega t - 90^\circ - \theta_{bc})\mathbf{b} + Y_{ca}\cos(\omega t + 150^\circ - \theta_{ca})\mathbf{c}). \tag{3.108}$$

To obtain the three-phase Q-current, the relations between phase currents and line currents in a Δ load are used, i.e., $i_a = i_{ab} - i_{ca}$, $i_b = i_{bc} - i_{ab}$ and $i_c = i_{ca} - i_{bc}$. Since $\mathbf{I}_{pp}(t) = i_{ab}\mathbf{a} + i_{bc}\mathbf{b} + i_{ca}\mathbf{c}$,

$$\mathbf{I}(t) = i_a\mathbf{a} + i_b\mathbf{b} + i_c\mathbf{c}, \tag{3.109}$$

where

$$i_a(t) = \sqrt{6}V_o(Y_{ab}\cos(\omega t + 30^\circ - \theta_{ab}) - Y_{ca}\cos(\omega t + 150^\circ - \theta_{ca})), \tag{3.110}$$

$$i_b(t) = \sqrt{6}V_o(Y_{bc}\cos(\omega t - 90^\circ - \theta_{bc}) - Y_{ab}\cos(\omega t + 30^\circ - \theta_{ab})), \tag{3.111}$$

$$i_c(t) = \sqrt{6}V_o(Y_{ca}\cos(\omega t + 150^\circ - \theta_{ca}) - Y_{bc}\cos(\omega t - 90^\circ - \theta_{bc})). \tag{3.112}$$

The Q-admittance is given by

$$\mathbf{Y} = \mathbf{I}\mathbf{V}^{-1}, \tag{3.113}$$

where $\mathbf{V}^{-1}$ is given by

$$\mathbf{V}^{-1} = -\frac{\sqrt{2}}{3V_o}\left(\cos(\omega t)\mathbf{a} + \cos(\omega t - 120^\circ)\mathbf{b} + \cos(\omega t + 120^\circ)\mathbf{c}\right). \tag{3.114}$$

Using eq. (3.113), the scalar and vectorial part of the Q-admittance for this case is obtained. Calculating its scalar part

$$\begin{aligned}\mathrm{Re}(\mathbf{Y}) = \frac{2}{\sqrt{3}}&(Y_{ab}\cos(\omega t + 30^\circ - \theta_{ab}) - Y_{ca}\cos(\omega t + 150^\circ - \theta_{ca}))\cos(\omega t)\\ &+ (Y_{bc}\cos(\omega t - 90^\circ - \theta_{bc}) - Y_{ab}\cos(\omega t + 30^\circ - \theta_{ab}))\cos(\omega t - 120^\circ)\\ &+ (Y_{ca}\cos(\omega t + 150^\circ - \theta_{ca}) - Y_{bc}\cos(\omega t - 90^\circ - \theta_{bc}))\cos(\omega t + 120^\circ)).\end{aligned} \tag{3.115}$$

Using that $\cos(\alpha) - \cos(\alpha - 120^\circ) = \sqrt{3}\cos(\alpha + 30^\circ)$,

$$\begin{aligned}\mathrm{Re}(\mathbf{Y}) = 2(&Y_{ab}\cos(\omega t + 30^\circ - \theta_{ab})\cos(\omega t + 30^\circ) + Y_{bc}\cos(\omega t - 90^\circ - \theta_{bc})\cos(\omega t - 90^\circ)\\ &+ Y_{ca}\cos(\omega t + 150^\circ - \theta_{ca})\cos(\omega t + 150^\circ)).\end{aligned} \tag{3.116}$$

The scalar part of $\mathbf{Y}$ is then obtained using the identity $\cos(\alpha)\cos(\alpha-\beta) = 1/2\,(\cos(2\alpha - \beta) + \cos(\beta)))$

$$\begin{aligned}\mathrm{Re}(\mathbf{Y}) = \Big[&Y_{ab}\cos(\theta_{ab}) + Y_{bc}\cos(\theta_{bc}) + Y_{ca}\cos(\theta_{ca}) + Y_{ab}\cos\left(2\omega t + 60^\circ - \theta_{ab}\right)\\ &+ Y_{bc}\cos(2\omega t - 180^\circ - \theta_{bc}) + Y_{ca}\cos\left(2\omega t - 60^\circ - \theta_{ca}\right)\Big].\end{aligned} \tag{3.117}$$

Next, the vectorial part of Q-admittance $\vec{\mathbf{Y}}$ is calculated.

$$\vec{\mathbf{Y}} = \begin{vmatrix} \mathbf{a} & \mathbf{b} & \mathbf{c} \\ i_a & i_b & i_c \\ (\mathbf{V}^{-1})_a & (\mathbf{V}^{-1})_b & (\mathbf{V}^{-1})_c \end{vmatrix}.$$

$$\vec{\mathbf{Y}} = \mathbf{Y}_a + \mathbf{Y}_b + \mathbf{Y}_c, \tag{3.118}$$

in which the components of $\vec{\mathbf{Y}}$ are given by

$$\begin{aligned}\mathbf{Y}_a = \frac{2}{\sqrt{3}}&[-\cos(\omega t + 120^\circ)(Y_{bc}\cos(\omega t - 90^\circ - \theta_{bc}) - Y_{ab}\cos(\omega t + 30^\circ - \theta_{ab}))\\ &+ \cos(\omega t - 120^\circ)(Y_{ca}\cos(\omega t + 150^\circ - \theta_{ca}) - Y_{bc}\cos(\omega t - 90^\circ - \theta_{bc}))]\mathbf{a},\end{aligned} \tag{3.119}$$

$$\begin{aligned}\mathbf{Y}_b = \frac{2}{\sqrt{3}}&[-\cos(\omega t)(Y_{ca}\cos(\omega t + 150^\circ - \theta_{ca}) - Y_{bc}\cos(\omega t - 90^\circ - \theta_{bc}))\\ &+ \cos(\omega t + 120^\circ)(Y_{ab}\cos(\omega t + 30^\circ - \theta_{ab}) - Y_{ca}\cos(\omega t + 150^\circ - \theta_{ca}))]\mathbf{b},\end{aligned} \tag{3.120}$$

$$\mathbf{Y}_c = \frac{2}{\sqrt{3}}[-\cos(\omega t - 120^\circ)(Y_{ab}\cos(\omega t + 30^\circ - \theta_{ab}) - Y_{ca}\cos(\omega t + 150^\circ - \theta_{ca}))$$
$$+ \cos(\omega t)(Y_{bc}\cos(\omega t - 90^\circ - \theta_{bc}) - Y_{ab}\cos(\omega t + 30^\circ - \theta_{ab}))]\mathbf{c}. \quad (3.121)$$

Using that $\cos(\alpha) + \cos(\alpha + 120^\circ) = \cos(\alpha + 60^\circ)$

$$\mathbf{Y}_a = \frac{2}{\sqrt{3}}[-Y_{bc}\cos(\omega t + 180^\circ)\cos(\omega t - 90^\circ - \theta_{bc}) + Y_{ab}\cos(\omega t + 120^\circ)\cos(\omega t + 30^\circ - \theta_{ab}))$$
$$+ Y_{ca}\cos(\omega t - 120^\circ)\cos(\omega t + 150^\circ - \theta_{ca})]\mathbf{a}, \quad (3.122)$$

$$\mathbf{Y}_b = \frac{2}{\sqrt{3}}[-Y_{ca}\cos(\omega t + 60^\circ)\cos(\omega t + 150^\circ - \theta_{ca}) - Y_{bc}\cos(\omega t - 90^\circ - \theta_{bc}))$$
$$+ Y_{ab}\cos(\omega t + 120^\circ)\cos(\omega t + 30^\circ - \theta_{ab})]\mathbf{b}, \quad (3.123)$$

$$\mathbf{Y}_c = \frac{2}{\sqrt{3}}[-Y_{ab}\cos(\omega t - 60^\circ)\cos(\omega t + 30^\circ - \theta_{ab}) + Y_{ca}\cos(\omega t - 120^\circ)\cos(\omega t + 150^\circ - \theta_{ca}))$$
$$+ Y_{bc}\cos(\omega t)\cos(\omega t - 90^\circ - \theta_{bc})]\mathbf{c}. \quad (3.124)$$

Given that $-\cos(\alpha) = \cos(\alpha + 180^\circ)$, it is noticed that all components are equal

$$|\mathbf{Y}_a| = |\mathbf{Y}_b| = |\mathbf{Y}_c| = \frac{2}{\sqrt{3}}[Y_{ab}\cos(\omega t + 120^\circ)\cos(\omega t + 30^\circ - \theta_{ab})) + Y_{bc}\cos(\omega t)\cos(\omega t - 90^\circ - \theta_{bc})$$
$$+ Y_{ca}\cos(\omega t - 120^\circ)\cos(\omega t + 150^\circ - \theta_{ca})]. \quad (3.125)$$

It follows that the vectorial part of $\mathbf{Y}$ can be written as

$$\vec{\mathbf{Y}} = 2\mathbf{n}[Y_{ab}\cos(\omega t + 120^\circ)\cos(\omega t + 30^\circ - \theta_{ab}) + Y_{bc}\cos(\omega t)\cos(\omega t - 90^\circ - \theta_{bc})$$
$$+ Y_{ca}\cos(\omega t - 120^\circ)\cos(\omega t + 150^\circ - \theta_{ca})], \quad (3.126)$$

where

$$\mathbf{n} = \frac{1}{\sqrt{3}}(\mathbf{a} + \mathbf{b} + \mathbf{c}). \quad (3.127)$$

Using the trigonometric identity $\cos(\alpha)\cos(\beta) = 1/2(\cos(\alpha + \beta) + \cos(\alpha - \beta))$

$$\vec{\mathbf{Y}} = \mathbf{n}[Y_{ab}\cos(\theta_{ab} + 90^\circ) + Y_{ab}\cos(2\omega t + 150^\circ - \theta_{ab}) + Y_{bc}\cos(\theta_{bc} + 90^\circ) + Y_{bc}\cos(2\omega t - 90^\circ - \theta_{bc})$$
$$+ Y_{ca}\cos(\theta_{ca} + 90^\circ) + Y_{ca}\cos(2\omega t + 30^\circ - \theta_{ca})]. \quad (3.128)$$

Finally, the cosines are substituted by sines using that $\cos(\alpha + 90^\circ) = -\sin(\alpha)$

$$\vec{\mathbf{Y}} = -\mathbf{n}[Y_{ab}\sin(\theta_{ab}) + Y_{bc}\sin(\theta_{bc}) + Y_{ca}\sin(\theta_{ca}) + Y_{ab}\sin(2\omega t + 60^\circ - \theta_{ab}) + Y_{bc}\sin(2\omega t - 180^\circ - \theta_{bc}) + Y_{ca}\sin(2\omega t - 60^\circ - \theta_{ca})]. \quad (3.129)$$

Comparing eqs. (3.117) and (3.129), $\mathbf{Y}$ can be rewritten as a sum of 6 quaternions in polar form as

$$\boxed{\mathbf{Y} = Y_{ab}e^{-\mathbf{n}\theta_{ab}} + Y_{bc}e^{-\mathbf{n}\theta_{bc}} + Y_{ca}e^{-\mathbf{n}\theta_{ca}} + Y_{ab}e^{-\mathbf{n}\phi_{ab}(t)} + Y_{bc}e^{-\mathbf{n}\phi_{bc}(t)} + Y_{ca}e^{-\mathbf{n}\phi_{ca}(t)},} \quad (3.130)$$

where $\phi_{ab}(t) = 2\omega t + \frac{\pi}{3} - \theta_{ab}$, $\phi_{bc}(t) = 2\omega t - \pi - \theta_{bc}$, and $\phi_{ca}(t) = 2\omega t - \frac{\pi}{3} - \theta_{ca}$.

Analyzing eq. (3.130), it is observed that the Q-admittance of an unbalanced three-phase load is equivalent to the sum of the admittances of six different balanced three-phase loads: three balanced consisting of the admittances between each phase and three balanced with varying in time phases.

Summing the three constant quaternions, eq. (3.130) can be rewritten as

$$\mathbf{Y} = Y_{pl}e^{-\mathbf{n}\theta_{pl}} + Y_{ab}e^{-\mathbf{n}\phi_{ab}(t)} + Y_{bc}e^{-\mathbf{n}\phi_{bc}(t)} + Y_{ca}e^{-\mathbf{n}\phi_{ca}(t)}, \quad (3.131)$$

where

$$Y_{pl}^2 = Y_{ab}^2 + Y_{bc}^2 + Y_{ca}^2 + 2Y_{ab}Y_{bc}\cos(\theta_{ab} - \theta_{bc}) + 2Y_{bc}Y_{ca}\cos(\theta_{bc} - \theta_{ca}) + 2Y_{ca}Y_{ab}\cos(\theta_{ca} - \theta_{ab}), \quad (3.132)$$

$$\theta_{pl} = k_{pl}\pi + tg^{-1}\left(\frac{Y_{ab}\sin(\theta_{ab}) + Y_{bc}\sin(\theta_{bc}) + Y_{ca}\sin(\theta_{ca})}{Y_{ab}\cos(\theta_{ab}) + Y_{bc}\cos(\theta_{bc}) + Y_{ca}\cos(\theta_{ca})}\right), \quad (3.133)$$

in which $k_{pl} = 1$ if the denominator is negative and $k_{pl} = 0$ otherwise.

These values of Y_{pl} and θ_{pl} correspond to the association of the admittances in parallel, that is,

$$Y_{pl}e^{-j\theta_{pl}} = Y_{ab}e^{-j\theta_{ab}} + Y_{bc}e^{-j\theta_{bc}} + Y_{ca}e^{-j\theta_{ca}}.$$

The other terms can be simplified as well, which is equivalent to two associate the three balanced loads with varying in time phases in parallel. The Q-admittance can then be written as

$$\boxed{\mathbf{Y} = Y_{pl}e^{-\mathbf{n}\theta_{pl}} + Y_{\omega}e^{-\mathbf{n}\phi_{\omega}(t)},} \quad (3.134)$$

where

$$\phi_{\omega} = k_{\omega}\pi + tg^{-1}\left(\frac{Y_{ab}\sin(\phi_{ab}) + Y_{bc}\sin(\phi_{bc}) + Y_{ca}\sin(\phi_{ca})}{Y_{ab}\cos(\phi_{ab}) + Y_{bc}\cos(\phi_{bc}) + Y_{ca}\cos(\phi_{ca})}\right), \quad (3.135)$$

in which $k_\omega = 1$ if the denominator is negative and $k_\omega = 0$ otherwise.

$$Y_\omega^2 = Y_{ab}^2 + Y_{bc}^2 + Y_{ca}^2 + 2Y_{ab}Y_{bc}\cos\left(\theta_{ab} - \theta_{bc} + \frac{2\pi}{3}\right) + 2Y_{bc}Y_{ca}\cos\left(\theta_{bc} - \theta_{ca} + \frac{2\pi}{3}\right) + 2Y_{ca}Y_{ab}\cos\left(\theta_{ca} - \theta_{ab} + \frac{2\pi}{3}\right). \quad (3.136)$$

Notice that, if the three-phase load is balanced, $Y_\omega = 0$.

The result in eq. (3.131) can also be interpreted as the Q-admittance of one balanced three-phase load and three unbalanced loads with admittances between phases A-B, B-C, and C-A, respectively

$$\frac{Y_{ab}}{3}e^{-j\theta_{ab}},\ \frac{Y_{ab}}{3}e^{-j(2\pi/3+\theta_{ab})} \text{ and } \frac{Y_{ab}}{3}e^{j(2\pi/3-\theta_{ab})}$$

for the first three-phase load,

$$\frac{Y_{bc}}{3}e^{j(2\pi/3-\theta_{bc})},\ \frac{Y_{bc}}{3}e^{-j\theta_{bc}} \text{ and } \frac{Y_{bc}}{3}e^{-j(2\pi/3+\theta_{bc})}$$

for the second and

$$\frac{Y_{ca}}{3}e^{-j(2\pi/3+\theta_{ca})},\ \frac{Y_{ca}}{3}e^{j(2\pi/3-\theta_{ca})} \text{ and } \frac{Y_{ca}}{3}e^{-j\theta_{ca}}$$

for the third. This can easily be proven calculating Q-admittance for each of these loads. Fig. 3.27 shows these admittances connected in parallel.

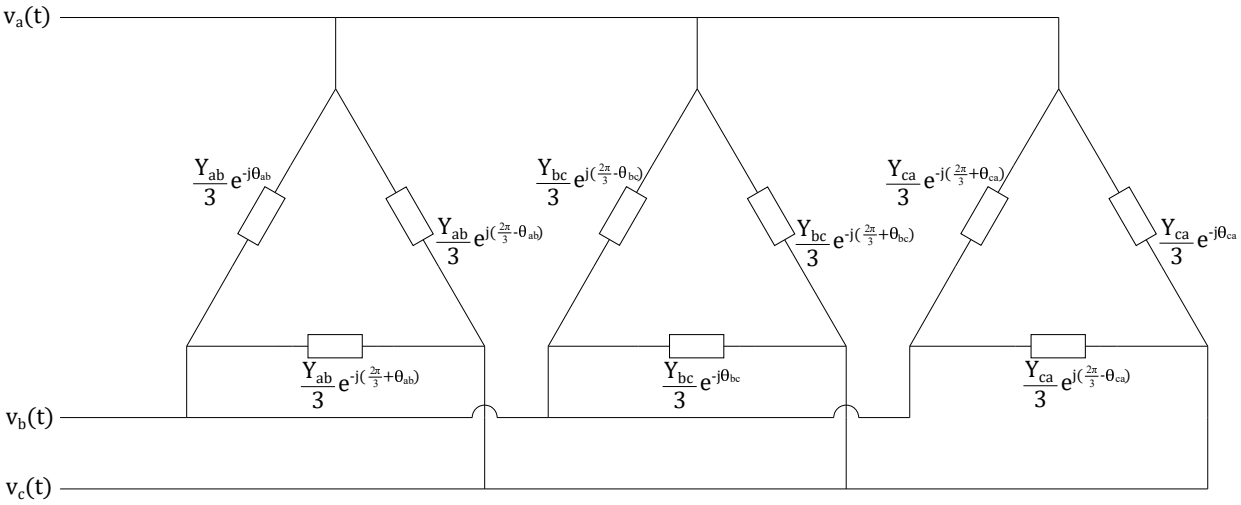

Figure 3.27: Equivalent admittances.

Associating these admittances in parallel, a three-phase load with the followings admittances is obtained

$$Y'_{ab}e^{-j\theta'_{ab}} = \frac{Y_{ab}}{3}e^{-j\theta_{ab}} + \frac{Y_{bc}}{3}e^{j(2\pi/3-\theta_{bc})} + \frac{Y_{ca}}{3}e^{-j(2\pi/3+\theta_{ca})}, \quad (3.137)$$

$$Y'_{bc}e^{-j\theta'_{bc}} = \frac{Y_{ab}}{3}e^{-j(2\pi/3+\theta_{ab})} + \frac{Y_{bc}}{3}e^{-j\theta_{bc}} + \frac{Y_{ca}}{3}e^{j(\frac{2\pi}{3}-\theta_{ca})}, \tag{3.138}$$

$$Y'_{ca}e^{-j\theta'_{ca}} = \frac{Y_{ab}}{3}e^{j(2\pi/3-\theta_{ab})} + \frac{Y_{bc}}{3}e^{-j(2\pi/3+\theta_{bc})} + \frac{Y_{ca}}{3}e^{-j\theta_{ca}}. \tag{3.139}$$

It is noticeable that eqs. (3.137) to (3.139) are not the unique possible representation of the unbalanced term of the three-phase load. Another representation would be obtained if the balanced admittance is subtracted from the original unbalanced three-phase load. For obtaining all equivalent representations of the unbalanced term, the generic unbalanced load with admittances between phases A-B, B-C, and C-A, respectively, $Me^{-j\theta_M}$, $Ne^{-j\theta_N}$ and $Oe^{-j\theta_O}$ is considered. The line current of this load in parallel with the balanced load should have line currents equal to line currents of the initial unbalanced load, which implies

$$Me^{-j\theta_M} - Oe^{j(\frac{2\pi}{3}-\theta_O)} + \frac{\sqrt{3}}{3}Y_{pl}e^{-j(\frac{\pi}{6}+\theta_{pl})} = Y_{ab}e^{-j\theta_{ab}} - Y_{ca}e^{j(\frac{2\pi}{3}-\theta_{ca})}, \tag{3.140}$$

$$Ne^{-j(\frac{2\pi}{3}+\theta_N)} - Me^{-j\theta_M} + \frac{\sqrt{3}}{3}Y_{pl}e^{-j(\frac{5\pi}{6}+\theta_{pl})} = Y_{bc}e^{-j(\frac{2\pi}{3}+\theta_{bc})} - Y_{ab}e^{-j\theta_{ab}}, \tag{3.141}$$

$$Oe^{j(\frac{2\pi}{3}-\theta_O)} - Ne^{-j(\frac{2\pi}{3}+\theta_N)} + \frac{\sqrt{3}}{3}Y_{pl}e^{j(\frac{\pi}{2}-\theta_{pl})} = Y_{ca}e^{j(\frac{2\pi}{3}-\theta_{ca})} - Y_{bc}e^{-j(\frac{2\pi}{3}+\theta_{bc})}. \tag{3.142}$$

Since eq. (3.142) is a linear combination of eqs. (3.140) and (3.141), this equation can be eliminated. Solving in terms of $Me^{-j\theta_M}$

$$\boxed{Ne^{-j\theta_N} = Me^{j(\frac{2\pi}{3}-\theta_M)} - \frac{\sqrt{3}}{3}Y_{ab}e^{j(\frac{\pi}{2}-\theta_{ab})} + \frac{\sqrt{3}}{3}Y_{bc}e^{j(\frac{\pi}{6}-\theta_{bc})} - \frac{\sqrt{3}}{3}Y_{ca}e^{-j(\frac{\pi}{6}+\theta_{ca})},} \tag{3.143}$$

$$\boxed{Oe^{-j\theta_O} = Me^{-j(\frac{2\pi}{3}+\theta_M)} - \frac{\sqrt{3}}{3}Y_{ab}e^{-j(\frac{\pi}{2}+\theta_{ab})} + \frac{\sqrt{3}}{3}Y_{bc}e^{-j(\frac{5\pi}{6}+\theta_{bc})} + \frac{\sqrt{3}}{3}Y_{ca}e^{j(\frac{\pi}{6}-\theta_{ca})}.} \tag{3.144}$$

The admittance $Me^{-j\theta_M}$ can be chosen arbitrarily, which implies that there are infinite equivalent unbalanced loads to the admittances shown in eqs. (3.137) to (3.139). As a consequence, any unbalanced delta load connected to a balanced voltage source has infinite equivalents. The derivation of the existence of infinite equivalents presented in this work is an alternative to that [45], which followed a different approach without quaternions. Furthermore, the unbalanced three-phase load represented by eqs. (3.143) and (3.144) has also the propriety of null average three-phase power. This is a consequence of the expression of Q-admittance eq. (3.134), where the first term accounts for the average three-phase power of the load.

Returning to eq. (3.134), the expression can be simplified summing both quaternions. This sum results in the shortest version of Q-admittance, analogous to the balanced case presented in eq. (3.26)

$$\boxed{\mathbf{Y} = Y_\delta(t)e^{-\mathbf{n}\phi_\delta(t)},} \tag{3.145}$$

where

$$Y_\delta(t)^2 = Y_{pl}^2 + Y_\omega^2 + 2Y_{pl}Y_\omega \cos\left(\theta_{pl} - \phi_\omega(t)\right), \tag{3.146}$$

$$\phi_\delta(t) = k_\delta \pi + tg^{-1}\left(\frac{Y_{pl}\sin(\theta_{pl}) + Y_\omega \sin(\phi_\omega(t))}{Y_{pl}\cos(\theta_{pl}) + Y_\omega \cos(\phi_\omega(t))}\right), \tag{3.147}$$

in which $k_\delta = 1$ if the denominator is negative and $k_\delta = 0$ otherwise.

Analyzing eq. (3.145), it is possible to conclude that the three-phase unbalanced load can be represented by a three-phase balanced load, with modulus and phase varying in time.

3.4.1.2 Wye load

In this subsection, an unbalanced wye load as presented in Fig. 3.28 is analyzed. Its admittances are, respectively, $Y_a e^{-j\theta_a}$, $Y_b e^{-j\theta_b}$ and $Y_c e^{-j\theta_c}$, where $Y_m e^{-j\theta_m}$ is the complex representation of the admittance connected to phase m.

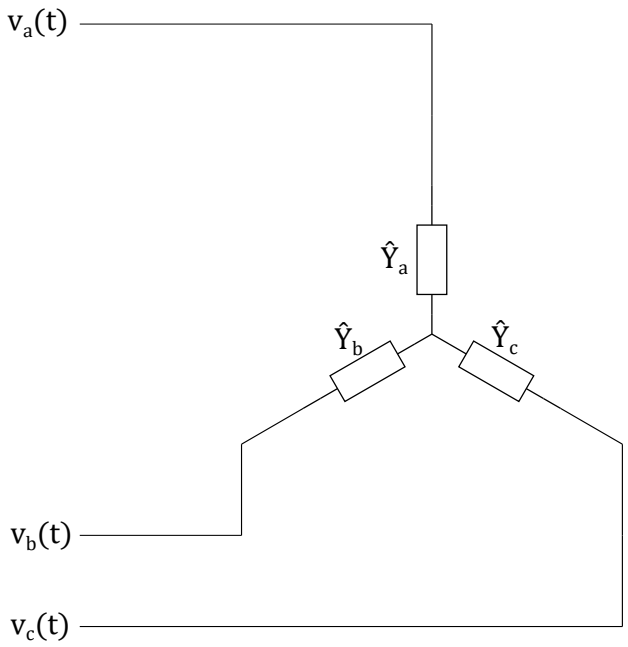

Figure 3.28: Balanced three-phase load.

To determine the line currents of this load the phasorial notation is employed. It is noteworthy that phasors are used separately of quaternions, since the first represent individual electrical quantities in the frequency domain and the latter three-phase electrical quantities in the time domains.

The source voltage $\mathbf{V}(t)$ is given by eq. (3.4). The voltage on the central node can be written with

phasors as

$$V_w e^{j\theta_w} = \frac{V_a e^{j0} Y_a e^{-j\theta_a} + V_b e^{j\frac{2\pi}{3}} Y_b e^{-j\theta_b} + V_c e^{-j\frac{2\pi}{3}} Y_c e^{-j\theta_c}}{Y_a e^{-j\theta_a} + Y_b e^{-j\theta_b} + Y_c e^{-j\theta_c}}, \tag{3.148}$$

and the line currents can be computed as

$$I_a e^{j\Theta_a} = (V_a e^{j0} - V_w e^{j\theta_w}) Y_a e^{-j\theta_a}, \tag{3.149}$$

$$I_b e^{j\Theta_b} = (V_b e^{-j\frac{2\pi}{3}} - V_w e^{j\theta_w}) Y_b e^{-j\theta_b}, \tag{3.150}$$

$$I_c e^{j\Theta_c} = (V_c e^{j\frac{2\pi}{3}} - V_w e^{j\theta_w}) Y_c e^{-j\theta_c}, \tag{3.151}$$

which results in

$$I_a e^{j\Theta_a} = \frac{(V_{ab} e^{j\frac{\pi}{6}} Y_b e^{-j\theta_b} - V_{ca} e^{j\frac{5\pi}{6}} Y_c e^{-j\theta_c}) Y_a e^{-j\theta_a}}{Y_a e^{-j\theta_a} + Y_b e^{-j\theta_b} + Y_c e^{-j\theta_c}}, \tag{3.152}$$

$$I_b e^{j\Theta_b} = \frac{(V_{bc} e^{-j\frac{\pi}{2}} Y_c e^{-j\theta_c} - V_{ab} e^{j\frac{\pi}{6}} Y_a e^{-j\theta_a}) Y_b e^{-j\theta_b}}{Y_a e^{-j\theta_a} + Y_b e^{-j\theta_b} + Y_c e^{-j\theta_c}}, \tag{3.153}$$

$$I_c e^{j\Theta_c} = \frac{(V_{ca} e^{j\frac{5\pi}{6}} Y_a e^{-j\theta_a} - V_{bc} e^{-j\frac{\pi}{2}} Y_b e^{-j\theta_b}) Y_c e^{-j\theta_c}}{Y_a e^{-j\theta_a} + Y_b e^{-j\theta_b} + Y_c e^{-j\theta_c}}. \tag{3.154}$$

The Y-Δ transformation, represented by the Fig. 3.29, is given by the formulas

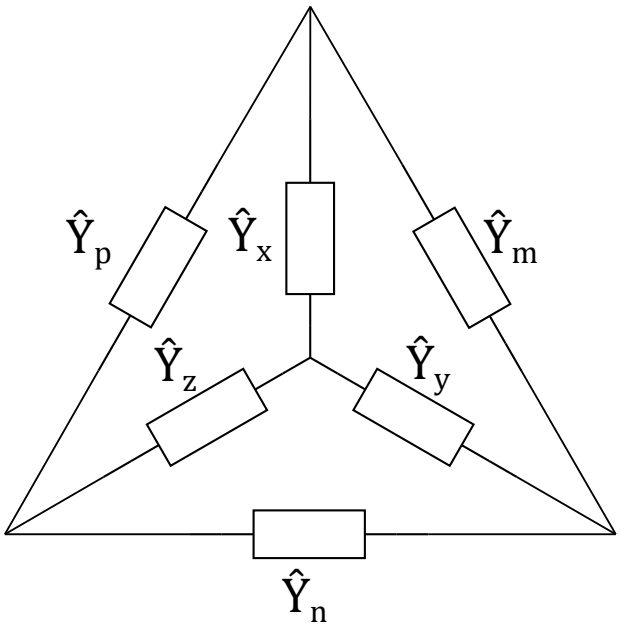

Figure 3.29: Y-Δ transformation.

$$\hat{Y}_m = \frac{\hat{Y}_x \hat{Y}_y}{\hat{Y}_x + \hat{Y}_y + \hat{Y}_z}, \tag{3.155}$$

$$\hat{Y}_n = \frac{\hat{Y}_y \hat{Y}_z}{\hat{Y}_x + \hat{Y}_y + \hat{Y}_z}, \tag{3.156}$$

$$\hat{Y}_p = \frac{\hat{Y}_z \hat{Y}_x}{\hat{Y}_x + \hat{Y}_y + \hat{Y}_z}. \tag{3.157}$$

Applying eqs. (3.155) to (3.157) to eqs. (3.152) to (3.154)

$$I_a e^{j\Theta_a} = V_{ab} e^{j\frac{\pi}{6}} Y_{ab} e^{-j\theta_{ab}} - V_{ca} e^{j\frac{5\pi}{6}} Y_{ca} e^{-j\theta_{ca}}, \tag{3.158}$$

$$I_b e^{j\Theta_b} = V_{bc} e^{-j\frac{\pi}{2}} Y_{bc} e^{-j\theta_{bc}} - V_{ab} e^{j\frac{\pi}{6}} Y_{ab} e^{-j\theta_{ab}}, \tag{3.159}$$

$$I_c e^{j\Theta_c} = V_{ca} e^{j\frac{5\pi}{6}} Y_{ca} e^{-j\theta_{ca}} - V_{bc} e^{-j\frac{\pi}{2}} Y_{bc} e^{-j\theta_{bc}}, \tag{3.160}$$

which can be written in the time-domain as

$$i_a(t) = V_{ab}(Y_{ab}\cos(\omega t + 30^\circ - \theta_{ab}) - Y_{ca}\cos(\omega t + 150^\circ - \theta_{ca})), \tag{3.161}$$

$$i_b(t) = V_{bc}(Y_{bc}\cos(\omega t - 90^\circ - \theta_{bc}) - Y_{ab}\cos(\omega t + 30^\circ - \theta_{ab})), \tag{3.162}$$

$$i_c(t) = V_{ca}(Y_{ca}\cos(\omega t + 150^\circ - \theta_{ca}) - Y_{bc}\cos(\omega t - 90^\circ - \theta_{bc})). \tag{3.163}$$

Notice that $V_{ab} = V_{bc} = V_{ca} = \sqrt{6}V_o$, implying that eqs. (3.161) to (3.163) and eqs. (3.110) to (3.112) are the same line currents. This result is expected, since the wye load is a transformed version of the delta load. As a consequence, all development made for the delta case is also valid in the wye case. In particular, the expression for the Q-admittance eq. (3.130) can be used for representing the wye load. The expression is rewritten here for the sake of the demonstration.

$$\mathbf{Y} = Y_{ab} e^{-\mathbf{n}\theta_{ab}} + Y_{bc} e^{-\mathbf{n}\theta_{bc}} + Y_{ca} e^{-\mathbf{n}\theta_{ca}} + Y_{ab} e^{-\mathbf{n}(2\omega t + \frac{\pi}{3} - \theta_{ab})} + Y_{bc} e^{-\mathbf{n}(2\omega t - \pi - \theta_{bc})} + Y_{ca} e^{-\mathbf{n}(2\omega t - \frac{\pi}{3} - \theta_{ca})}. \tag{3.164}$$

Since this expression consists only of quaternions in the form $a + \mathbf{n}b$, which form a commutative subset of $\mathbb{H}$, the Y-Δ transform expressions eqs. (3.155) to (3.157) can be applied to eq. (3.164). First, eq. (3.164) can be written as

$$\mathbf{Y} = Y_{ab} e^{-\mathbf{n}\theta_{ab}} + Y_{bc} e^{-\mathbf{n}\theta_{bc}} + Y_{ca} e^{-\mathbf{n}\theta_{ca}} + (Y_{ab} e^{-\mathbf{n}\theta_{ab}})^* e^{-\mathbf{n}(2\omega t + \frac{\pi}{3})} + (Y_{bc} e^{-\mathbf{n}\theta_{bc}})^* e^{-\mathbf{n}(2\omega t - \pi)} + (-Y_{ca} e^{\mathbf{n}\theta_{ca}})^* e^{-\mathbf{n}(2\omega t - \frac{\pi}{3})}. \tag{3.165}$$

Them, applying eqs. (3.155) to (3.157)

$$\boxed{\begin{aligned}\mathbf{Y} = {} & (Y_\sigma e^{-\mathbf{n}\theta_\sigma})^{-1}(Y_a Y_b e^{-\mathbf{n}(\theta_a+\theta_b)} + Y_b Y_c e^{-\mathbf{n}(\theta_b+\theta_c)} + Y_c Y_a e^{-\mathbf{n}(\theta_c+\theta_a)}) + \\ & (Y_\sigma e^{\mathbf{n}\theta_\sigma})^{-1}(Y_a Y_b e^{-\mathbf{n}(2\omega t + \frac{\pi}{3} - \theta_a - \theta_b)} + Y_b Y_c e^{-\mathbf{n}(2\omega t - \pi - \theta_b - \theta_c)} + Y_c Y_a e^{-\mathbf{n}(2\omega t - \frac{\pi}{3} - \theta_c - \theta_a)}),\end{aligned}} \tag{3.166}$$

where Y_σ and θ_σ are defined by

$$Y_\sigma e^{-\mathbf{n}\theta_\sigma} = Y_a e^{-\mathbf{n}\theta_a} + Y_b e^{-\mathbf{n}\theta_b} + Y_c e^{-\mathbf{n}\theta_c}, \tag{3.167}$$

which implies that it is equivalent to the admittance of the loads in each phase in parallel.

Comparing eqs. (3.130) and (3.166), it is observed that the expression for the Delta load is more compact and easier to analyze. Nevertheless, if the load is given by its wye parameters, eq. (3.166) may be used to obtain the corresponding Q-admittance. It is observed that

$$\frac{Y_a Y_b}{Y_\sigma} = Y_{ab}, \tag{3.168}$$

$$\frac{Y_b Y_c}{Y_\sigma} = Y_{bc}, \tag{3.169}$$

$$\frac{Y_c Y_a}{Y_\sigma} = Y_{ca}, \tag{3.170}$$

$$\theta_a + \theta_b - \theta_\sigma = \theta_{ab}, \tag{3.171}$$

$$\theta_b + \theta_c - \theta_\sigma = \theta_{bc}, \tag{3.172}$$

$$\theta_c + \theta_a - \theta_\sigma = \theta_{ca}, \tag{3.173}$$

as expected from the Δ-Y transform. Using eqs. (3.168) to (3.173), eq. (3.134) can be obtained in terms of wye parameters.

3.4.2 Four-wire systems

3.4.2.1 Solidly grounded wye load

In this case, the Q-admittance of the three-phase load presented in Fig. 3.30 will be analyzed. Its admittances are, respectively, $Y_a e^{-j\theta_a}$, $Y_b e^{-j\theta_b}$ and $Y_c e^{-j\theta_c}$, where $Y_m e^{-j\theta_m}$ is the complex representation of the admittance connected to phase m. Since the connection to the ground isolates each phase, the Q-current is easily determined.

$$\mathbf{I}(t) = \sqrt{2}V_o[Y_a \cos(\omega t - \theta_a)\mathbf{a} + Y_b \cos(\omega t - 120^\circ - \theta_b)\mathbf{b} + Y_c \cos(\omega t + 120^\circ - \theta_c)\mathbf{c}]. \tag{3.174}$$

Using eq. (3.18) and eq. (3.114), the Q-admittance can be determined. First, calculating its real part

$$\begin{aligned}\mathrm{Re}(\mathbf{Y}) = \frac{2}{3}(&Y_a \cos(\omega t)\cos(\omega t - \theta_a) + Y_b \cos(\omega t - 120^\circ)\cos(\omega t - 120^\circ - \theta_b) \\ &+ Y_c \cos(\omega t + 120^\circ)\cos(\omega t + 120^\circ - \theta_c)).\end{aligned} \tag{3.175}$$

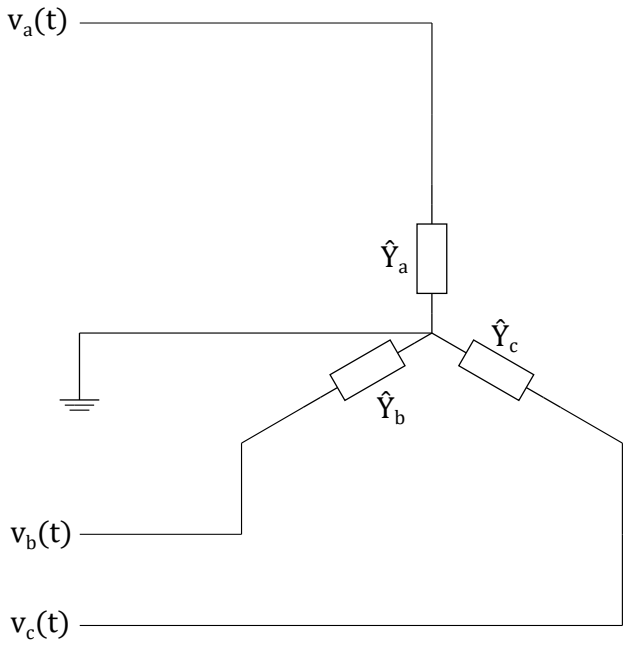

Figure 3.30: Solidly grounded three-phase load.

Applying the trigonometric relation $\cos(\alpha)\cos(\alpha-\beta) = 1/2(\cos(2\alpha-\beta)+\cos(\beta))$

$$\mathrm{Re}(\mathbf{Y}) = \frac{1}{3}[Y_a\cos(\theta_a) + Y_a\cos(2\omega t-\theta_a) + Y_b\cos(\theta_b) + Y_b\cos(2\omega t+120^\circ-\theta_b) + Y_c\cos(\theta_c) + Y_c\cos(2\omega t-120^\circ-\theta_c)]. \quad (3.176)$$

Next, the vectorial part of the Q-admittance $\vec{\mathbf{Y}}$ is determined by eq. (3.118). Determining its components as in eq. (3.118)

$$\mathbf{Y}_a = \frac{2}{3}[Y_c\cos(\omega t-120^\circ)\cos(\omega t+120^\circ-\theta_c) - Y_b\cos(\omega t+120^\circ)\cos(\omega t-120^\circ-\theta_b)]\mathbf{a}, \quad (3.177)$$

$$\mathbf{Y}_b = \frac{2}{3}[Y_a\cos(\omega t+120^\circ)\cos(\omega t-\theta_a) - Y_c\cos(\omega t)\cos(\omega t+120^\circ-\theta_c)]\mathbf{b}, \quad (3.178)$$

$$\mathbf{Y}_c = \frac{2}{3}[Y_b\cos(\omega t)\cos(\omega t-120^\circ-\theta_b) - Y_a\cos(\omega t-120^\circ)\cos(\omega t-\theta_a)]\mathbf{c}. \quad (3.179)$$

Using $\cos(\alpha)\cos(\beta) = 1/2[\cos(\alpha+\beta)+\cos(\alpha-\beta)]$

$$\mathbf{Y}_a = \frac{1}{3}[Y_c\cos(\theta_c+120^\circ) + Y_c\cos(2\omega t-\theta_c) - Y_b\cos(\theta_b-120^\circ) - Y_b\cos(2\omega t-\theta_b)]\mathbf{a}, \quad (3.180)$$

$$\mathbf{Y}_b = \frac{1}{3}[Y_a\cos(\theta_a+120^\circ) + Y_a\cos(2\omega t+120^\circ-\theta_a) - Y_c\cos(\theta_c-120^\circ) - Y_c\cos(2\omega t+120^\circ-\theta_c)]\mathbf{b}, \quad (3.181)$$

$$\mathbf{Y}_c = \frac{1}{3}[Y_b \cos(\theta_b + 120^\circ) + Y_b \cos(2\omega t - 120^\circ - \theta_b) \\ - Y_a \cos(\theta_a - 120^\circ) - Y_a \cos(2\omega t - 120^\circ - \theta_a)]\mathbf{c}. \quad (3.182)$$

Then, the Q-admittance of this load can be expressed as

$$\mathbf{Y} = \mathrm{Re}(\mathbf{Y}) + \mathbf{Y}_a + \mathbf{Y}_b + \mathbf{Y}_c \quad (3.183)$$

Alternatively, grouping the terms that are associated to the same admittance, it can be rewritten as

$$\mathbf{Y} = \mathbf{Y}_A + \mathbf{Y}_B + \mathbf{Y}_C, \quad (3.184)$$

where

$$\mathbf{Y}_A = \frac{Y_a}{3}[(\cos(\theta_a) + \cos(2\omega t - \theta_a)) + (\cos(\theta_a + 120^\circ) + \cos(2\omega t + 120^\circ - \theta_a))\mathbf{b} \\ - (\cos(\theta_a - 120^\circ) + \cos(2\omega t - 120^\circ - \theta_a))\mathbf{c}], \quad (3.185)$$

$$\mathbf{Y}_B = \frac{Y_b}{3}[(\cos(\theta_b) + \cos(2\omega t + 120^\circ - \theta_b)) - (\cos(\theta_b - 120^\circ) + \cos(2\omega t - \theta_b))\mathbf{a} \\ + (\cos(\theta_b + 120^\circ) + \cos(2\omega t - 120^\circ - \theta_b))\mathbf{c}], \quad (3.186)$$

$$\mathbf{Y}_C = \frac{Y_c}{3}[(\cos(\theta_c) + \cos(2\omega t - 120^\circ - \theta_c)) + (\cos(\theta_c + 120^\circ) + \cos(2\omega t - \theta_c))\mathbf{a} \\ - (\cos(\theta_c - 120^\circ) + \cos(2\omega t + 120^\circ - \theta_c))\mathbf{b}]. \quad (3.187)$$

It is noteworthy that each of the components of this Q-admittance relates two imaginary axis and the real axis. A further simplification can be achieved using the missing basic quaternion in each component.

$$\mathbf{a}\mathbf{Y}_A = \frac{Y_a}{3}[(\cos(\theta_a) + \cos(2\omega t - \theta_a))\mathbf{a} + (\cos(\theta_a + 120^\circ) + \cos(2\omega t + 120^\circ - \theta_a))\mathbf{c} \\ + (\cos(\theta_a - 120^\circ) + \cos(2\omega t - 120^\circ - \theta_a))\mathbf{b}], \quad (3.188)$$

$$\mathbf{b}\mathbf{Y}_B = \frac{Y_b}{3}[(\cos(\theta_b) + \cos(2\omega t + 120^\circ - \theta_b))\mathbf{b} + (\cos(\theta_b - 120^\circ) + \cos(2\omega t - \theta_b))\mathbf{c} \\ + (\cos(\theta_b + 120^\circ) + \cos(2\omega t - 120^\circ - \theta_b))\mathbf{a}], \quad (3.189)$$

$$\mathbf{c}\mathbf{Y}_C = \frac{Y_c}{3}[(\cos(\theta_c) + \cos(2\omega t - 120^\circ - \theta_c))\mathbf{c} + (\cos(\theta_c + 120^\circ) + \cos(2\omega t - \theta_c))\mathbf{b} \\ + (\cos(\theta_c - 120^\circ) + \cos(2\omega t + 120^\circ - \theta_c))\mathbf{a}]. \quad (3.190)$$

The expressions eqs. (3.188) to (3.190) are similar to eq. (3.4), except for the fact that the first refers to Q-admittance and the latter to Q-voltage. Nevertheless, eq. (3.23) can be used for simplifying even further.

$$\mathbf{a}\mathbf{Y}_A = \frac{Y_a}{\sqrt{6}}(e^{\mathbf{n}(\theta_a)}\mathbf{q}_p + e^{\mathbf{n}(2\omega t-\theta_a)}\mathbf{q}_p), \tag{3.191}$$

$$\mathbf{b}\mathbf{Y}_B = \frac{Y_b}{\sqrt{6}}(e^{\mathbf{n}(\theta_b+\frac{2\pi}{3})}\mathbf{q}_p + e^{\mathbf{n}(2\omega t-\frac{2\pi}{3}-\theta_b)}\mathbf{q}_p), \tag{3.192}$$

$$\mathbf{c}\mathbf{Y}_C = \frac{Y_c}{\sqrt{6}}(e^{\mathbf{n}(\theta_c-\frac{2\pi}{3})}\mathbf{q}_p + e^{\mathbf{n}(2\omega t+\frac{2\pi}{3}-\theta_c)}\mathbf{q}_p). \tag{3.193}$$

Finally, the Q-admittance of the unbalanced grounded wye load is expressed as

$$\begin{aligned}\mathbf{Y} = \mathbf{a}^{-1}\frac{Y_a}{\sqrt{6}}(e^{\mathbf{n}(\theta_a)}\mathbf{q}_p + e^{\mathbf{n}(2\omega t-\theta_a)}\mathbf{q}_p) + \mathbf{b}^{-1}\frac{Y_b}{\sqrt{6}}(e^{\mathbf{n}(\theta_b+\frac{2\pi}{3})}\mathbf{q}_p + e^{\mathbf{n}(2\omega t-\frac{2\pi}{3}-\theta_b)}\mathbf{q}_p)\\ + \mathbf{c}^{-1}\frac{Y_c}{\sqrt{6}}(e^{\mathbf{n}(\theta_c-\frac{2\pi}{3})}\mathbf{q}_p + e^{\mathbf{n}(2\omega t+\frac{2\pi}{3}-\theta_c)}\mathbf{q}_p).\end{aligned} \tag{3.194}$$

Since the ground isolates each phase, the Q-admittance is made up of three independent components. Each component represents a rotating circle, but the three circles are in different spaces. As a consequence, the geometric representation of the composition lies in the hyper-complex space. However, this decomposed form already produces interesting results. It is noticeable, e.g., that

$$\mathbf{Y}_A\mathbf{V}(t) = i_a(t)\mathbf{a} = \sqrt{2}V_oY_a\cos(\omega t-\theta_a)\mathbf{a}, \tag{3.195}$$

$$\mathbf{Y}_B\mathbf{V}(t) = i_b(t)\mathbf{b} = \sqrt{2}V_oY_b\cos(\omega t-120^\circ-\theta_b)\mathbf{b}, \tag{3.196}$$

$$\mathbf{Y}_C\mathbf{V}(t) = i_c(t)\mathbf{c} = \sqrt{2}V_oY_c\cos(\omega t+120^\circ-\theta_c)\mathbf{c}, \tag{3.197}$$

that is, the expression allows obtaining each current separately, which is expected with the addition of the ground wire.

The Q-admittance of the solidly grounded wye can also be written in terms of a constant part and a varying in time part. Using eqs. (3.176) and (3.180) to (3.182), eq. (3.183) can be written as

$$\begin{aligned}\mathbf{Y} = \frac{1}{3}[&Y_a\cos(2\omega t-\theta_a) + Y_b\cos(2\omega t+120^\circ-\theta_b) + Y_c\cos(2\omega t-120^\circ-\theta_c)\\ &+ (Y_c\cos(2\omega t-\theta_c) - Y_b\cos(2\omega t-\theta_b))\mathbf{a}\\ &+ (Y_a\cos(2\omega t+120^\circ-\theta_a) - Y_c\cos(2\omega t+120^\circ-\theta_c))\mathbf{b}\\ &+ (Y_b\cos(2\omega t-120^\circ-\theta_b) - Y_a\cos(2\omega t-120^\circ-\theta_a))\mathbf{c} + \mathbf{Y}_o],\end{aligned} \tag{3.198}$$

where

$$\mathbf{Y}_o = Y_a\cos(\theta_a) + Y_b\cos(\theta_b) + Y_c\cos(\theta_c) + (Y_c\cos(\theta_c + 120^\circ) - Y_b\cos(\theta_b - 120^\circ))\mathbf{a}$$
$$+ (Y_a\cos(\theta_a + 120^\circ) - Y_c\cos(\theta_c - 120^\circ))\mathbf{b} + (Y_b\cos(\theta_b + 120^\circ) - Y_a\cos(\theta_a - 120^\circ))\mathbf{c}, \quad (3.199)$$

Then, applying the trigonometric identity $\cos(\alpha - \beta) = \cos(\alpha)\cos(\beta) + \sin(\alpha)\sin(\beta)$

$$\boxed{\mathbf{Y} = \frac{1}{3}[\cos(2\omega t)\mathbf{Y}_\varphi + \sin(2\omega t)\mathbf{Y}_\psi + \mathbf{Y}_o],} \quad (3.200)$$

where

$$\mathbf{Y}_\varphi = Y_a\cos(\theta_a) + Y_b\cos(\theta_b - 120^\circ) + Y_c\cos(\theta_c + 120^\circ) + (Y_c\cos(\theta_c) - Y_b\cos(\theta_b))\mathbf{a}$$
$$+ (Y_a\cos(\theta_a - 120^\circ) - Y_c\cos(\theta_c - 120^\circ))\mathbf{b} + (Y_b\cos(\theta_b + 120^\circ) - Y_a\cos(\theta_a + 120^\circ))\mathbf{c}, \quad (3.201)$$

$$\mathbf{Y}_\psi = Y_a\sin(\theta_a) + Y_b\sin(\theta_b - 120^\circ) + Y_c\sin(\theta_c + 120^\circ) + (Y_c\sin(\theta_c) - Y_b\sin(\theta_b))\mathbf{a}$$
$$+ (Y_a\sin(\theta_a - 120^\circ) - Y_c\sin(\theta_c - 120^\circ))\mathbf{b} + (Y_b\sin(\theta_b + 120^\circ) - Y_a\sin(\theta_a + 120^\circ))\mathbf{c}. \quad (3.202)$$

From eq. (3.200) it is observed that the Q-admittance locus is a circumference in the $\mathbb{H}$ space, with center in $^{\mathbf{Y}_o}/_3$ and radius $^{Y_r}/_3$ determined by

$$Y_r^2 = |\cos(2\omega t)\mathbf{Y}_\varphi + \sin(2\omega t)\mathbf{Y}_\psi|^2 = \frac{3}{2}(Y_a^2 + Y_b^2 + Y_c^2) + \sqrt{3}(Y_aY_bcos(\theta_a - \theta_b + 150^\circ)$$
$$+ Y_bY_ccos(\theta_b - \theta_c + 150^\circ) + Y_cY_acos(\theta_c - \theta_a + 150^\circ)). \quad (3.203)$$

It is also noteworthy that $\mathbf{Y}_\varphi$ and $\mathbf{Y}_\psi$ are orthogonal, that is, their dot product is null.

3.4.2.2 Grounded wye load

In this subsection, an unbalanced grounded wye load as presented in Fig. 3.31 is analyzed. Its phase admittances are, respectively, $Y_ae^{-j\theta_a}$, $Y_be^{-j\theta_b}$ and $Y_ce^{-j\theta_c}$, where $Y_me^{-j\theta_m}$ is the complex representation of the admittance connected to phase m. Additionally, the central node is connected to the ground with and admittance $Y_ne^{-j\theta_n}$

The source voltage $\mathbf{V}(t)$ is given by eq. (3.4). The voltage on the central node can be written with phasors as

$$V_ne^{j\theta_n} = \frac{V_ae^{j0}Y_ae^{-j\theta_a} + V_be^{j\frac{2\pi}{3}}Y_be^{-j\theta_b} + V_ce^{-j\frac{2\pi}{3}}Y_ce^{-j\theta_c}}{Y_ae^{-j\theta_a} + Y_be^{-j\theta_b} + Y_ce^{-j\theta_c} + Y_ne^{-j\theta_n}}, \quad (3.204)$$

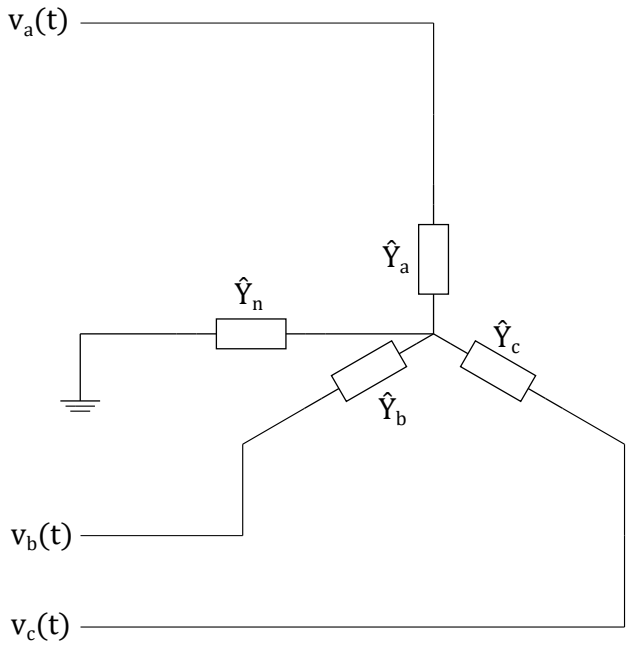

Figure 3.31: Grounded three-phase load.

and the line currents can be computed as

$$I_a e^{j\Theta_a} = (V_a e^{j0} - V_n e^{j\theta_n}) Y_a e^{-j\theta_a}, \tag{3.205}$$

$$I_b e^{j\Theta_b} = (V_b e^{-j\frac{2\pi}{3}} - V_n e^{j\theta_n}) Y_b e^{-j\theta_b}, \tag{3.206}$$

$$I_c e^{j\Theta_c} = (V_c e^{j\frac{2\pi}{3}} - V_n e^{j\theta_n}) Y_c e^{-j\theta_c}, \tag{3.207}$$

which results in

$$I_a e^{j\Theta_a} = \frac{(V_{ab} e^{j\frac{\pi}{6}} Y_b e^{-j\theta_b} - V_{ca} e^{j\frac{5\pi}{6}} Y_c e^{-j\theta_c} + V_a e^{j0} Y_n e^{-j\theta_n}) Y_a e^{-j\theta_a}}{Y_\varsigma e^{-j\theta_\varsigma}}, \tag{3.208}$$

$$I_b e^{j\Theta_b} = \frac{(V_{bc} e^{-j\frac{\pi}{2}} Y_c e^{-j\theta_c} - V_{ab} e^{j\frac{\pi}{6}} Y_a e^{-j\theta_a} + V_b e^{-j\frac{2\pi}{3}} Y_n e^{-j\theta_n}) Y_b e^{-j\theta_b}}{Y_\varsigma e^{-j\theta_\varsigma}}, \tag{3.209}$$

$$I_c e^{j\Theta_c} = \frac{(V_{ca} e^{j\frac{5\pi}{6}} Y_a e^{-j\theta_a} - V_{bc} e^{-j\frac{\pi}{2}} Y_b e^{-j\theta_b} + V_c e^{j\frac{2\pi}{3}} Y_n e^{-j\theta_n}) Y_c e^{-j\theta_c}}{Y_\varsigma e^{-j\theta_\varsigma}}, \tag{3.210}$$

where

$$Y_\varsigma e^{-j\theta_\varsigma} = Y_a e^{-j\theta_a} + Y_b e^{-j\theta_b} + Y_c e^{-j\theta_c} + Y_n e^{-j\theta_n}. \tag{3.211}$$

In the time-domain, each current can be written as

$$\begin{aligned} i_a(t) = \frac{\sqrt{2}V_o}{Y_\varsigma} [&Y_a Y_b \sqrt{3} \cos(\omega t + 30^\circ - \theta_a - \theta_b + \theta_\varsigma) \\ &- Y_c Y_a \sqrt{3} \cos(\omega t + 150^\circ - \theta_c - \theta_a + \theta_\varsigma) + Y_a Y_n \cos(\omega t - \theta_a - \theta_n + \theta_\varsigma)], \end{aligned} \tag{3.212}$$

$$i_b(t) = \frac{\sqrt{2}V_o}{Y_\varsigma}[Y_bY_c\sqrt{3}\cos(\omega t - 90^\circ - \theta_b - \theta_c + \theta_\varsigma) \\ - \sqrt{3}Y_aY_b\cos(\omega t + 30^\circ - \theta_a - \theta_b + \theta_\varsigma) + Y_bY_n\cos(\omega t - 120^\circ - \theta_b - \theta_n + \theta_\varsigma)], \quad (3.213)$$

$$i_c(t) = \frac{\sqrt{2}V_o}{Y_\varsigma}[Y_cY_a\sqrt{3}\cos(\omega t + 150^\circ - \theta_c - \theta_a + \theta_\varsigma) \\ - Y_bY_c\sqrt{3}\cos(\omega t - 90^\circ - \theta_b - \theta_c + \theta_\varsigma) + Y_cY_n\cos(\omega t + 120^\circ - \theta_c - \theta_n + \theta_\varsigma)]. \quad (3.214)$$

The Q-current is given by

$$\mathbf{I}(t) = i_a(t)\mathbf{a} + i_b(t)\mathbf{b} + i_c(t)\mathbf{c}, \quad (3.215)$$

which can also be written in the form

$$\mathbf{I}(t) = \mathbf{I}_\Delta(t) + \mathbf{I}_\Upsilon(t), \quad (3.216)$$

where

$$\mathbf{I}_\Delta(t) = \frac{\sqrt{6}V_o}{Y_\varsigma}[(Y_aY_b\cos(\omega t + 30^\circ - \theta_a - \theta_b + \theta_\varsigma) - Y_cY_a\cos(\omega t + 150^\circ - \theta_c - \theta_a + \theta_\varsigma))\mathbf{a} \\ + (Y_bY_c\cos(\omega t - 90^\circ - \theta_b - \theta_c + \theta_\varsigma) - Y_aY_b\cos(\omega t + 30^\circ - \theta_a - \theta_b + \theta_\varsigma))\mathbf{b} \\ + (Y_cY_a\cos(\omega t + 150^\circ - \theta_c - \theta_a + \theta_\varsigma) - Y_bY_c\cos(\omega t - 90^\circ - \theta_b - \theta_c + \theta_\varsigma))\mathbf{c}], \quad (3.217)$$

$$\mathbf{I}_\Upsilon(t) = \frac{\sqrt{2}Y_nV_o}{Y_\varsigma}[Y_a\cos(\omega t - \theta_a - \theta_n + \theta_\varsigma)\mathbf{a} + Y_b\cos(\omega t - 120^\circ - \theta_b - \theta_n + \theta_\varsigma)\mathbf{b} \\ + Y_c\cos(\omega t + 120^\circ - \theta_c - \theta_n + \theta_\varsigma)\mathbf{c}]. \quad (3.218)$$

As a consequence, Q-admittance can also be decomposed in two components

$$\boxed{\mathbf{Y} = \mathbf{I}\mathbf{V}^{-1} = \mathbf{I}_\Delta(t)\mathbf{V}^{-1} + \mathbf{I}_\Upsilon(t)\mathbf{V}^{-1} = \mathbf{Y}_\Delta(t) + \mathbf{Y}_\Upsilon(t).} \quad (3.219)$$

It can be noticed that $\mathbf{I}_\Upsilon(t)$ is similar to the Q-current obtained in eq. (3.174). The difference is that each angle is added $\theta_\varsigma - \theta_n$ and $\mathbf{I}(t)$ is multiplied by Y_n/Y_ς. Considering these adjustments, eq. (3.218) can be rewritten using eq. (3.194) as

$$\mathbf{Y}_\Upsilon(t) = \frac{Y_n}{Y_\varsigma}[\mathbf{a}^{-1}\frac{Y_a}{\sqrt{6}}(e^{\mathbf{n}(\theta_a+\theta_n-\theta_\varsigma)}\mathbf{q}_p + e^{\mathbf{n}(2\omega t-\theta_a-\theta_n+\theta_\varsigma)}\mathbf{q}_p) \\ + \mathbf{b}^{-1}\frac{Y_b}{\sqrt{6}}(e^{\mathbf{n}(\theta_b+\theta_n-\theta_\varsigma+\frac{2\pi}{3})}\mathbf{q}_p + e^{\mathbf{n}(2\omega t-\frac{2\pi}{3}-\theta_b-\theta_n+\theta_\varsigma)}\mathbf{q}_p) \\ + \mathbf{c}^{-1}\frac{Y_c}{\sqrt{6}}(e^{\mathbf{n}(\theta_c+\theta_n-\theta_\varsigma-\frac{2\pi}{3})}\mathbf{q}_p + e^{\mathbf{n}(2\omega t+\frac{2\pi}{3}-\theta_c-\theta_n+\theta_\varsigma)}\mathbf{q}_p)], \quad (3.220)$$

which can also be written as

$$\begin{aligned}\mathbf{Y}_{\Upsilon}(t) = (&\mathbf{a}^{-1}\frac{Y_a}{\sqrt{6}}\mathbf{q}_p e^{-\mathbf{n}(\theta_a)} + \mathbf{b}^{-1}\frac{Y_b}{\sqrt{6}}\mathbf{q}_p e^{-\mathbf{n}(\theta_b+\frac{2\pi}{3})} \\ &+ \mathbf{c}^{-1}\frac{Y_c}{\sqrt{6}}\mathbf{q}_p e^{-\mathbf{n}(\theta_c-\frac{2\pi}{3})})Y_n e^{-\mathbf{n}(\theta_n)}(Y_\varsigma e^{-\mathbf{n}(\theta_\varsigma)})^{-1} + (\mathbf{a}^{-1}\frac{Y_a}{\sqrt{6}}\mathbf{q}_p e^{-\mathbf{n}(2\omega t-\theta_a)} \\ &+ \mathbf{b}^{-1}\frac{Y_b}{\sqrt{6}}\mathbf{q}_p e^{-\mathbf{n}(2\omega t-\frac{2\pi}{3}-\theta_b)} + \mathbf{c}^{-1}\frac{Y_c}{\sqrt{6}}\mathbf{q}_p e^{-\mathbf{n}(2\omega t+\frac{2\pi}{3}-\theta_c)})Y_n e^{\mathbf{n}(\theta_n)}(Y_\varsigma e^{\mathbf{n}(\theta_\varsigma)})^{-1},\end{aligned} \tag{3.221}$$

where

$$Y_\varsigma e^{-\mathbf{n}\theta_\varsigma} = Y_a e^{-\mathbf{n}\theta_a} + Y_b e^{-\mathbf{n}\theta_b} + Y_c e^{-\mathbf{n}\theta_c} + Y_n e^{-\mathbf{n}\theta_n}. \tag{3.222}$$

Next, $\mathbf{Y}_{\Delta}(t)$ is calculated. Computing its real part

$$\begin{aligned}\mathrm{Re}(\mathbf{Y}_{\Delta}(t)) = \frac{2}{\sqrt{3}}[&\frac{\cos(\omega t)}{Y_\varsigma}(Y_a Y_b\cos(\omega t+30^\circ-\theta_a-\theta_b+\theta_\varsigma) - Y_c Y_a\cos(\omega t+150^\circ-\theta_c-\theta_a+\theta_\varsigma)) \\ &+ \frac{\cos(\omega t-120^\circ)}{Y_\varsigma}(Y_b Y_c\cos(\omega t-90^\circ-\theta_b-\theta_c+\theta_\varsigma) - Y_a Y_b\cos(\omega t+30^\circ-\theta_a-\theta_b+\theta_\varsigma)) \\ &+ \frac{\cos(\omega t+120^\circ)}{Y_\varsigma}(Y_c Y_a\cos(\omega t+150^\circ-\theta_c-\theta_a+\theta_\varsigma) - Y_b Y_c\cos(\omega t-90^\circ-\theta_b-\theta_c+\theta_\varsigma))]\end{aligned} \tag{3.223}$$

Using that $\cos(\alpha) - \cos(\alpha-120^\circ) = \sqrt{3}\cos(\alpha+30^\circ)$,

$$\begin{aligned}\mathrm{Re}(\mathbf{Y}_{\Delta}(t)) = 2[&\frac{1}{Y_\varsigma}(Y_a Y_b\cos(\omega t+30^\circ)\cos(\omega t+30^\circ-\theta_a-\theta_b+\theta_\varsigma)) \\ &+ \frac{1}{Y_\varsigma}(Y_b Y_c\cos(\omega t-90^\circ)\cos(\omega t-90^\circ-\theta_b-\theta_c+\theta_\varsigma)) \\ &+ \frac{1}{Y_\varsigma}(Y_c Y_a\cos(\omega t+150^\circ)\cos(\omega t+150^\circ-\theta_c-\theta_a+\theta_\varsigma))].\end{aligned} \tag{3.224}$$

Applying the trigonometric relation $\cos(\alpha)\cos(\alpha-\beta) = 1/2(\cos(2\alpha-\beta)+\cos(\beta))$

$$\begin{aligned}\mathrm{Re}(\mathbf{Y}_{\Delta}(t)) = \frac{1}{Y_\varsigma}[&Y_a Y_b\cos(\theta_a+\theta_b-\theta_\varsigma) + Y_b Y_c\cos(\theta_b+\theta_c-\theta_\varsigma) + Y_c Y_a\cos(\theta_c+\theta_a-\theta_\varsigma) \\ &+ Y_a Y_b\cos(2\omega t+60^\circ-\theta_a-\theta_b+\theta_\varsigma) + Y_b Y_c\cos(2\omega t-180^\circ-\theta_b-\theta_c+\theta_\varsigma) \\ &+ Y_c Y_a\cos(2\omega t-60^\circ-\theta_c-\theta_a+\theta_\varsigma)].\end{aligned} \tag{3.225}$$

The vectorial part of the Q-admittance $\vec{\mathbf{Y}}_{\Delta}(t)$ is determined by eq. (3.118). Determining its components.

$$\begin{aligned}\mathbf{Y}_{\Delta_a} = \frac{2}{\sqrt{3}}[&\frac{\cos(\omega t)}{Y_\varsigma}(Y_c Y_a\cos(\omega t+150^\circ-\theta_c-\theta_a+\theta_\varsigma) - Y_b Y_c\cos(\omega t-90^\circ-\theta_b-\theta_c+\theta_\varsigma)) \\ &- \frac{\cos(\omega t+120^\circ)}{Y_\varsigma}(Y_b Y_c\cos(\omega t-90^\circ-\theta_b-\theta_c+\theta_\varsigma) - Y_a Y_b\cos(\omega t+30^\circ-\theta_a-\theta_b+\theta_\varsigma))]\mathbf{a},\end{aligned} \tag{3.226}$$

$$\mathbf{Y}_{\Delta_b} = \frac{2}{\sqrt{3}}[\frac{\cos(\omega t - 120^\circ)}{Y_\varsigma}(Y_a Y_b \cos(\omega t + 30^\circ - \theta_a - \theta_b + \theta_\varsigma)$$
$$- Y_c Y_a \cos(\omega t + 150^\circ - \theta_c - \theta_a + \theta_\varsigma)) - \frac{\cos(\omega t)}{Y_\varsigma}(Y_c Y_a \cos(\omega t + 150^\circ - \theta_c - \theta_a + \theta_\varsigma)$$
$$- Y_b Y_c \cos(\omega t - 90^\circ - \theta_b - \theta_c + \theta_\varsigma))]\mathbf{b}, \quad (3.227)$$

$$\mathbf{Y}_{\Delta_c} = \frac{2}{\sqrt{3}}[\frac{\cos(\omega t + 120^\circ)}{Y_\varsigma}(Y_b Y_c \cos(\omega t - 90^\circ - \theta_b - \theta_c + \theta_\varsigma)$$
$$- Y_a Y_b \cos(\omega t + 30^\circ - \theta_a - \theta_b + \theta_\varsigma))$$
$$- \frac{\cos(\omega t - 120^\circ)}{Y_\varsigma}(Y_a Y_b \cos(\omega t + 30^\circ - \theta_a - \theta_b + \theta_\varsigma)$$
$$- Y_c Y_a \cos(\omega t + 150^\circ - \theta_c - \theta_a + \theta_\varsigma))]\mathbf{c}. \quad (3.228)$$

Using that $\cos(a) + \cos(a + 120^\circ) = -\cos(a - 120^\circ)$

$$\mathbf{Y}_{\Delta_a} = \frac{2}{\sqrt{3}}[\frac{\cos(\omega t)}{Y_\varsigma} Y_c Y_a \cos(\omega t + 150^\circ - \theta_c - \theta_a + \theta_\varsigma)$$
$$+ \frac{\cos(\omega t - 120^\circ)}{Y_\varsigma} Y_b Y_c \cos(\omega t - 90^\circ - \theta_b - \theta_c + \theta_\varsigma)$$
$$+ \frac{\cos(\omega t + 120^\circ)}{Y_\varsigma} Y_a Y_b \cos(\omega t + 30^\circ - \theta_a - \theta_b + \theta_\varsigma)]\mathbf{a}, \quad (3.229)$$

$$\mathbf{Y}_{\Delta_b} = \frac{\cos(\omega t + 120^\circ)}{Y_\varsigma} Y_a Y_b \cos(\omega t + 30^\circ - \theta_a - \theta_b + \theta_\varsigma)$$
$$+ \frac{2}{\sqrt{3}}[\frac{\cos(\omega t)}{Y_\varsigma} Y_c Y_a \cos(\omega t + 150^\circ - \theta_c - \theta_a + \theta_\varsigma)$$
$$+ \frac{\cos(\omega t - 120^\circ)}{Y_\varsigma} Y_b Y_c \cos(\omega t - 90^\circ - \theta_b - \theta_c + \theta_\varsigma)]\mathbf{b}, \quad (3.230)$$

$$\mathbf{Y}_{\Delta_c} = \frac{\cos(\omega t - 120^\circ)}{Y_\varsigma} Y_b Y_c \cos(\omega t - 90^\circ - \theta_b - \theta_c + \theta_\varsigma)$$
$$+ \frac{\cos(\omega t + 120^\circ)}{Y_\varsigma} Y_a Y_b \cos(\omega t + 30^\circ - \theta_a - \theta_b + \theta_\varsigma)$$
$$+ \frac{2}{\sqrt{3}}[\frac{\cos(\omega t)}{Y_\varsigma} Y_c Y_a \cos(\omega t + 150^\circ - \theta_c - \theta_a + \theta_\varsigma)]\mathbf{c}. \quad (3.231)$$

It is observed that $|\mathbf{Y}_{\Delta_a}| = |\mathbf{Y}_{\Delta_b}| = |\mathbf{Y}_{\Delta_c}|$. So, $\vec{\mathbf{Y}}_\Delta(t) = \sqrt{3}|\mathbf{Y}_{\Delta_a}|\mathbf{n}$. Using $\cos(\alpha)\cos(\beta) = {}^1\!/_2[\cos(\alpha + \beta) + \cos(\alpha - \beta)]$ to calculate $\mathbf{Y}_{\Delta_a}$

$$\mathbf{Y}_{\Delta_a} = \frac{1}{\sqrt{3}Y_\varsigma}[Y_c Y_a \cos(\theta_c + \theta_a - \theta_\varsigma + 90^\circ) + Y_b Y_c \cos(\theta_b + \theta_c - \theta_\varsigma + 90^\circ)$$
$$+ Y_a Y_b \cos(\theta_a + \theta_b - \theta_\varsigma + 90^\circ) + Y_c Y_a \cos(2\omega t + 30^\circ - \theta_c - \theta_a + \theta_\varsigma)$$
$$+ Y_b Y_c \cos(2\omega t - 90^\circ - \theta_b - \theta_c + \theta_\varsigma) + Y_a Y_b \cos(2\omega t + 150^\circ - \theta_a - \theta_b + \theta_\varsigma)]\mathbf{a}, \quad (3.232)$$

Applying $\cos(\alpha + 90^\circ) = -\sin(\alpha)$

$$\begin{aligned}\mathbf{Y}_{\Delta_a} = \frac{1}{\sqrt{3}Y_\varsigma}[&Y_cY_a\sin(\theta_c+\theta_a-\theta_\varsigma) + Y_bY_c\sin(\theta_b+\theta_c-\theta_\varsigma) + Y_aY_b\sin(\theta_a+\theta_b-\theta_\varsigma)\\ &+ Y_cY_a\sin(2\omega t - 60^\circ - \theta_c - \theta_a + \theta_\varsigma) + Y_bY_c\sin(2\omega t - 180^\circ - \theta_b - \theta_c + \theta_\varsigma)\\ &+ Y_aY_b\sin(2\omega t + 60^\circ - \theta_a - \theta_b + \theta_\varsigma)]\mathbf{a}, \quad (3.233)\end{aligned}$$

The polar form of $\mathbf{Y}_\Delta$ can by written as

$$\begin{aligned}\mathbf{Y}_\Delta(t) = \frac{1}{Y_\varsigma}[&Y_cY_ae^{-\mathbf{n}(\theta_c+\theta_a-\theta_\varsigma)} + Y_bY_ce^{-\mathbf{n}(\theta_b+\theta_c-\theta_\varsigma)} + Y_aY_be^{-\mathbf{n}(\theta_a+\theta_b-\theta_\varsigma)}\\ &+ Y_cY_ae^{-\mathbf{n}(2\omega t-\frac{\pi}{3}-\theta_c-\theta_a+\theta_\varsigma)} + Y_bY_ce^{-\mathbf{n}(2\omega t-\pi-\theta_b-\theta_c+\theta_\varsigma)} + Y_aY_be^{-\mathbf{n}(2\omega t+\frac{\pi}{3}-\theta_a-\theta_b+\theta_\varsigma)}], \quad (3.234)\end{aligned}$$

Alternatively

$$\begin{aligned}&\mathbf{Y}_\Delta(t) = (Y_\varsigma e^{-\mathbf{n}(\theta_\varsigma)})^{-1}(Y_aY_be^{-\mathbf{n}(\theta_a+\theta_b)} + Y_bY_ce^{-\mathbf{n}(\theta_b+\theta_c)} + Y_cY_ae^{-\mathbf{n}(\theta_c+\theta_a)})\\ &+ (Y_\varsigma e^{\mathbf{n}(\theta_\varsigma)})^{-1}(Y_aY_be^{-\mathbf{n}(2\omega t+\frac{\pi}{3}-\theta_a-\theta_b)} + Y_bY_ce^{-\mathbf{n}(2\omega t-\pi-\theta_b-\theta_c)} + Y_cY_ae^{-\mathbf{n}(2\omega t-\frac{\pi}{3}-\theta_c-\theta_a)}). \quad (3.235)\end{aligned}$$

Next, the replacement of the neutral impedance by an short-circuit is considered. Since

$$\lim_{Y_n\to\infty}(Y_ae^{-\mathbf{n}\theta_a} + Y_be^{-\mathbf{n}\theta_b} + Y_ce^{-\mathbf{n}\theta_c} + Y_ne^{-\mathbf{n}\theta_n})^{-1} = 0, \quad (3.236)$$

$$\begin{aligned}&\lim_{Y_n\to\infty} Y_ne^{-\mathbf{n}(\theta_n)}(Y_ae^{-\mathbf{n}\theta_a} + Y_be^{-\mathbf{n}\theta_b} + Y_ce^{-\mathbf{n}\theta_c} + Y_ne^{-\mathbf{n}\theta_n})^{-1} =\\ &\lim_{Y_n\to\infty} e^{-\mathbf{n}(\theta_n)}\left(\frac{Y_a}{Y_n}e^{-\mathbf{n}\theta_a} + \frac{Y_b}{Y_n}e^{-\mathbf{n}\theta_b} + \frac{Y_c}{Y_n}e^{-\mathbf{n}\theta_c} + e^{-\mathbf{n}\theta_n}\right)^{-1} = 1, \quad (3.237)\end{aligned}$$

it can be concluded that

$$\lim_{Y_n\to\infty}\mathbf{Y} = \lim_{Y_n\to\infty}\mathbf{Y}_\Delta(t) + \lim_{Y_n\to\infty}\mathbf{Y}_\Upsilon(t) = \lim_{Y_n\to\infty}\mathbf{Y}_\Upsilon(t), \quad (3.238)$$

$$\begin{aligned}\lim_{Y_n\to\infty}\mathbf{Y} = \mathbf{a}^{-1}\frac{Y_a}{\sqrt{6}}(e^{\mathbf{n}(\theta_a)}\mathbf{q}_p + e^{\mathbf{n}(2\omega t-\theta_a)}\mathbf{q}_p) + \mathbf{b}^{-1}\frac{Y_b}{\sqrt{6}}(e^{\mathbf{n}(\theta_b+\frac{2\pi}{3})}\mathbf{q}_p + e^{\mathbf{n}(2\omega t-\frac{2\pi}{3}-\theta_b)}\mathbf{q}_p)\\ + \mathbf{c}^{-1}\frac{Y_c}{\sqrt{6}}(e^{\mathbf{n}(\theta_c-\frac{2\pi}{3})}\mathbf{q}_p + e^{\mathbf{n}(2\omega t+\frac{2\pi}{3}-\theta_c)}\mathbf{q}_p). \quad (3.239)\end{aligned}$$

It is observed that eqs. (3.194) and (3.239) are the same expressions. This result is expected since an infinite admittance is equivalent to a short-circuit. So, the Q-admittance of the grounded wye becomes equal to the Q-admittance of the solidly grounded wye if the neutral impedance is substituted by a short-circuit.

Afterwards, the replacement of the neutral impedance by an open circuit is considered. Since

$$\lim_{Y_n\to 0}(Y_a e^{-\mathbf{n}\theta_a}+Y_b e^{-\mathbf{n}\theta_b}+Y_c e^{-\mathbf{n}\theta_c}+Y_n e^{-\mathbf{n}\theta_n})^{-1}= \\ (Y_a e^{-\mathbf{n}\theta_a}+Y_b e^{-\mathbf{n}\theta_b}+Y_c e^{-\mathbf{n}\theta_c})^{-1}=Y_\sigma e^{-\mathbf{n}\theta_\sigma}, \quad (3.240)$$

$$\lim_{Y_n\to 0} Y_n e^{-\mathbf{n}(\theta_n)}(Y_a e^{-\mathbf{n}\theta_a}+Y_b e^{-\mathbf{n}\theta_b}+Y_c e^{-\mathbf{n}\theta_c}+Y_n e^{-\mathbf{n}\theta_n})^{-1}=0, \quad (3.241)$$

it can be concluded that

$$\lim_{Y_n\to 0}\mathbf{Y}=\lim_{Y_n\to 0}\mathbf{Y}_\Delta(t)+\lim_{Y_n\to 0}\mathbf{Y}_\Upsilon(t)=\lim_{Y_n\to 0}\mathbf{Y}_\Delta(t), \quad (3.242)$$

$$\lim_{Y_n\to 0}\mathbf{Y}=(Y_\sigma e^{-\mathbf{n}\theta_\sigma})^{-1}(Y_aY_b e^{-\mathbf{n}(\theta_a+\theta_b)}+Y_bY_c e^{-\mathbf{n}(\theta_b+\theta_c)}+Y_cY_a e^{-\mathbf{n}(\theta_c+\theta_a)})+ \\ (Y_\sigma e^{\mathbf{n}\theta_\sigma})^{-1}(Y_aY_b e^{-\mathbf{n}(2\omega t+\frac{\pi}{3}-\theta_a-\theta_b)}+Y_bY_c e^{-\mathbf{n}(2\omega t-\pi-\theta_b-\theta_c)}+Y_cY_a e^{-\mathbf{n}(2\omega t-\frac{\pi}{3}-\theta_c-\theta_a)}). \quad (3.243)$$

It is observed that eqs. (3.166) and (3.243) are the same expressions. This result is also expected, since removing the admittance, the load loses the connection to the neutral, becoming an ungrounded wye load. In this case, the four-wire system becomes a three-wire system.

From the results of eqs. (3.239) and (3.243). it is observed that the grounded wye load is a combination of the solidly grounded wye load and the ungrounded wye load. More specifically, these expressions indicate that the grounded wye load is a parallel combination of the aforementioned loads. Consider $\mathbf{Y}_\Upsilon(t)$ as presented in eq. (3.220). Defining

$$Y_\alpha=\frac{Y_aY_n}{Y_\varsigma}, \quad (3.244)$$

$$Y_\beta=\frac{Y_bY_n}{Y_\varsigma}, \quad (3.245)$$

$$Y_\gamma=\frac{Y_cY_n}{Y_\varsigma}, \quad (3.246)$$

$$\theta_\alpha=\theta_a+\theta_n-\theta_\varsigma, \quad (3.247)$$

$$\theta_\beta=\theta_b+\theta_n-\theta_\varsigma, \quad (3.248)$$

$$\theta_\gamma=\theta_c+\theta_n-\theta_\varsigma, \quad (3.249)$$

the Q-admittance eq. (3.220) can be written as

$$\mathbf{Y}=\mathbf{a}^{-1}\frac{Y_\alpha}{\sqrt{6}}(e^{\mathbf{n}(\theta_\alpha)}\mathbf{q}_p+e^{\mathbf{n}(2\omega t-\theta_\alpha)}\mathbf{q}_p)+\mathbf{b}^{-1}\frac{Y_\beta}{\sqrt{6}}(e^{\mathbf{n}(\theta_\beta+\frac{2\pi}{3})}\mathbf{q}_p+e^{\mathbf{n}(2\omega t-\frac{2\pi}{3}-\theta_\beta)}\mathbf{q}_p) \\ +\mathbf{c}^{-1}\frac{Y_\gamma}{\sqrt{6}}(e^{\mathbf{n}(\theta_\beta-\frac{2\pi}{3})}\mathbf{q}_p+e^{\mathbf{n}(2\omega t+\frac{2\pi}{3}-\theta_\gamma)}\mathbf{q}_p). \quad (3.250)$$

According to eq. (3.194), eq. (3.250) represents the Q-admittance of a solidly grounded wye load with admittances $Y_\alpha e^{-j\theta_\alpha}, Y_\beta e^{-j\theta_\beta}$ and $Y_\gamma e^{-j\theta_\gamma}$, connected to phases A, B and C, respectively.

Next for the delta load, $\mathbf{Y}_\Delta(t)$ as presented in eq. (3.234) is considered. Defining.

$$Y_{\Delta_{ab}} = \frac{Y_a Y_b}{Y_\varsigma}, \tag{3.251}$$

$$Y_{\Delta_{bc}} = \frac{Y_b Y_c}{Y_\varsigma}, \tag{3.252}$$

$$Y_{\Delta_{ca}} = \frac{Y_c Y_a}{Y_\varsigma}, \tag{3.253}$$

$$\theta_{\Delta_{ab}} = \theta_a + \theta_b - \theta_\varsigma, \tag{3.254}$$

$$\theta_{\Delta_{bc}} = \theta_b + \theta_c - \theta_\varsigma, \tag{3.255}$$

$$\theta_{\Delta_{ca}} = \theta_c + \theta_a - \theta_\varsigma, \tag{3.256}$$

the Q-admittance in eq. (3.234) can be written as

$$\begin{aligned}\mathbf{Y}_\Delta(t) = Y_{\Delta_{ab}} e^{-\mathbf{n}\theta_{\Delta_{ab}}} + Y_{\Delta_{bc}} e^{-\mathbf{n}\theta_{\Delta_{bc}}} + Y_{\Delta_{ca}} e^{-\mathbf{n}\theta_{\Delta_{ca}}} + Y_{\Delta_{ab}} e^{-\mathbf{n}(2\omega t + \frac{\pi}{3} - \theta_{\Delta_{ab}})} \\ + Y_{\Delta_{bc}} e^{-\mathbf{n}(2\omega t - \pi - \theta_{\Delta_{bc}})} + Y_{\Delta_{ca}} e^{-\mathbf{n}(2\omega t - \frac{\pi}{3} - \theta_{\Delta_{ca}})},\end{aligned} \tag{3.257}$$

It is observed comparing eq. (3.257) and eq. (3.130) that $\mathbf{Y}_\Delta(t)$ is the Q-admittance of an delta load with admittances $Y_{\Delta_{ab}} e^{-j\theta_{ab}}, Y_{\Delta_{bc}} e^{-j\theta_{\Delta_{bc}}}$ and $Y_{\Delta_{ca}} e^{-j\theta_{\Delta_{ca}}}$ between phases A-B, B-C and C-A, respectively.

Considering eq. (3.250) and eq. (3.257), it is observed that the grounded wye load can be decomposed into a delta load and a solidly grounded wye load. The neutral impedance acts as an converting factor that relates these loads. Fig. 3.32 shows the decomposition of the grounded load.

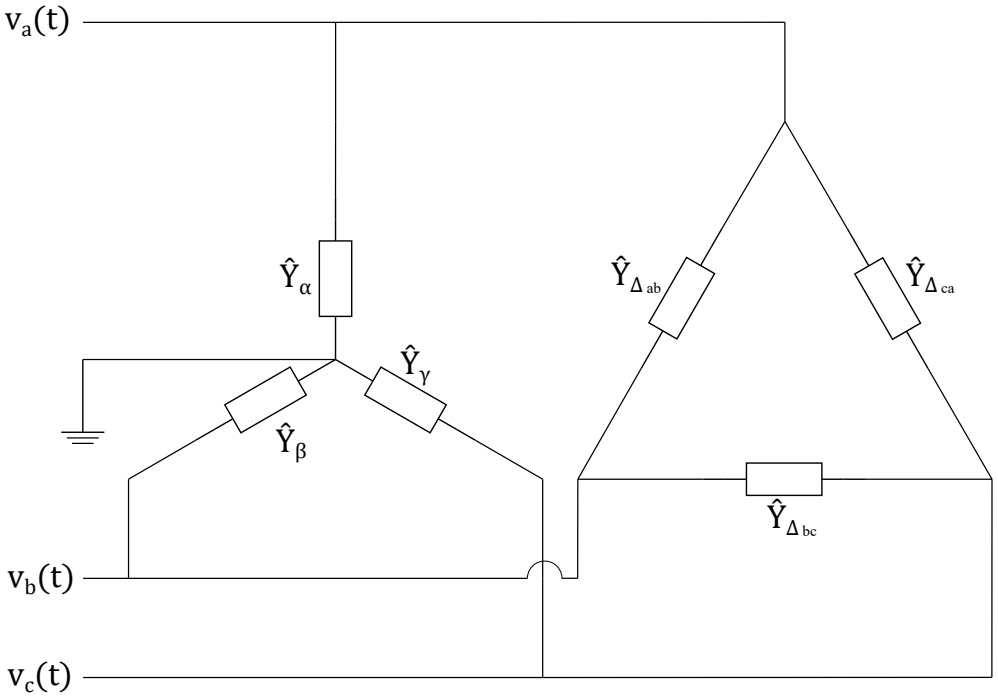

Figure 3.32: Equivalent of the grounded three-phase load.

3.5 Q-POWER ANALYSIS

In this section, the Q-power of some of the loads studied in this chapter is analyzed. In the balanced case, the RL, RC, RLC, and LC loads are considered. In the unbalanced case, only the delta and solidly grounded wye are evaluated. The analysis of an ungrounded wye load is equivalent to the analysis of the delta load, due to Δ-Y transform, so it is not presented here. On the other hand, the grounded wye load was shown to be equivalent to the parallel association of a delta load and a solidly grounded wye. For this reason, the Q-power of the grounded wye load is also not shown.

Starting the analysis, a balanced three-phase load in the steady-state is considered. The Q-power of this load can be calculated using eq. (3.26) in eq. (3.20)

$$Ye^{\mathbf{n}\theta}|\mathbf{V}|^2 = 3V_o^2 Ye^{\mathbf{n}\theta}. \tag{3.258}$$

It is noteworthy that eq. (3.258) is equivalent to the definition of three-phase power of the same load using phasors. If the **n** in eq. (3.258) is substituted by j, the complex power would be obtained. In this sense, a representation of Q-power in a plane, denoted by N_R, formed by the real axis and the axis in the direction of **n** is possible. Considering three three-phase balanced loads in the wye configuration with admittances connected to each phase equal to 1 for the first load, $e^{-j\frac{\pi}{2}}$ for the second and $e^{j\frac{\pi}{6}}$ for the third.

The Q-admittance of these loads is $\mathbf{Y}_1 = e^{\mathbf{n}0}$, $\mathbf{Y}_2 = e^{-\mathbf{n}\frac{\pi}{2}}$ and $\mathbf{Y}_3 = e^{\mathbf{n}\frac{\pi}{6}}$, for the first, second and third load, respectively. Using the admittance of these loads, the Q-power is calculated applying eq. (3.258), with $V_o = 220V$. The representation of the Q-power in the N_R plane is presented in Fig. 3.33.

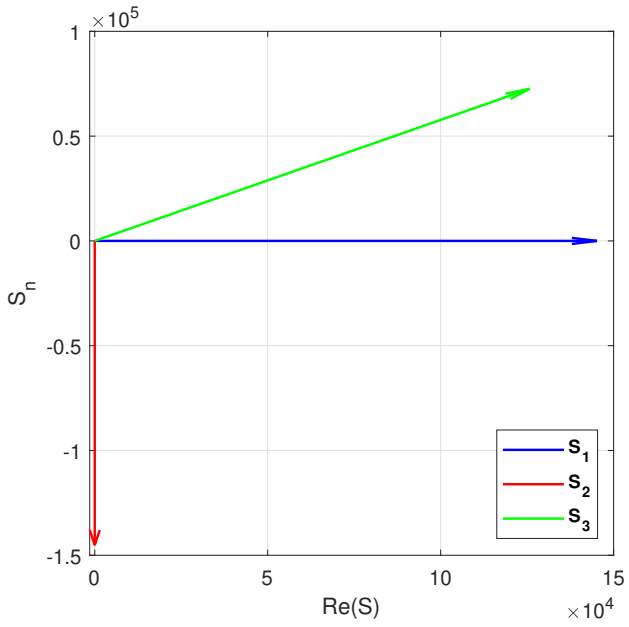

Figure 3.33: Q-power of loads $\mathbf{Y}_1$, $\mathbf{Y}_2$ and $\mathbf{Y}_3$.

It is observed in Fig. 3.33 that the Q-power lies in the real axis for the pure resistive load $\mathbf{Y}_1$ as expected. Analogously, it is located under the real axis for capacitive loads and above it for inductive loads, as observed from the Q-power of pure capacitive load $\mathbf{Y}_2$ and inductive load $\mathbf{Y}_3$. The Q-power is represented in Fig. 3.33 by a vector, since it is a single point in the N_R plane in the steady-state for balanced loads. Nevertheless, it varies in time if the transient state is considered or if the load is unbalanced. Considering this fact, in the rest of this section, the Q-power is represented by its locus.

3.5.1 RL and RC balanced loads

The Q-power can be determined considering the transient and the steady-states using eq. (3.104). Applying eqs. (3.60) and (3.70) in eq. (3.104) the Q-power for RL and RC loads, respectively, can be written as

$$\mathbf{S}_T(t) = 3V_o^2 Y e^{\mathbf{n}\theta} + \sqrt{3}V_o e^{-\frac{R}{L}t} e^{\mathbf{n}\omega t}\mathbf{q}_p\mathbf{k}^*. \tag{3.259}$$

$$\mathbf{S}_T(t) = 3V_o^2 Y e^{\mathbf{n}\theta} + \sqrt{3}V_o e^{-\frac{t}{RC}} e^{\mathbf{n}\omega t}\mathbf{q}_p\mathbf{k}^*. \tag{3.260}$$

Figs. 3.34 and 3.35 present the Q-power of three-phase RL and RC loads, respectively. In the RL load,

$R = 100\,\Omega$ and $L = 1$ H and, in the RC load, $R = 100\,\Omega$ and $C = 100\,\mu$F. In both cases, $\mathbf{I}(0) = 0$ and $V_o = 220$ V.

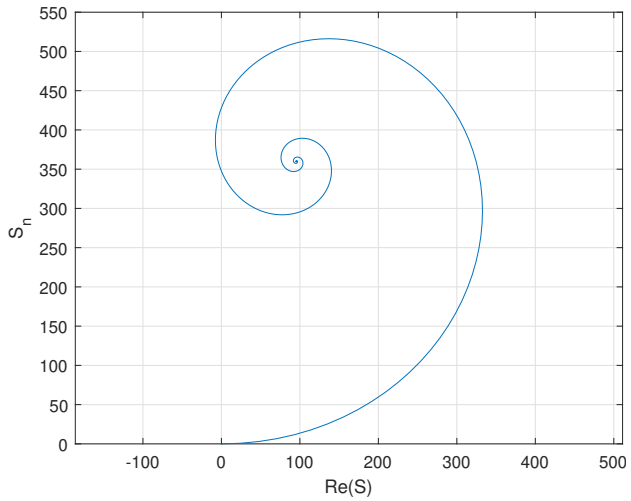

Figure 3.34: Q-power of a three-phase RL load.

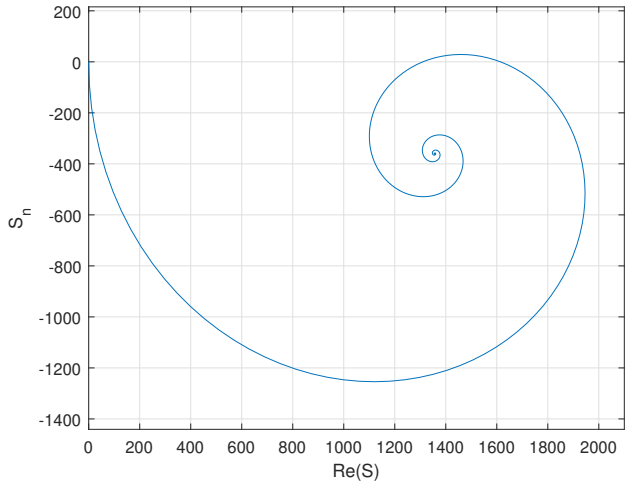

Figure 3.35: Q-power of a three-phase RC load.

It is observed from Figs. 3.34 and 3.35 that the Q-power starts at 0, since the initial value of Q-current is null, and then varies until it stabilizes in the steady-state. In the case of the RC load, for a short period of time, the Q-power is above the real axis, indicating an inductive characteristic. It is concluded that in the transient state, loads can alternate between capacitive and inductive characteristics. Naturally, as time increases, the Q-power stabilizes at its steady-state, as discussed in the previous section.

3.5.2 RLC balanced loads

As discussed in section 3.2, RLC loads can be divided into overdamped, critically damped, and underdamped cases. Applying eqs. (3.82), (3.86) and (3.90) in eq. (3.104) the Q-power for overdamped, critically damped and underdamped RLC loads, respectively, can be written as

$$\mathbf{S}_T(t) = 3V_o^2 Y e^{\mathbf{n}\theta} + \sqrt{3}V_o e^{-\zeta\omega_0 t} e^{\mathbf{n}\omega t}\mathbf{q}_p(e^{\omega_0\sqrt{\zeta^2-1}t}\mathbf{k}_1^* + e^{-\omega_0\sqrt{\zeta^2-1}t}\mathbf{k}_2^*). \tag{3.261}$$

$$\mathbf{S}_T(t) = 3V_o^2 Y e^{\mathbf{n}\theta} + \sqrt{3}V_o e^{-\zeta\omega_0 t} e^{\mathbf{n}\omega t}\mathbf{q}_p(\mathbf{k}_1^* + t\mathbf{k}_2^*). \tag{3.262}$$

$$\mathbf{S}_T(t) = 3V_o^2 Y e^{\mathbf{n}\theta} + \sqrt{3}V_o e^{-\zeta\omega_0 t} e^{\mathbf{n}\omega t}\mathbf{q}_p[\cos(\omega_0\sqrt{1-\zeta^2}t)\mathbf{k}_1^* + \sin(\omega_0\sqrt{1-\zeta^2}t)\mathbf{k}_2^*]. \tag{3.263}$$

Figs. fig. 3.36, 3.37 and 3.38 present the Q-power of three-phase RLC loads for the overdamped, critically damped and underdamped cases, respectively. The impedances connected to each phase are $R = 100\,\Omega$, $L = 50$ mH and $C = 100\,\mu$F for the overdamped load, $R = 200\,\Omega$, $L = 1$ H, $C = 100\,\mu$F for the critically damped load and $R = 100\,\Omega$, $L = 1$ H, $C = 100\,\mu$F for the underdamped load. In both cases, $\mathbf{I}(0) = 0$ and $V_o = 220$ V.

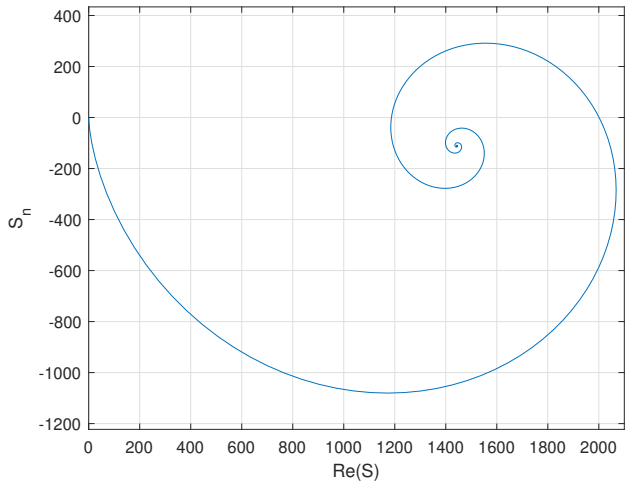

Figure 3.36: Q-power of a three-phase RLC load (overdamped).

It is observed from Figs. 3.36, 3.37 and 3.38 that as in the case of first-order loads, the Q-power of quaternion loads varies in time in a spiral shape, converging to the steady-state value. The Q-power also crosses the real axis, indicating that Q-power alternates between capacitive and inductive behavior. From Figs. 3.37 and 3.38 it is also observed that the Q-power crosses the **n** axis, which indicates that the instantaneous power is negative for a short period of time. So, in the critically damped and the underdamped cases, the load has behaved as a source during part of the transient state.

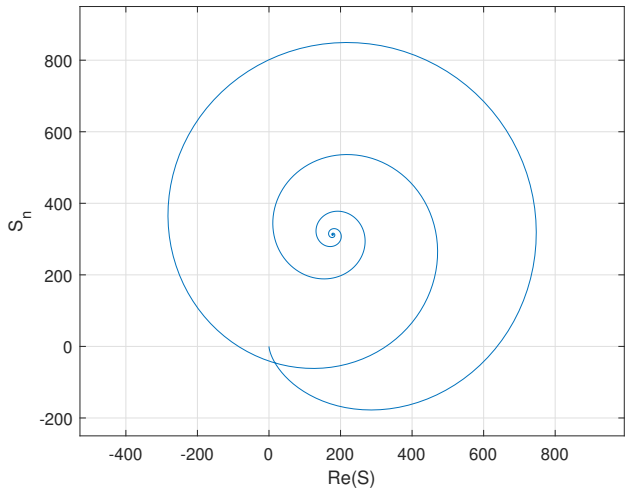

Figure 3.37: Q-power of a three-phase RLC load (critically damped).

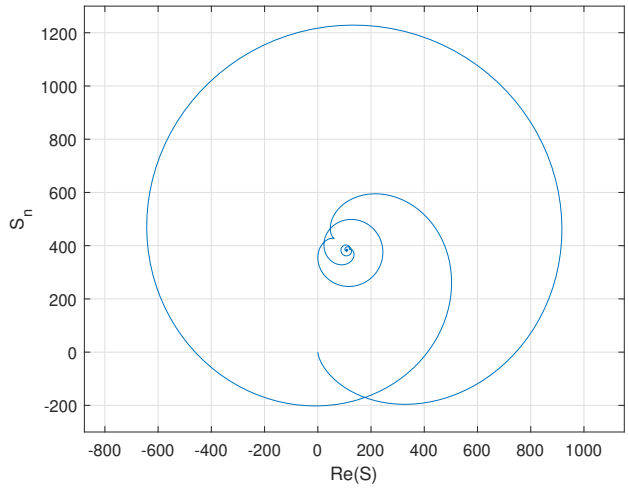

Figure 3.38: Q-power of a three-phase RLC load (underdamped)

3.5.3 LC balanced load

The Q-power of the three-phase balanced LC load is also determined. Applying eq. (3.102) in eq. (3.104) the Q-power for LC loads can be written as

$$\mathbf{S}_T(t) = 3V_o^2 Y e^{\mathbf{n}\theta} + \sqrt{3}V_o e^{\mathbf{n}\omega t}\mathbf{q}_p(\cos(\omega_0 t)\mathbf{k}_1^* - \sin(\omega_0 t)\mathbf{k}_2^*). \tag{3.264}$$

Fig. 3.39 present the Q-power of a three-phase LC load, considering $L = 1$ H, $C = 1\ \mu$F, $\mathbf{I}(0) = 0$ and $V_o = 220$ V.

As observed from Fig. 3.39, the Q-power does not converge to the steady-state, as expected. Additionally, the Q-power locus oscillates between the **n** axis, so that the average active power consumption of this load is null.

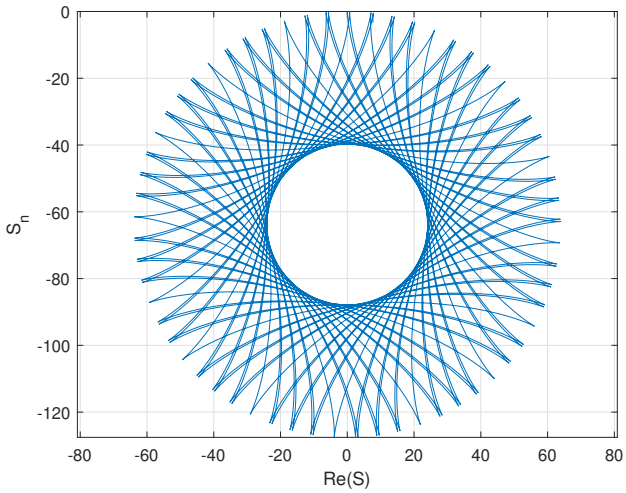

Figure 3.39: Q-power of a three-phase LC load.

3.5.4 Unbalanced delta load

In this subsection, the Q-power of unbalanced delta loads is analyzed. The expressions for Q-power of the delta load are obtained from eqs. (3.134) and (3.145) using eq. (3.20).

$$\mathbf{S} = 3Y_{pl}V_o^2 e^{\mathbf{n}\theta_{pl}} + 3Y_\omega V_o^2 e^{\mathbf{n}\phi_\omega(t)}, \tag{3.265}$$

$$\mathbf{S} = 3Y_\delta(t)V_o^2 e^{\mathbf{n}\phi_\delta(t)}. \tag{3.266}$$

For analyzing the behavior of Q-power, several loads will be considered. Table 3.5.4 presents the admittance connected to each pair of phases of these loads, as well as Q-admittance terms.

Table 3.1: Three-phase delta load admittances.

	$Y_{ab}e^{-j\theta_{ab}}$	$Y_{bc}e^{-j\theta_{bc}}$	$Y_{ca}e^{-j\theta_{ca}}$	Y_{pl}	θ_{pl}	Y_ω
$\mathbf{Y}_1$	3	2	2	7	0	1
$\mathbf{Y}_2$	4	2	2	8	0	2
$\mathbf{Y}_3$	5	2	2	9	0	3
$\mathbf{Y}_4$	4	3	3	10	0	1
$\mathbf{Y}_5$	5	3	2	10	0	2.65
$\mathbf{Y}_6$	6	3	1	10	0	4.36
$\mathbf{Y}_7$	$2e^{j\frac{\pi}{6}}$	$2e^{-j\frac{\pi}{12}}$	$2e^{-j\frac{\pi}{12}}$	5.60	$-0.36°$	1.53
$\mathbf{Y}_8$	$2e^{j\frac{\pi}{2}}$	$2e^{-j\frac{\pi}{12}}$	$2e^{-j\frac{\pi}{12}}$	4.91	$-38.15°$	3.17
$\mathbf{Y}_9$	$2e^{-j\frac{\pi}{2}}$	$2e^{-j\frac{\pi}{12}}$	$2e^{-j\frac{\pi}{12}}$	3.98	$14.02°$	2.44

The loads in Table 3.5.4 are separated into three groups. The first group consist of the Q-admittances $\mathbf{Y}_1$, $\mathbf{Y}_2$ and $\mathbf{Y}_3$. It consists of a set of resistive loads in which the resistance connected to phases A and B

is decreased. The second group consists of the Q-admittances $\mathbf{Y}_4$, $\mathbf{Y}_5$ and $\mathbf{Y}_6$. This group is also a set of resistive three-phase loads, but in this case, the Y_{ab} is increased and Y_{ca} is decreased by the same value. The third group consists of the Q-admittances $\mathbf{Y}_7$, $\mathbf{Y}_8$ and $\mathbf{Y}_9$. In this group, the admittances have the same absolute value, but the argument θ_{ab} is varied.

Fig. 3.40 presents the Q-power of the first group of loads.

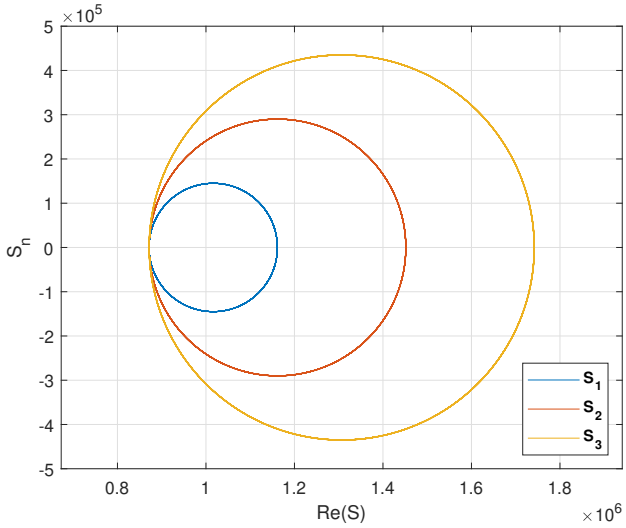

Figure 3.40: Q-power of Q-admittances $\mathbf{Y}_1$, $\mathbf{Y}_2$ and $\mathbf{Y}_3$.

From Fig. 3.40 it is observed that the Q-power of resistive unbalanced delta loads describes a circle centered in the real axis. As one of the admittances is increased, the center of this circle moves away from the origin. The radius of the circle is increased as well.

Fig. 3.41 presents the Q-power of the second group of loads.

From Fig. 3.41 it is observed that if one of the admittances is increased by the same amount that a second is decreased, the center of the Q-power locus does not change. However, as the load is more unbalanced, the radius of the circle increases.

Fig. 3.42 presents the Q-power of the third group of loads.

From Fig. 3.42 it is observed that as the argument of one of the admittances is varied, the center of Q-power locus also varies. The radius also varies depending on the difference between the arguments of the admittances in each phase.

Analyzing eq. (3.265), it is observed that the center of the Q-power locus is its constant part, $3Y_{pl}V_o^2 e^{\mathbf{n}\theta_{pl}}$. It indicates the Q-power of the balanced load obtained by the decomposition of the delta load. The radius

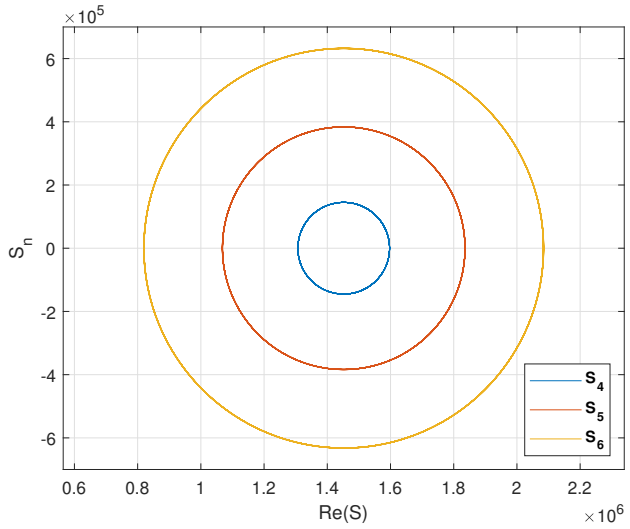

Figure 3.41: Q-power of Q-admittances $\mathbf{Y}_4$, $\mathbf{Y}_5$ and $\mathbf{Y}_6$.

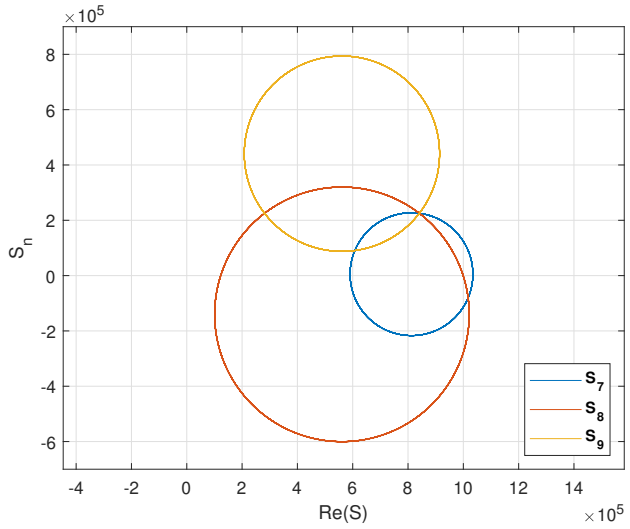

Figure 3.42: Q-power of Q-admittances $\mathbf{Y}_7$, $\mathbf{Y}_8$ and $\mathbf{Y}_9$.

of the circle is given by $3Y_\omega V_o^2$. In this sense, Y_ω is a measure of load unbalance, since it increases if the unbalances between phases are increased as observed from Figs. 3.40, 3.41 and 3.42. It accounts for absolute values and arguments of each admittance, as described in eq. (3.136).

3.5.5 Unbalanced solidly grounded wye load

In this subsection, the Q-power of a three-phase solidly grounded wye load is analyzed. The Q-power of this load can be obtained applying eq. (3.184) in eq. (3.20)

$$\mathbf{S} = 3V_o^2(\mathbf{Y}_A^* + \mathbf{Y}_B^* + \mathbf{Y}_C^*), \tag{3.267}$$

or alternatively using eq. (3.194)

$$\mathbf{S} = \frac{3V_o^2}{\sqrt{6}}[Y_a(e^{\mathbf{n}(\theta_a)}\mathbf{q}_p^* + e^{\mathbf{n}(2\omega t-\theta_a)}\mathbf{q}_p^*)\mathbf{a} + Y_b(e^{\mathbf{n}(\theta_b+\frac{2\pi}{3})}\mathbf{q}_p^* + e^{\mathbf{n}(2\omega t-\frac{2\pi}{3}-\theta_b)}\mathbf{q}_p^*)\mathbf{b} + Y_c(e^{\mathbf{n}(\theta_c-\frac{2\pi}{3})}\mathbf{q}_p^* + e^{\mathbf{n}(2\omega t+\frac{2\pi}{3}-\theta_c)}\mathbf{q}_p^*)\mathbf{c}]. \quad (3.268)$$

which can be written analogously to eq. (3.184) as

$$\mathbf{S} = \mathbf{S}_A + \mathbf{S}_B + \mathbf{S}_C. \quad (3.269)$$

Next, the Q-power a solidly grounded wye load is obtained. It has admittances $Y_a e^{-j\theta_a} = 100$, $Y_b e^{-j\theta_b} = 2^{j\frac{\pi}{6}}$ and $Y_c e^{-j\theta_c} = e^{-j\frac{\pi}{2}}$ connected to phases A, B and C, respectively is obtained.

Figs. 3.43, 3.44 and 3.45 presents the components $\mathbf{S}_A$, $\mathbf{S}_B$ and $\mathbf{S}_C$ of Q-power of this load.

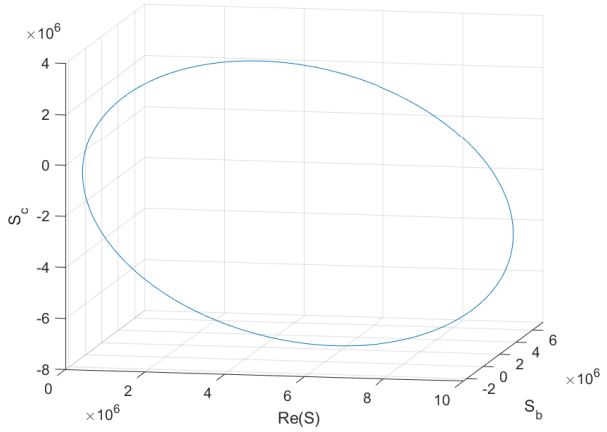

Figure 3.43: $\mathbf{S}_A$ component of the Q-power of a solidly-grounded unbalanced wye.

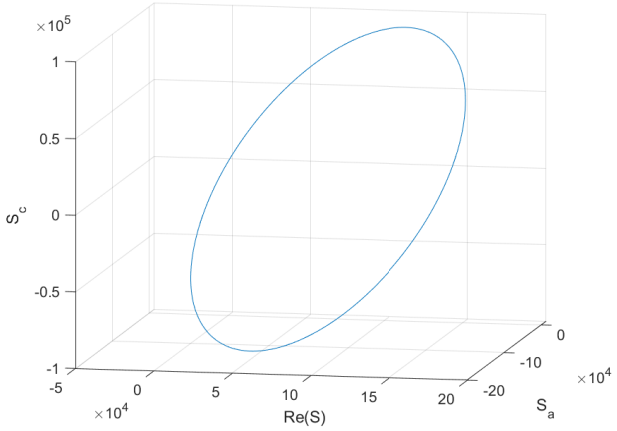

Figure 3.44: $\mathbf{S}_B$ component of the Q-power of a solidly-grounded unbalanced wye.

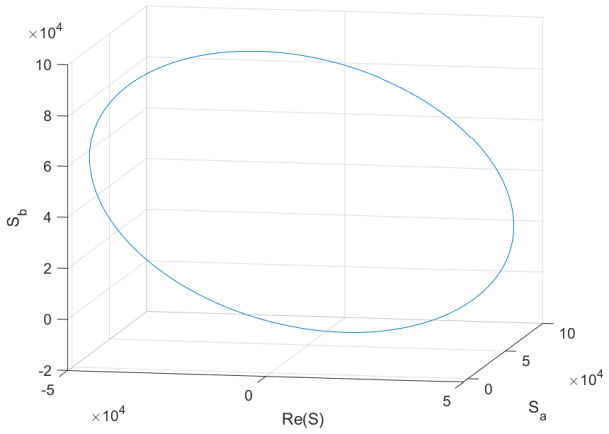

Figure 3.45: $\mathbf{S}_C$ component of the Q-power of a solidly-grounded unbalanced wye.

From Figs. 3.43, 3.44 and 3.45 it is observed that each component of the Q-power is in a space lacing one of the three basic quaternion units. Moreover, each component is an ellipse with parameters determined by its constant and varying in time components.

The Q-power of the three-phase load is them obtained summing these three components. It has all four quaternionic components and its vectorial part is not restricted to a direction as in the case of the delta load. To represent the Q-power, another expression for this quantity is used. Substituting eq. (3.200) in eq. (3.20)

$$\mathbf{S} = V_o^2[\cos(2\omega t)\mathbf{Y}_\varphi^* + \sin(2\omega t)\mathbf{Y}_\psi^* + \mathbf{Y}_o^*]. \tag{3.270}$$

For representing the Q-power in a three-dimensional space, the axis direction have to be chosen accordingly to eq. (3.270). Since $\mathbf{Y}_\varphi^*$ and $\mathbf{Y}_\psi^*$ are orthogonal, their directions can be defined as two of the space axis, that is

$$\mathbf{q}_1 = \frac{\mathbf{Y}_\varphi^*}{|\mathbf{Y}_\varphi^*|}, \tag{3.271}$$

$$\mathbf{q}_2 = \frac{\mathbf{Y}_\psi^*}{|\mathbf{Y}_\psi^*|}. \tag{3.272}$$

The third direction is defined by the direction of $\mathbf{Y}_o^*$ subtracted by its projections in $\mathbf{q}_1$ and $\mathbf{q}_2$. This method used to normalizing vectors is known as Gram-Schmidt process.

$$\mathbf{q}_3 = \frac{\mathbf{Y}_o^* - (\mathbf{Y}_o^* \cdot \mathbf{q}_1)\mathbf{q}_1 - (\mathbf{Y}_o^* \cdot \mathbf{q}_2)\mathbf{q}_2}{|\mathbf{Y}_o^* - (\mathbf{Y}_o^* \cdot \mathbf{q}_1)\mathbf{q}_1 - (\mathbf{Y}_o^* \cdot \mathbf{q}_2)\mathbf{q}_2|} \tag{3.273}$$

Fig. 3.46 presents the Q-power in the space formed by the direction q_1, q_2 and q_3

It is observed from Fig. 3.46 that the locus of the Q-power of the solidly grounded load is a circumference. In this case, differently than in the delta load, the axis directions depend on load parameters. So,

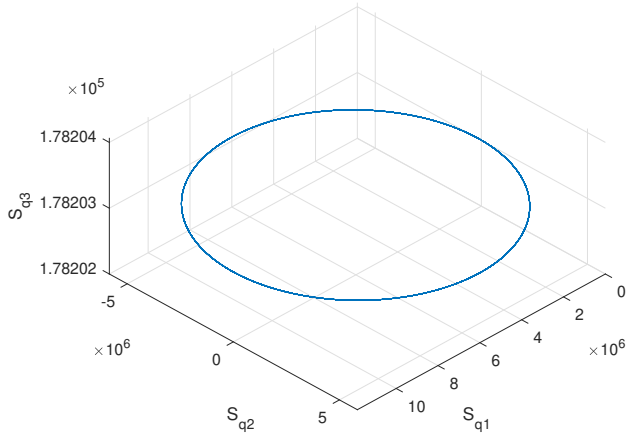

Figure 3.46: Q-power of a solidly-grounded unbalanced wye.

it is not possible to represent different loads in the same subspace of $\mathbb{H}$. Nevertheless, the radius of the Q-power circumference is also related unbalance levels.

3.6 FINAL CONSIDERATIONS

In this chapter, three-phase linear loads were modeled in the time-domain using a quaternion framework. Initially, the definitions of Q-voltage, Q-current, instantaneous Q-power, Q-impedance, and Q-impedance were shown. The definition of Q-admittance was presented and the power expressions were rewritten in terms of this definition. Then, three-phase balanced loads were analyzed in terms of Q-admittance and power. Resistive, inductive, and capacitive loads, as well as their combinations, were considered in the time-domain. Afterward, unbalanced loads in three-wire systems were analyzed. The delta and wye configurations were evaluated considering the steady-state. It was shown that in the quaternion framework, the unbalanced load expressions for admittance and power resemble those of a combination of balanced loads. It was concluded that the unbalanced three-phase load is equivalent to a time-varying balanced three-phase load. Expressions for the steady-state Q-admittance of solidly grounded and grounded wye were obtained. It was shown that the grounded wye is a parallel combination of the solidly grounded wye and the delta load. All expressions obtained for these loads are not obtainable with the usual time-domain theory. Nevertheless, these expressions provide simple rules for obtaining the Q-admittance if the admittance of each phase is known. Furthermore, the proposed formulation is a novel and compact representation of three-phase loads.

In the following chapter, conclusions and suggestions of future works are addressed.

4 CONCLUSIONS

In this study, three-phase balanced and unbalanced linear loads were analyzed in a quaternion framework. Expressions for Q-admittance and Q-power were obtained considering transient and steady-states in the balanced case. The Q-current locus was described for several types of three-phase loads. Several formulas were derived for Q-admittance and Q-power of unbalanced delta loads in the steady-state. It was shown that the Y-Δ transform allows for accounting for the Q-admittance and the Q-power of wye loads as well. Additionally, Q-power and Q-admittance of grounded and solidly grounded wye loads were presented. With the model proposed, Q-power and Q-current can easily be obtained if the three-phase voltages and parameters of load are known.

The definitions of impedance and admittance are normally introduced in the frequency domain. Nevertheless, their generalization to the time domain in the presented quaternion framework provides useful information about loads. It also allows for considering impedance and admittance in scenarios in which phasorial theory was not able to, e.g. in the presence of harmonics.

For three-wire loads, it was shown that the Q-admittance can be expressed with two terms: one that is equivalent to the usual complex admittance and other that accounts for the time-variant contribution of the load imbalance on the power. The second component of the Q-admittance can be used as a measure of the load unbalance level. It is an unbiased measure in the sense that for a balanced load this second term is zero. This decomposition also makes it natural to introduce the idea of decomposition of the unbalanced load in terms of a balanced load in parallel with an unbalanced load with null average power.

The Q-admittance can be expressed as well in a form that makes clear that any unbalanced delta load can be represented as a time-varying balanced load. It is noteworthy that the Q-admittance of this load is restricted to a plane in the hypercomplex space. As a consequence, operating this quantity uses the same computational effort as operating with complex numbers.

In four-wire systems, it was shown that the Q-admittance of the solidly grounded load is composed of three linearly independent parts due to the direct connection to the ground. Given this, the quaternionic analysis of this case is analogous to considering each phase separately. The Q-admittance of the grounded load is shown to be equivalent to the Q-admittance of delta load plus the Q-admittance of the solidly

grounded load. Thus, it can be decomposed into a parallel combination of these loads.

For future works, the investigation of the proposed formulation in an environment with harmonics is suggested. In this sense, the modeling of non-linear three-phase loads is a possible guideline. The quaternion framework allows for the unification of the transient and the steady-state in a compact and consistent algebra. So, the development of power system algorithms based on the proposed model is encouraged. The use of Y_ω and Y_r as indicators of load unbalance also needs further investigations. Proposed formulations of three-phase loads also indicate the possibility of designing compensators in the $\mathbb{H}$ domain.

Bibliography

[1] BOSE, B. K. Global energy scenario and impact of power electronics in 21st century. *IEEE Transactions on Industrial Electronics*, IEEE, v. 60, n. 7, p. 2638–2651, 2013. ISSN 02780046.

[2] JANNESAR, M. R. et al. Optimal probabilistic planning of passive harmonic filters in distribution networks with high penetration of photovoltaic generation. *International Journal of Electrical Power Energy Systems*, Elsevier, v. 110, p. 332–348, 2019. ISSN 0142-0615.

[3] MAI, A.; WAGNER, B.; STREIT, F. Elimination of Current Harmonics in Electrical Machines with Iterative Learning Control. In: *2020 10th International Electric Drives Production Conference (EDPC)*. [S.l.]: IEEE, 2020. p. 1–5. ISBN 1728184584.

[4] LIU, Y. et al. Sensorless control of standalone brushless doubly fed induction generator feeding unbalanced loads in a ship shaft power generation system. *IEEE Transactions on Industrial Electronics*, IEEE, v. 66, n. 1, p. 739–749, 2018. ISSN 0278-0046.

[5] AHMED, E. M. et al. Multifunctional distributed MPPT controller for 3P4W grid-connected PV systems in distribution network with unbalanced loads. *Energies*, Multidisciplinary Digital Publishing Institute, v. 12, n. 24, p. 4799, 2019.

[6] CZARNECKI, L. S. Energy flow and power phenomena in electrical circuits: Illusions and reality. *Electrical Engineering*, v. 82, n. 3, p. 119–126, 2000. ISSN 09487921.

[7] STEINMETZ, C. P. Does phase displacement occur in the current of electric arcs? *ETZ*, v. 587, 1892.

[8] USTARIZ, A. J.; CANO, E. A.; TACCA, H. E. Evaluación, Interpretación y Visualización de la Potencia Instantánea en Sistemas Eléctricos. *V Simposio Internacional sobre Calidad de la Energia Eléctrica*, p. 7, 2009.

[9] EMANUEL, A. et al. IEEE Std 1459–2010. IEEE Standard Definitions for the Measurement of Electric Power Quantities under Sinusoidal, Nonsinusoidal, Balanced or Unbalanced Conditions. IEEE, 2010. ISSN 0738160598.

[10] AKAGI, H.; KANAZAWA, Y.; NABAE, A. Instantaneous reactive power compensators comprising switching devices without energy storage components. *IEEE Transactions on industry applications*, IEEE, n. 3, p. 625–630, 1984.

[11] WILLEMS, J. L. A New Interpretation of the Akagi-Nabae Power Components for Nonsinusoidal Three-Phase Situations. *IEEE Transactions on Instrumentation and Measurement*, v. 41, n. 4, p. 523–527, 1992. ISSN 15579662.

[12] PENG, F. Z.; LAI, J. S. Generalized instantaneous reactive power theory for three-phase power systems. *IEEE Transactions on Instrumentation and Measurement*, v. 45, n. 1, p. 293–297, 1996. ISSN 00189456.

[13] MENTI, A.; ZACHARIAS, T.; MILIAS-ARGITIS, J. Geometric algebra: A powerful tool for representing power under nonsinusoidal conditions. *IEEE Transactions on Circuits and Systems I: Regular Papers*, v. 54, n. 3, p. 601–609, 2007. ISSN 10577122.

[14] MONTOYA, F. G. et al. A new approach to single-phase systems under sinusoidal and non-sinusoidal supply using geometric algebra. *Electric Power Systems Research*, Elsevier, v. 189, n. July, p. 106605, 2020. ISSN 03787796. Disponível em: <https://doi.org/10.1016/j.epsr.2020.106605>.

[15] DAI, X.; LIU, G.; GRETSCH, R. Generalized theory of instantaneous reactive quantity for multiphase power system. *IEEE Transactions on Power Delivery*, IEEE, v. 19, n. 3, p. 965–972, 2004. ISSN 08858977.

[16] Ustariz-Farfan, A. J.; Cano-Plata, E. A.; Arias-Guzman, S. Identification of protection coordination break points: A power quality approach. *IEEE Industry Applications Magazine*, v. 25, n. 5, p. 68–82, 2019.

[17] NOS, O. V. Linear transformations in mathematical models of an induction motor by quaternions. *International Workshop and Tutorials on Electron Devices and Materials, EDM - Proceedings*, v. 1, p. 295–298, 2012. ISSN 18153712.

[18] BRASIL, V. D. P.; De Leles Ferreira Filho, A.; ISHIHARA, J. Y. Electrical three phase circuit analysis using quaternions. *Proceedings of International Conference on Harmonics and Quality of Power, ICHQP*, v. 2018-May, n. 1, p. 1–6, 2018. ISSN 21640610.

[19] BARRY, N. Electrical circuit analysis using four dimensional complex numbers, in the form of quaternions. *Proceedings of the Universities Power Engineering Conference*, IEEE, 2013.

[20] NOS, O. V. et al. Quaternion control of four-leg inverter for distribution system with harmonic-producing load. In: IEEE. *2020 XI International Conference on Electrical Power Drive Systems (ICEPDS)*. [S.l.], 2020. p. 1–6.

[21] MORAIS, J. P.; GEORGIEV, S.; SPRÖSSIG, W. *Real quaternionic calculus handbook*. [S.l.]: Springer, 2014.

[22] KUIPERS, J. B. *Quaternions and rotation sequences: a primer with applications to orbits, aerospace, and virtual reality*. [S.l.]: Princeton university press, 1999. ISBN 0691102988.

[23] CRASSIDIS, J. L.; MARKLEY, F. L.; CHENG, Y. Survey of nonlinear attitude estimation methods. *Journal of guidance, control, and dynamics*, v. 30, n. 1, p. 12–28, 2007. ISSN 0731-5090.

[24] SPRING, K. W. Euler parameters and the use of quaternion algebra in the manipulation of finite rotations: a review. *Mechanism and machine theory*, Elsevier, v. 21, n. 5, p. 365–373, 1986. ISSN 0094-114X.

[25] SHOEMAKE, K. Animating rotation with quaternion curves. In: *Proceedings of the 12th annual conference on Computer graphics and interactive techniques*. [S.l.: s.n.], 1985. p. 245–254.

[26] MIRON, S.; BIHAN, N. L.; MARS, J. I. Quaternion-MUSIC for Vector-Sensor Array Processing. v. 54, n. 4, p. 1218–1229, 2006.

[27] MANDIC, D. P.; JAHANCHAHI, C.; TOOK, C. C. A quaternion gradient operator and its applications. *IEEE Signal Processing Letters*, IEEE, v. 18, n. 1, p. 47–50, 2011. ISSN 10709908.

[28] JAHANCHAHI, C.; MANDIC, D. P. A class of quaternion kalman filters. *IEEE Transactions on Neural Networks and Learning Systems*, IEEE, v. 25, n. 3, p. 533–544, 2014. ISSN 21622388.

[29] CHOUKROUN, D.; BAR-ITZHACK, I. Y.; OSHMAN, Y. Novel quaternion Kalman filter. *IEEE Transactions on Aerospace and Electronic Systems*, IEEE, v. 42, n. 1, p. 174–190, 2006. ISSN 00189251.

[30] CRISTALDI, L.; FERRERO, A. Mathematical foundations of the instantaneous power concepts: an algebraic approach. *European transactions on electrical power*, Wiley Online Library, v. 6, n. 5, p. 305–309, 1996.

[31] WILLEMS, J. L. Mathematical foundations of the instantaneous power concepts: a geometrical approach. *European transactions on electrical power*, Wiley Online Library, v. 6, n. 5, p. 299–304, 1996.

[32] MALYAVKO, E. Y.; NOS, O. V. Control strategy of inactive instantaneous power compensation in quaternion basis. *International Conference of Young Specialists on Micro/Nanotechnologies and Electron Devices, EDM*, IEEE, p. 411–414, 2014. ISSN 2325419X.

[33] NOS, O. V. Control strategy of active power filter for ineffective instantaneous power compensation. *International Conference of Young Specialists on Micro/Nanotechnologies and Electron Devices, EDM*, IEEE, n. 6, p. 370–374, 2014. ISSN 2325419X.

[34] NOS, O. V. Control strategy of shunt active power filter based on an algebraic approach. *International Conference of Young Specialists on Micro/Nanotechnologies and Electron Devices, EDM*, IEEE, v. 2015-August, n. 2, p. 459–463, 2015. ISSN 2325419X.

[35] NOS, O. V.; BROVANOV, S. V.; DYBKO, M. A. Development of active filtering algorithms for higher harmonics in electrical power circuits. *Optoelectronics, Instrumentation and Data Processing*, v. 52, n. 6, p. 557–562, 2016. ISSN 19347944.

[36] TALEBI, S. P.; MANDIC, D. P. A quaternion frequency estimator for three-phase power systems. *ICASSP, IEEE International Conference on Acoustics, Speech and Signal Processing - Proceedings*, v. 2015-August, n. 1, p. 3956–3960, 2015. ISSN 15206149.

[37] BARRY, N. The application of quaternions in electrical circuits. *2016 27th Irish Signals and Systems Conference, ISSC 2016*, IEEE, 2016.

[38] BARRY, N. Electrical motor force analysis using quaternions. *Proceedings of the Universities Power Engineering Conference*, IEEE, v. 2015-November, p. 1–4, 2015.

[39] GOU, X. et al. Quaternion-valued single-phase model for three-phase power systems. *arXiv preprint arXiv:1601.01557*, 2016.

[40] NOS, O. V.; TOKAREV, V. G. Dynamic model of induction motor in the hyper-complex space. *2016 13th International Scientific-Technical Conference on Actual Problems of Electronic Instrument Engineering, APEIE 2016 - Proceedings*, IEEE, v. 3, n. 2, p. 55–59, 2016.

[41] NOS, O. V.; DUDIN, A.; PETZOLDT, J. The instantaneous power quaternion of the three-phase electric circuit with linear load. *International Conference of Young Specialists on Micro/Nanotechnologies and Electron Devices, EDM*, v. 2016-August, p. 526–531, 2016. ISSN 2325419X.

[42] ARTAMONOV, D. V. et al. Application of a Hyper-Complex Impedance Model for Indirect Measurements of Materials Parameters of Functional Electronics. *International Conference of Young Specialists on Micro/Nanotechnologies and Electron Devices, EDM*, IEEE, v. 2019-June, p. 760–764, 2019. ISSN 2325419X.

[43] TALEBI, S. P.; WERNER, S.; MANDIC, D. P. Quaternion-Valued Distributed Filtering and Control. *IEEE Transactions on Automatic Control*, v. 65, n. 10, p. 4246–4257, 2020. ISSN 15582523.

[44] KOMENO, A. S. et al. Three-phase quaternion power in three-wire systems. *Renewable Energy and Power Quality Journal*, v. 19, n. 19, p. 493–498, 2021. ISSN 2172038X.

[45] CZARNECKI, L. Equivalent circuits of unbalanced loads supplied with symmetrical and asymmetrical voltage and their identification. *Electrical Engineering*, Springer, v. 78, n. 3, p. 165–168, 1995.